Spring 1997

Quantified sea level history for the middle Jurassic (Bajocian) through Cretaceous (Santonian) based on Russian platform and Siberian stratigraphic data

Oleg Vladimir Pinous
University of New Hampshire, Durham

INFORMATION TO USERS

This manuscript has been reproduced from the microfilm master. UMI films the text directly from the original or copy submitted. Thus, some thesis and dissertation copies are in typewriter face, while others may be from any type of computer printer.

The quality of this reproduction is dependent upon the quality of the copy submitted. Broken or indistinct print, colored or poor quality illustrations and photographs, print bleedthrough, substandard margins, and improper alignment can adversely affect reproduction.

In the unlikely event that the author did not send UMI a complete manuscript and there are missing pages, these will be noted. Also, if unauthorized copyright material had to be removed, a note will indicate the deletion.

Oversize materials (e.g., maps, drawings, charts) are reproduced by sectioning the original, beginning at the upper left-hand corner and continuing from left to right in equal sections with small overlaps. Each original is also photographed in one exposure and is included in reduced form at the back of the book.

Photographs included in the original manuscript have been reproduced xerographically in this copy. Higher quality 6" x 9" black and white photographic prints are available for any photographs or illustrations appearing in this copy for an additional charge. Contact UMI directly to order.

UMI

A Bell & Howell Information Company
300 North Zeeb Road, Ann Arbor MI 48106-1346 USA
313/761-4700 800/521-0600

QUANTIFIED SEA LEVEL HISTORY FOR THE MIDDLE JURASSIC (BAJOCIAN) THROUGH CRETACEOUS (SANTONIAN) BASED ON RUSSIAN PLATFORM AND SIBERIAN STRATIGRAPHIC DATA

BY

Oleg V. Pinous
Baccalaureate Degree, Novosibirsk State University, 1992
Master's Degree, Novosibirsk State University, 1993

DISSERTATION

Submitted to the University of New Hampshire
in Partial Fulfillment of
the requirements for the Degree of

Doctor of Philosophy

in

Earth Sciences: Geology

May, 1997

APPROVAL PAGE

This dissertation has been examined and approved.

Dissertation Director, Dork Sahagian,
Research Associate Professor

Wallace Bothner, Professor

Jo Laird, Associate Professor

Herbert Tischler, Professor

Lawrence Ward, Research Associate Professor

May 8 1997
Date

TABLE OF CONTENTS

ACKNOWLEDGEMENTS

Deepest thanks go to my graduate advisor Dork Sahagian for his help and supervision throughout my doctoral studies. In addition to specific guidance for my research, he served as a fine example of a modern scientist, showing me how to put my results into the context of the scientific community. I am particularly grateful to Victor Zakharov whose help and supervision ranged from data interpretation and consulting in numerous scientific problems to organization of fieldwork and providing me cooperative working environment in the Institute of Geology, Russian Academy of Science (Novosibirsk, Russia). Without his regional insights, participation and assistance this project would have been practically impossible to complete. Detailed comments by Steve Jacobson helped me clarify many of the sequence stratigraphic interpretations. Special thanks go to B.N. Shurygin and M.A. Levchuk form the Institute of Geology for consulting on West Siberian regional data. I also appreciate the helpful guidance and reviews of my committee members: Wally Bothner, Jo Laird, Herb Tischler, and Larry Ward.

This project was supported by NSF grant (EAR 9218945), a Doctoral Research Fellowship from the Graduate School of UNH, and two student research grants from Geological Society of America and American Association of Petroleum Geologists.

The dissertation is dedicated to the memory of my mother, Larisa Pinous.

LIST OF FIGURES

ABSTRACT

QUANTIFIED SEA LEVEL HISTORY FOR THE MIDDLE JURASSIC (BAJOCIAN) THROUGH CRETACEOUS (SANTONIAN) BASED ON RUSSIAN PLATFORM AND SIBERIAN STRATIGRAPHIC DATA

by

Oleg V. Pinous
University of New Hampshire, May, 1997

Quantified Eustatic Curve (QEC) for Bajocian (Mid Jurassic) through Santonian (Upper Cretaceous) was constructed on the basis of the stratigraphy of the Russian Platform. The Mesozoic tectonic stability of the central part of the Russian Platform provided a valid frame of reference upon which to base the eustatic curve. As such, this curve can be considered a reliable representation of eustasy. The stratigraphic hiatuses left by unconformities in the central part of the Russian Platform were filled with stratigraphic information from the more continuous stratigraphy of the subsiding regions such as Ryazan Saratov Trough and Northern Siberia. The curve makes it possible to filter the eustatic signal from basin stratigraphic data (in any basin) and thereby quantify basin subsidence and sedimentation history more accurately than previously possible.

In order to test its validity the QEC was compared to the existing eustatic reconstructions for Jurassic-Cretaceous of the European and U.S. mid-continent sections. Good correlation (within limits of biostratigraphic resolution) of sea-level events interpreted from the regions with different tectonic histories made it possible to prove eustatic nature of several sea-level events. These include transgressive/highstand episodes: 1) late Bathonian; 2) late Callovian; 3) middle Oxfordian; 4) late Oxfordian; 5) late Albian; 6) Cenomanian/Turonian boundary; 7) mid-Volgian, and regressive events such as: 1) latest early Oxfordian; 2) middle late Oxfordian. Good agreement with some discrepancies was found for: early-mid Callovian, Kimmeridgian, Hauterivian, Aptian,

Late Albian-Turonian intervals of the QEC. Additional testing is needed to prove their eustatic origin.

West Siberian basin served as a first site for an application of the QEC. Sequence stratigraphic analysis of the Jurassic and Neocomian sections of the selected regions in West Siberia led to identification of depositional sequences and an improved understanding of their depositional histories. Good correlation (100% correspondence for Oxfordian) was found between the QEC and sea-level change patterns inferred from Late Bathonian-Kimmeridgian and Valanginian-Hauterivian stratigraphic intervals of West Siberia. This result demonstrates the main role of eustasy as a factor controlling the deposition of the Mid-Upper Jurassic and "Clinoform Neocomian" sections.

INTRODUCTION

One of the most difficult problems in stratigraphy is the interpretation of sea-level rise and fall from record of earth's history as preserved in sedimentary rocks. One way sea level change can occur is by local vertical movements of the continents (tectonic subsidence or uplift). This leads to ***relative*** sea level change which simply pertains to the position of the sea surface relative to any point of interest along the coastline. Different places experience different relative sea level histories. Another way sea level can change is by a shift in the relationship between volume of the Earth's ocean basins and the volume of the Earth's ocean water. This leads to a uniform sea level change throughout the entire earth and is termed ***eustatic*** sea level change.

The documentation of eustasy is one of the most elusive problems in modern geology because it is very difficult to distinguish relative sea level changes from eustatic changes. Nevertheless, the documentation of eustatic changes which have occurred in the past is important because:

- Sea-level change directly controls sedimentation processes. Understanding of the relationship between depositional patterns and sea-level variations would make it possible to reconstruct geologic history much more accurately than presently possible.
- Global sea-level change is always associated with global climatic and geographic changes and is an essential part of paleoclimatic and paleogeographic studies.
- Predictions of future sea-level change may greatly benefit from deeper understanding of the measurement, causes, and consequences of sea-level changes of the past.

Eustatic sea level-change, however, is not easy to document uniquely because stratigraphic records of most regions are also affected by local tectonic processes and

varying rates of sedimentation and therefore provide misleading information. It thus becomes problematical to separate the global (eustatic) sea level signal from local (relative) sea level.

Mesozoic sea-level change (65-250 Million Years ago) has been extensively studied for the last 20 years. Much of the interest in these seemingly esoteric investigations has been driven by industry due to the presence of significant oil reservoirs in the Mesozoic strata of many sedimentary basins throughout the world. Documentation of the history of eustatic sea level change and application to specific regions makes it possible to greatly improve our understanding of local geology and depositional history which in turn provide the foundation for predictions of oil and gas reservoir distribution.

Several eustatic curves for the Mesozoic have been compiled from stratigraphic interpretations of continental margins and subsiding basins (Gygi, 1986; Hallam, 1988; Haq et al., 1988). However, this approach has been extensively (and justly) criticized for a number of important reasons. Perhaps the most important criticism is that these curves rely on data from tectonically active regions where local variations may largely or even completely obscure the record of eustatic change. With stratigraphic data from continental margins (or subsiding basins), it is necessary (but unrealistic) to assume that tectonic subsidence can be independently documented accurately enough to filter it from the raw stratigraphic data and thus obtain a residual eustatic signal. This is impractical because the magnitude of the errors inherent in calculating subsidence is greater than the entire eustatic signal, so the desired signal is smaller than the "noise".

While some have considered it impossible to accurately determine eustatic variations (Kendall and Lerche, 1988) others suggest that a eustatic curve should ideally be based on the stratigraphy of a tectonically quiescent region for each time interval of consideration (Hallam, 1992). On the basis of its generally flatlying and otherwise relatively undisturbed stratigraphy, we have identified the central part of the Russian

Platform as a useful reference frame for eustatic sea-level quantification for the time interval mid-Jurassic through Cretaceous.

Thus, the ***primary objective*** of this study was to develop a Quantified Eustatic Curve based on stratigraphy of the central Russian Platform. The Russian Platform was relatively flat and at an elevation very close to sea level during most of the Jurassic and Cretaceous. This interpretation is based on the uniformly thin strata and numerous unconformities (erosional surfaces) observed in the stratigraphic record. These data also suggest that the Russian Platform remained tectonically quiescent throughout the period of Mesozoic sediment deposition. The Russian Platform thus provides a unique opportunity for the quantification of eustatic history during the Mesozoic because there is no other region in the world which was stable for such a long period and has preserved the sedimentary record to document it.

In order to establish any sea-level curve as a eustatic curve, it is necessary to test it against relative sea level curves derived from basins with contrasting tectonic environments, and the eustatic curve developed in this study is no exception. However, there is no method demonstrated to date to prove the validity of any eustatic curve in terms of representation of the relative volumes of ocean basins and ocean water (our definition of eustasy). Nevertheless, most authors (Hallam, 1992; Lawrence, 1993; Miall, 1992) agree that a eustasy can be inferred if age equivalency of sea-level events (within limits of biostratigraphic resolution) is demonstrated in separate tectonically unrelated basins. Chronostratigraphic precision is of critical importance for such a test.

During the last decade, several analyses of relative sea-level change as well as attempts to extract eustasy have been conducted on Jurassic-Cretaceous strata from numerous sedimentary basins around the world. While, some of the resulting curves are claimed by the authors to be eustatic, none of them can be accepted as a universal representation of eustasy because of limitations inherent from the influence of tectonic

and sedimentation factors. However, these curves provide important material on regional sea-level change and serve for global testing of the Quantified Eustatic Curve.

Thus, the ***second objective*** of the dissertation is to test the Quantified Eustatic Curve obtained on Russian Platform stratigraphic data to the sea-level curves derived from sedimentary basins with different tectonic and sedimentation histories.

If the applicability test is successful, the Quantified Eustatic Curve may be used as a tool that can be applied to any basin world wide in order to:

- Quantify local factors (subsidence and sedimentation rates) by removing the eustatic signal from stratigraphic data
- Establish or refine geological ages where there is poor biostratigraphic control (using the synchroneity of major eustatic events);
- Provide the eustatic parameter for computer modelling of a basin sedimentation.

The text of the dissertation is organized into the three main parts.

The first is a detailed presentation of the methodology used for construction of the Quantified Eustatic curve. It includes description of the stratigraphy, paleogeography, and tectonic history of the central Russian Platform and two regions in North Siberia. Following is a description of all phases of data analysis and the final curve constructions. Finally, there is a discussion of all the potential problems involved in the procedure of curve construction, potential utility of the curve, and future prospects of its application.

The second part involves critical comparison (test) of the Quantified Eustatic Curve with existing sea-level curves from different regions in order to establish age equivalency of the inferred events, and thus, demonstrate their eustatic nature. This part is focused on the West European sections because they provide the most comprehensive data on Mesozoic sea-level change, to date. In addition, they are relatively straightforward to correlate biostratigraphically with the Russian Platform.

The third part is devoted to the West Siberian Basin. Because West Siberia is adjacent to the Russian Platform (divided by the Urals), there is particularly well established stratigraphic correspondence between the two for the Mesozoic, despite their contrasting tectonic environments (platform vs. basin). Therefore, the West Siberian basin provides an ideal case for testing the application of the eustatic sea level curve. In this part I focus on sequence stratigraphic analysis which provides tools for relative sea-level reconstructions as well as useful insights on various existing problems of the basin stratigraphy.

CHAPTER I

CONSTRUCTION OF THE QUANTIFIED EUSTATIC CURVE

Russian Platform

Tectonic setting

The Russian Platform is a large cratonic unit with an area of 5.5 million km^2 (Nalivkin, 1973). It generally consists of Precambrian crystalline basement and Phanerozoic cover. The accumulation of presently unmetamorphosed sediments began in the Late Proterozoic (Riphean) about 1400 Ma with the active formation of major aulacogens typical of the initial stages of platform development (Fedynsky et al., 1976). In the Vendo-Cambrian (650-550 Ma) the aulacogen stage terminated and sediments began to accumulate on the relatively flat-lying surface (compared to the modern basement relief) (Milanovsky, 1987). Subsequently, predominantly vertical tectonic movements occurred throughout the platform, resulting in differentiated structure of the sedimentary cover. In general it consists of large scale depressions and arches that themselves include smaller scale swells and troughs (Figure 1).

During the Paleozoic, significant subsidence and graben reactivation occurred throughout much of the platform resulting in the deposition of thick sedimentary units. Some of the graben were inverted in the late Mesozoic or early Cenozoic. The structure relevant to the present study is the Moscow Depression, a subsiding graben complex with thick Paleozoic sedimentary fill in the central part of the Russian Platform (Figure 1). The Mesozoic stratigraphy analyzed here is based on wells and outcrops on and near the

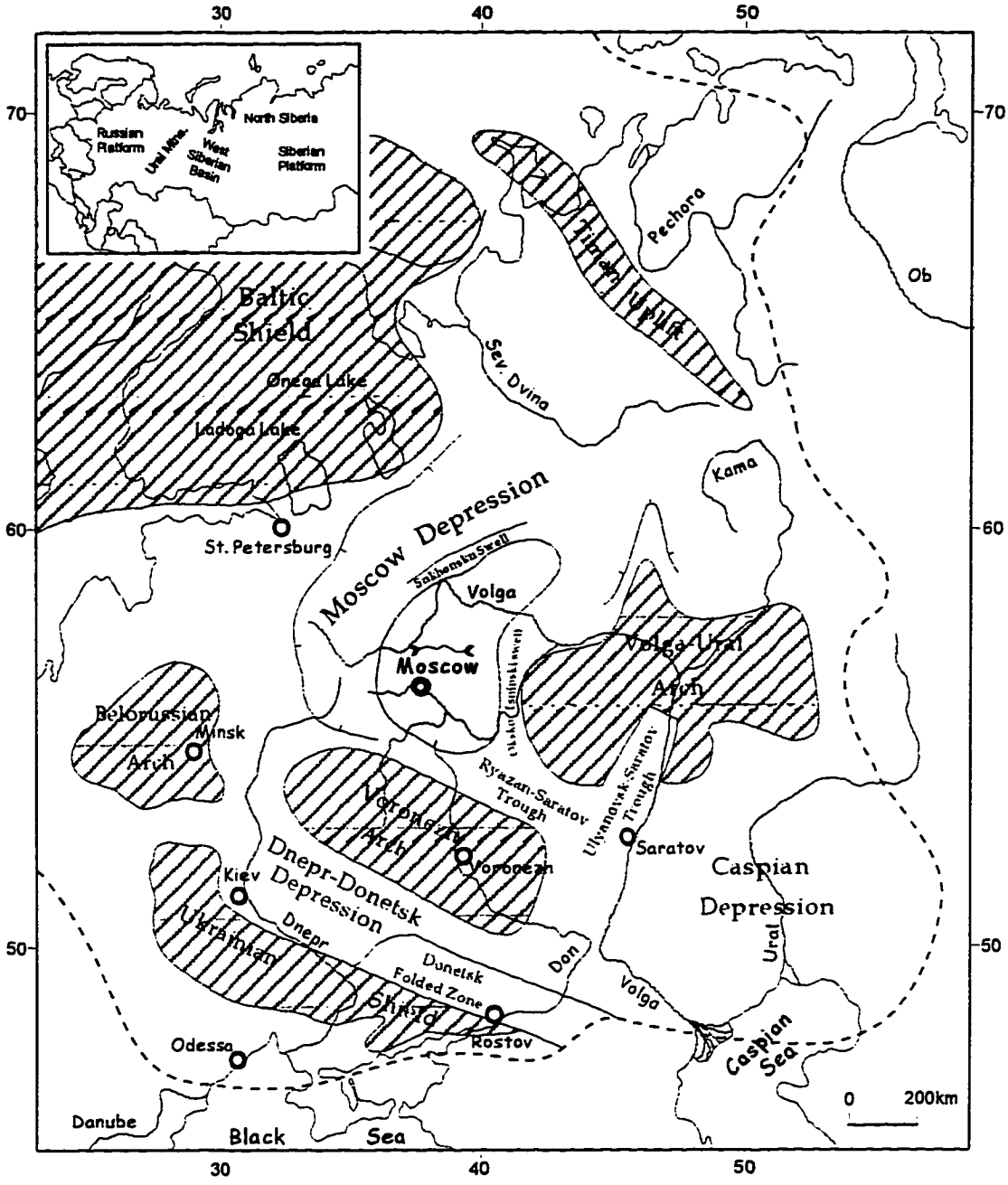

Figure 1. Sketch map of major structures of the Russian Platform

Legend:

- positive structures
- cross-section line
- stable area with preserved Jurassic and Cretaceous sediments
- boundary of the Platform

extinct Moscow Depression, referred to as the "Moscow Synclise" in the Russian literature.

By Jurassic time, the subsiding Moscow depression stabilized. This interpretation is supported by the uniformity and relatively thin nature of Mesozoic beds over great distances. For example, the Oxfordian shale facies between the Ryazan region and Unzha river sections (located about 600 km apart) displays similar isopachs down to the ammonite zone level. This is a typical situation for most of the central part of the Russian Platform. Sandy units are less uniform because of the variations typical of shoreface facies, different rates of sediment supply, and local erosion. The whole thickness of the marine Jurassic-Cretaceous sections usually varies from 5 to 250 meters, suggesting extremely slow rates of sedimentation and limited accommodational potential. The thickness of the entire Mesozoic package increases in the marginal regions (e.g. Caspian Depression, Dnepr-Donetsk Depression) where significant subsidence occurred during deposition.

The presence of a great number of unconformable surfaces and depositional hiatuses in the Jurassic-Cretaceous sections of the Moscow Depression represents additional evidence of stability. Due to very flat hypsometry and the lack of subsidence, even minor sea-level falls could have caused submarine erosion or subaerial exposure, resulting in unconformities. In contrast, the more continuous deposition observed toward the southeast (Lower Volga River Region and Caspian Depression) indicates significant subsidence and deeper water.

During Mesozoic time, limited reactivation of some aulacogen structures began on the Russian Platform. However, the aulacogens in the Moscow Depression apparently remained stable for the time interval from mid-Jurassic to at least Santonian. Tectonic activity resumed during the Campanian-Paleogene in some regions that had been stable since the Jurassic. The inversion of Proterozoic graben structures occurred in the Oksko-

Tsninsky swell and Sukhonsky swell (Figure 1) through uplift of the axis zones. Some minor local movements also occurred in other parts of the previously stable area. All this resulted in local areas with different altitudes of Mesozoic horizons. However, despite of the different vertical positions, the strata and facies are very uniform, even on the Oksko-Tsninsky swell where the relief of Mesozoic surfaces reaches 160 meters. This observation demonstrates the stability of the basin throughout the period of deposition in the Mesozoic.

The interpretation that uniform sedimentation indicates stability is based on the assumption that the Russian Platform did not rise or fall en masse. This assumption is supported by theoretical as well as observational considerations. The part of the Russian Platform which is covered by flat-lying Mesozoic sediments is broader than the flexural half-wavelength of the lithosphere (Sahagian and Holland, 1991; Watts, 1989), so any point source of uplift or subsidence would be expected to lead to large-scale deformation which is not observed. A broad source of epeirogeny such as low-order geoidal variations could affect the region's utility as a eustatic reference frame, but tomographic models suggest that this region has not experienced any significant variations in the relationship between dynamic topography and geoid since the Paleozoic (Gurnis, 1993). Consequently, we consider the Moscow Depression as the most reliable sea-level reference frame possible for the Jurassic and Cretaceous on an otherwise dynamic Earth. While there are other regions on other continents which suggest stability (Sahagian, 1988; Sahagian, 1987), the limited size and stratigraphic range make them inappropriate for construction of a eustatic curve for any appreciable interval in the Mesozoic.

Paleogeography

Paleogeographic maps of the Russian Platform have been compiled based on preserved stratigraphy (Milanovsky, 1987; Naidin, 1959; Naidin et al., 1986; Sazonov and Sazonova, 1967; Vinogradov, 1968). However, the extent of Mesozoic marine

deposition was considerably greater than that of preserved strata because facies generally do not vary as the outcrop edge is approached. Widespread post-Mesozoic erosion makes it difficult to make thorough paleogeographic reconstructions.

During Triassic time the Russian Platform was a low-elevation plain with deposition of alluvial and lacustrine sediments. Shallow marine sediments of Early and earliest Late Triassic age are present only in Caspian Depression (Milanovsky, 1987). In the Early Jurassic time marine transgressions from the Southern Tethyan basin are evident to the south in the Black Sea Depression, Dnepr-Donets Trough, and Caspian Depression. By the end of Bajocian time the central part of the Russian Platform was a low-elevation plain with local relief characterized by ravines and incised valleys (Zhukov and Konstantinovich, 1951). These sites of minor relief were the site of the first Bajocian marine deposition, and after several depositional cycles of incised valley fill, marine sedimentation spread uniformly over the region during the Callovian. Marine conditions subsequently dominated until at least the end of the Cretaceous and were interrupted for relatively short periods during eustatic sea level drops. Thus, during the Jurassic-Cretaceous, the Russian Platform was a shallow epicontinental sea that extended from Tethys to the Arctic, with occasional marine connections to the West (Figures 2, 3).

Marine deposition occurred with limited sediment supply from remote clastic sources (Baltic Shield, Hercinids of Urals, Caledonides). The lack of subsidence and low sediment supply caused eustatic sea level to be the main factor controlling sedimentation.

In our analysis, we use paleogeographic reconstructions as a secondary constraint for estimating paleowater depth. The main difficulties in this procedure arise from the ubiquitous unconformities and extensive areas of partial or complete erosion of depositional units.

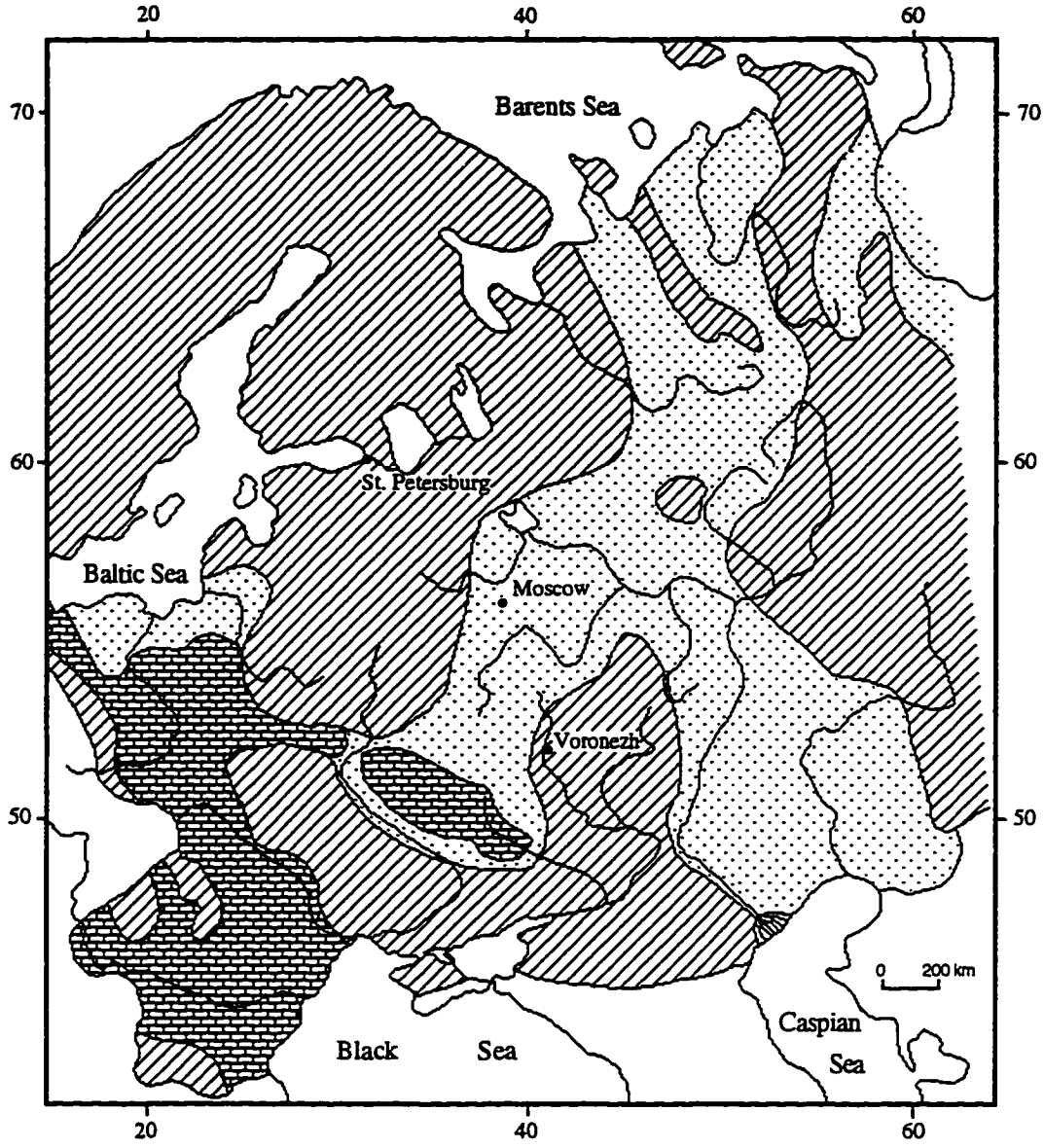

Figure 2. Late Oxfordian (Amoeboceras alternans time) paleogeography of the Russian Platform (after Sazonov and Sazonova, 1967)

Legend:

- Shallow marine clastic facies
- Facies of periodically flooded coastal plains
- Shallow marine carbonate facies
- Continental areas

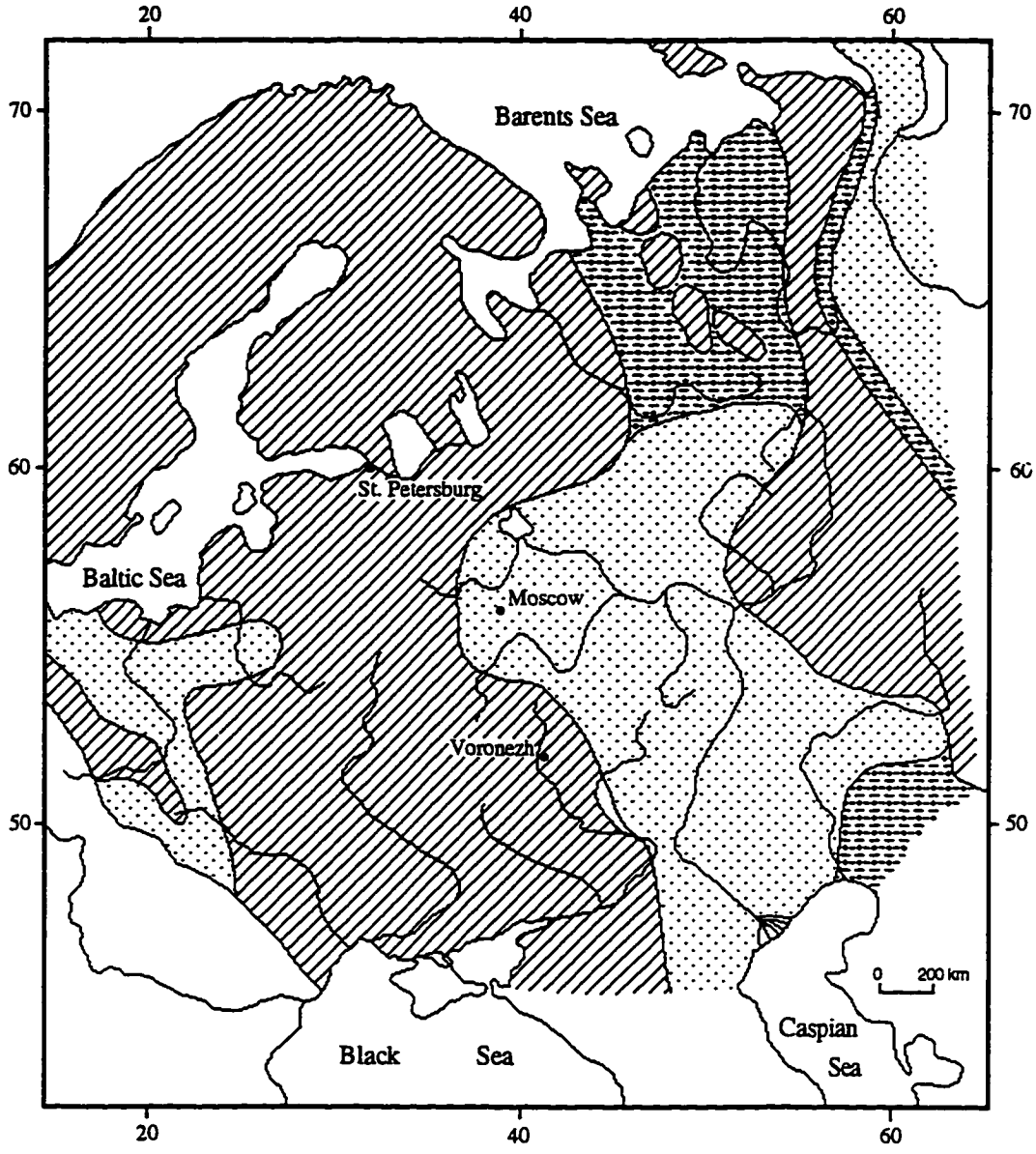

Figure 3. Late Hauterivian (Speetoniceras versicolor time) paleogeography of the Russian Platform (after Sazonov and Sazonova, 1967). See Figure 2 for legend.

According to Sazonov and Sazonova (1967), 4 major erosion events occurred on the Russian Platform since the beginning of Mesozoic marine deposition:

1. Pre-Berriasian - in the Moscow, Caspian, and Dnepr-Donets depressions.
2. Pre-Cenomanian - on the Belorussian and Voronezh arches and adjacent areas on Ukrainian Shield and Uralian Trough.
3. Tertiary.
4. Quaternary - due to glacial and fluvioglacial activities leading to locally complete removal of thick Jurassic-Cretaceous strata.

We have identified several additional important erosional events which potentially affect stratigraphic interpretation, as described below.

Pleistocene glacial activity resulted in significant redistribution and erosion of Mesozoic sediments especially in northern and north-eastern parts of the Platform. For example there is a glacial erratic of Upper Callovian shales up to 4 meters thick with area 4 km^2 located near Lukuva (Eastern Poland) which was transported 500 km from northern Lithuania. Smaller glacial erratics are reported from many places on the Russian Platform. Northeast of the Moscow Synclise (Kama, Vyatka, Sev. Dvina river basins), Jurassic-Cretaceous sediments have been completely removed (Sazonov and Sazonova, 1967).

In summary, during the Jurassic and Cretaceous, the central part of the Russian Platform was a shallow bay of an ephemeral Russian epicontinental sea. Slow rates of sedimentation and a lack of subsidence caused eustasy to be the primary factor controlling sedimentation. The area of preserved sediments is much smaller than the area of deposition because of subsequent widespread erosion. Paleogeographic analysis provided useful secondary constraint for paleodepth estimation, even though the extensive erosion makes it difficult to make thorough paleogeographic reconstructions.

Stratigraphic data

Middle Jurassic through Upper Cretaceous strata are widely distributed on the Russian Platform. Data were obtained for this study from wells and cores, as well as correlated outcrops throughout the Russian Platform (Figure 4). Mesozoic outcrops are numerous and widespread on the Russian Platform, and individual units are continuous and chemically, biostratigraphically, and lithostratigraphically uniform over long distances, allowing relatively reliable correlation between well and nearby outcrop data. The well data provide lithology, thickness, and elevation of depositional units, and the outcrops more closely constrain the age and small-scale lateral variability of lithology, sedimentary structures and depositional environments. The locations of the reference sections upon which our eustatic curve is based are indicated in Figure 4. These sections and associated wells and outcrops have been described in detail in published and unpublished reports (Gerasimov, 1962; Gerasimov, 1969; Krymholts, 1972; Olferiev, 1986; Olferiev, 1988; Sazonov, 1957).

Biostratigraphy. Biostratigraphic zonation is based primarily on ammonites, bivalves, forams, and palynomorphs (Baraboshkin, 1992; Baraboshkin and Mikhailova, 1987; Gerasimov, 1962; Krymholts et al., 1988; Mesezhnikov, 1984; Mitta, 1993; Naidin et al., 1984; Sazonov, 1957). The traditional approach taken by Russian geologists for subdivision of Russian Platform stratigraphy was strictly biostratigraphic at the stage and zone level (Gerasimov, 1971; Sazonov, 1957). More recently, Olferiev (Olferiev, 1986; Olferiev, 1988) subdivided units into formations based on lithostratigraphy (and constrained by biostratigraphy). This is the approach of the present study. Data were obtained for this study from wells, cores, and correlated outcrops throughout the central part of the Russian Platform (Figure 4).

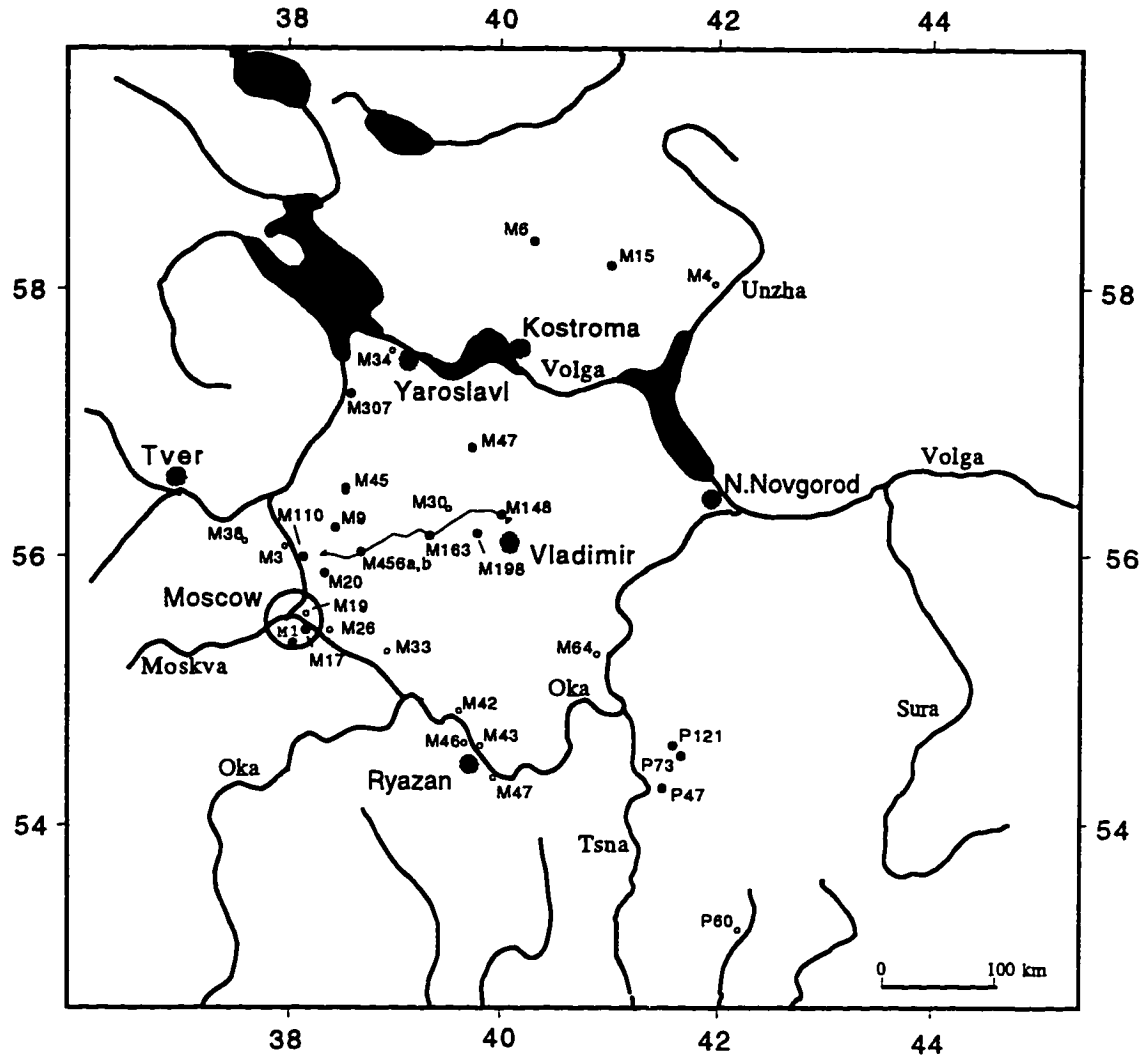

Figure 4. Locations of the main wells and outcrops used in the composite curve.

• - wells; ◦ - outcrops. ⌒ - cross section line

M1 - Teplyi Stan
M3 - Volgusha
M4 - B.Korovitsa (Unzha)
M6 - Yurino
M9 - Vorokhobino
M15 - Galich
M17 - Kolomenskaya
M19 - Khodynka
M20 - Tsernskoe
M26 - Kotelniki
M30 - Eza
M33 - Lopatino
M34 - Krest
M38 - Gavrilkovo
M42- Alpatievo
M43 - Novoselki
M45 - Skovorodino
M46 - Kuzminskoe
M47 - Yuriev-Polskii
M64 - Elatma
M110 - Paramonovo
M148 - Shikhobolovo
M163 - Savelievo
M198 - Boristsevo
M307 - Uglich
M456 - Varavino
P47 - Prosandeevka
P60 - Vorona
P73 - Lasitskyi ovrag
P121 - Lasitsy

Sequence stratigraphy. The sequence stratigraphy of the central Russian Platform generally consists of stacked transgressive and highstand systems tracts, as lowstand and lower parts of transgressive systems tracts were not generally deposited (Sahagian and Holland, 1991). This is due to the elevation and flat hypsometry of the Russian Platform, which experienced marine deposition only during eustatic highs. During sea-level lowerings lowstand deposits (such as, probably, stranded wedges that are typical for low gradient ramps) accumulated in deeper parts of the basin beyond the area of study. Absence of sandy lowstand units can also be explained by the concept of forced regression (Emery and Myers, 1996; Posamentier et al., 1992) that suggest significant acceleration of regression during sea-level falls with decrease of hypsometric gradient. In case of Moscow Depression, where the gradient is generally less than 0.2, rapid shoreline retreat accompanied every sea-level fall resulting in exposure of vast areas. At the same time, it is noticeable that no incised valley fill sediments have been found associated with regional erosional unconformities (sequence boundaries). This may suggest that no significant river systems existed on the area of study during the deposition. Rates of sediment supply were extremely slow, as a result.

Sediment sources. During times of highstands, the only clastic sources in the vicinity of the Moscow Synclise were the Urals, the Baltic Shield, Caledonides, and the Bohemian and other massifs to the southwest (Milanovsky, 1987; Ziegler, 1982), all at great distances. During times of slightly lower sea level, when these primary sources were still some distance from the shoreline on the Russian Platform, the dominant clastic source was redeposition of previously deposited material (Gerasimov, 1962). This recycling of sediment may have contributed to the transport of sands and their broad distribution across the Russian Platform, despite the lack of nearby primary clastic sources (Caledonides, Urals, etc.). Many examples have been found of faunas from several stages mixed together in redeposited strata on the Russian Platform. For instance, transgressive

beds at the base of Kostromskaya Formation (Middle Volgian) contain phosphorite pebbles of four generations. Many of these concretions contain well preserved ammonites which makes it possible to identify their ages. The oldest generation is present in the areas where transgressive Kostromskaya beds overlay Oxfordian clays of Alternans beds. In this case phosphorite pebbles reveal ammonites of *Amoeboceras alternans* group that are typical for Upper Oxfordian. Two other generations of phosphorites contain Early and Late Kimmeridgian ammonite complexes. The youngest generation includes rough surfaced concretions with ammonites that are characteristic for *Dorsoplanites panderi* Zone. It is noticeable that phosphorite pebbles of older generations are characterized by well polished (result of wave action) surfaces which is, sometimes, marked by drilling mollusks and worms (Gerasimov, 1971).

Unconformities and time hiatuses. The strata of the central Russian platform are riddled with unconformities, often representing more time than the preserved strata which they bound. Because of the unconformities, only the sea level highstands are recorded in the stratigraphic record, and it is not known by how much sea level dropped during unconformities. It is clearly advantageous to be able to fill the gaps in the stratigraphic record to obtain a more complete sea-level record. This can be done by incorporating data from marginal subsiding basins, which have a more complete stratigraphic record. Stratigraphic data from the adjacent basins are chosen for their completeness and reliability of stratigraphic correlation with the Russian Platform. In this study, we have filled the gaps left by unconformities on the Russian Platform with stratigraphic information from the more continuous stratigraphy of the neighboring subsiding regions such as northern Siberia and Ryazan-Saratov Trough. The biostratigraphic correlation between N. Siberia and Russian platform stratigraphy is not straightforward (the Urals are between), but has been clearly established to the level of zonal resolution (Krymholts et al., 1988; Sachs, 1976). Northern Siberian stratigraphy is described in the other chapter,

and so, will not be repeated here. The data from the western part of the nearby Ryazan-Saratov Trough were incorporated directly for the lowermost Aptian and upper Bajocian-Bathonian, because the similarity of overlying and underlying intervals to correlative intervals of the Moscow Depression suggests no significant subsidence during the short incorporated intervals. We have thus compiled a more complete eustatic curve than would be possible on the basis of Russian Platform stratigraphy alone. Stratigraphic descriptions of all the supplementary sections (North Siberia and Ryazan-Saratov Trough) as well as the most representative ones from the Russian Platform are available for reader in the Appendix.

Stage by Stage Stratigraphy The stable region of the Russian Platform (Moscow Synclise) includes the provinces of Moscow, Tver, Kostroma, Yaroslavl, Ivanovo, Vladimir, and Ryazan. Many of the sections are very thin and stratigraphically incomplete. Although each individual stratigraphic section includes only a portion of the Mesozoic section, a relatively complete composite section can be compiled from numerous sections throughout the stable region (Figures 5, 6). This provides the most reliable framework for building a eustatic curve.

Jurassic System

The Jurassic of the Russian Platform is represented by only clastic sediments such as sands, silts, clays, and bituminous shales and clays (Figure 5). Various facies are indicated including lagoon, shoreface, offshore and deeper marine. Minerals such as phosphorite and chamosite (often confused with glauconite in the Russian literature) are ubiquitous throughout the marine section. The average thickness of preserved Jurassic deposits is 120-140 m.

Traditionally, it has been thought that the oldest marine section on the Russian Platform was Callovian. However, more recently, upper Bajocian fauna including

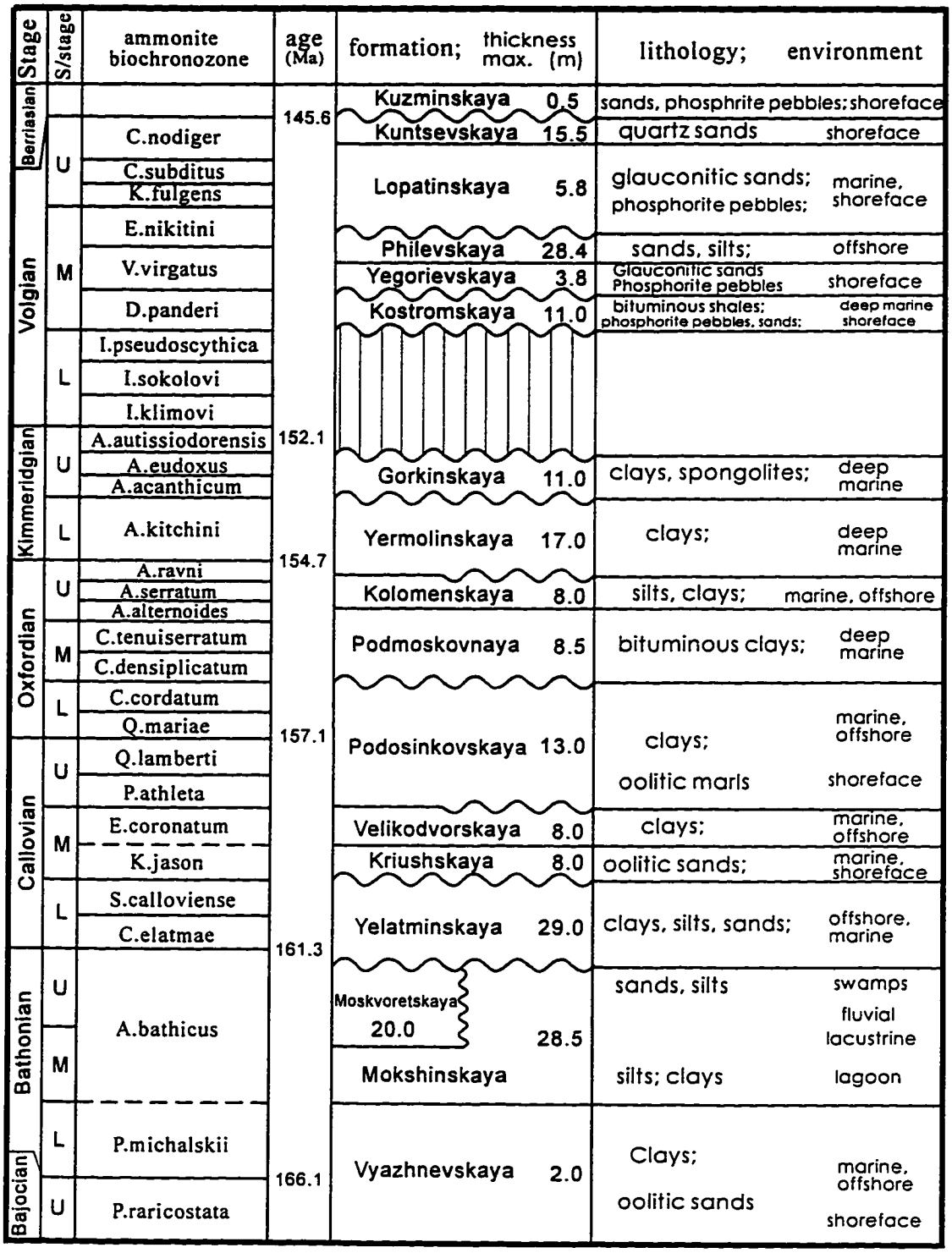

Figure 5. Middle and Upper Jurassic stratigraphy of the central Russian Platform

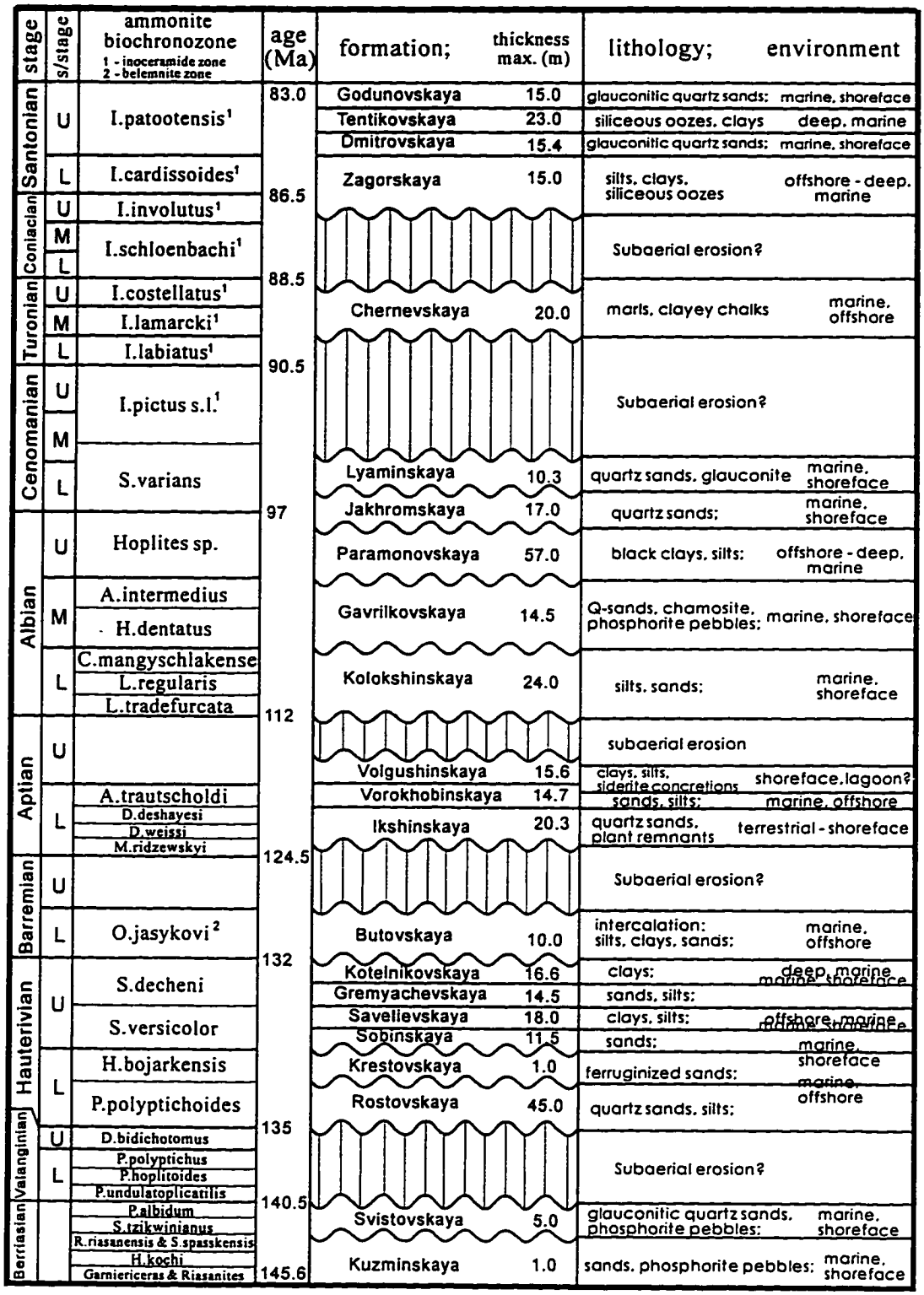

Figure 6. Cretaceous stratigraphy of the central Russian Platform

Parkinsonia doneziana Bor. and forams (*Lenticulina volganica*) were discovered from a well M121 in the basal oolitic sands of the Vyazhnevskaya Formation (Figure 5) in the western Ryazan Saratov trough (Olferiev, unpubl. data; Meledina, 1994 #70]. The upper portion of Vyazhnevskaya Formation consists of clays and is assigned to Lower Bathonian (Figure 5). The conformably overlying mid-upper Bathonian Mokshinskaya Formation is represented by intercalated lagoonal and lacustrine sands, silts and clays, and dated by forams (*Ammodiscus colchicus Thod.*), bivalves (*Meleagrinella aff. doneziana Bor.*), and palynomorphs (Olferiev, 1986).

The Elatminskaya Formation is composed of a coarsening upward succession of clays, silts and sands. The contact between the Mokshinskaya and Elatminskaya is an erosional unconformity overlain by an accumulation of belemnite fragments and pyritized wood. The Elatminskaya Formation has been considered a typical transgressive-regressive cycle (Olferiev, 1986). The lower part of Middle Callovian is represented by poorly sorted sands and silts with abundant iron oolites of the overlying Kriushskaya Formation. This distinct unit is characterized by uniform thickness and is often used as a marker bed for correlation. The Kriushskaya is conformably overlain by clays with abundant bivalves *Posidonomya buchi (Roem.)* of the Velikodvorskaya Formation which comprises the upper part of Middle Callovian section. The Kriushskaya is a transgressive deposit, whereas the Velikodvorskaya was formed during highstand and subsequent sea-level fall (Olferiev, 1986).

The overlying Late Callovian to Early Oxfordian Podosinkovskaya Formation consists of a basal oolitic marl overlain by light gray clay. The contact between the Podosinkovskaya Formation and the Velikodvorskaya is unconformable in many locations. No visible boundary exists between the Callovian and Oxfordian in well or outcrop sections (Unzha River near Makarievsk and Ryazan Province).

The Podmoskovnaya Formation (middle to upper Oxfordian) is represented by fine-laminated bituminous clays and shales with abundant ammonite fauna. The erosional

unconformity between the Podosinkovskaya and Podmoskovnaya Formations is widespread, extending across and beyond the Moscow Depression (Olferiev, 1986). The gray silty clays of the Late Oxfordian Kolomenskaya Formation conformably overlie the Podosinkovskaya Formation, but lenses of coarse sand and accumulations of bivalve and gastropod shells in the basal part suggest a shallowing event at the boundary of the two formations.

The Ermolinskaya Formation overlies the Kolomenskaya with an erosional unconformity in some places, and conformably, but with evidence of shallowing such as basal coarse-grained layers in others. It is generally composed of dark-gray to black clays with abundant pyrite nodules and sparse fossils.

The Upper Kimmeridgian has not been investigated in as much detail as have other parts of the Jurassic section because it has been almost completely removed by erosion, being adequately preserved in only several small areas in the Moscow depression (e.g. near Gorki village, Vladimir province). The Gorkinskaya Formation unconformably overlies the Ermolinskaya Formation and consists of dark clays with spongeolites and shell detritus. The Upper Kimmeridgian age of the unit corresponds to the *Aulacostephanus eudoxus* Zone (Gerasimov, 1971).

The presence of biostratigraphically defined Lower Volgian is reported only from the Kostroma province where calcareous silty clays (3.5 m) have been encountered in wells. The age of the clay is indicated by forams (*Pseudolamarckina polonica (Biel. et Pos.), Planularia polenovae Kuzn., Marginulina gluschisaensis Dain.*) but no ammonites have been encountered (Olferiev, 1986). Throughout most of the region however, the Middle Volgian overlies various Upper Jurassic strata with a significant erosional hiatus (Figure 5). The Middle Volgian is widespread throughout the Moscow Depression and is characterized by several marine facies that are represented by four middle Volgian formations (Figure 5). The fine-laminated bituminous shales and clays of the Kostromskaya Formation overlie a basal layer of coarse glauconite sands containing

numerous redeposited phosphorite nodules with ammonites of different ages including Upper Oxfordian, Kimmeridgian, and Middle Volgian. It should be noted that there is no lower Volgian fauna present in this layer.

The Egorievskaya Formation that unconformably overlies the Kostromskaya Formation consists of fine-grained glauconite sands with phosphorite nodules and pebbles. The gray-black clay-rich sands and silts of the Philevskaya Formation overlie the Egorievskaya Formation with no sign of sedimentary interruption. The Egorievskaya is interpreted to represent transgressive deposition, and the Philevskaya highstand and regressive deposition (Olferiev, 1986).

The Lopatinskaya Formation unconformably overlies the Philevskaya and is represented by very homogenous gray-green fine quartz-glauconite sands with an abundance of sandy phosphorite nodules in the upper part. The top of the Jurassic section is observed in outcrop in the vicinity of Moscow, and consists of a thick section of white fine well-sorted quartz-glauconite sands with phosphorite pebbles of the Kuntsevskaya Formation (Gerasimov, 1969).

Cretaceous System

Cretaceous strata of the Moscow Depression have an average thickness of 260-290 m. The section includes several significant erosional hiatuses (Figure 6) that developed local relief which was filled during subsequent transgressive episodes (Figure 7). The marine Cretaceous of the Russian Platform begins with the Berriasian stage (Ryazanian). Ryazanian and boreal Berriasian are used synonymously in the Russian literature. The relationship of boreal Berriasian biozones to Tethyan biozones and the position of the Jurassic/Cretaceous boundary is a separate problem which has been debated for over 30 years (Krymholts, 1984; Sachs, 1975) and will not be addressed here.

The most complete sections of the Berriasian are in the southern part of the Moscow Depression in the Oka River basin. At this locality there are two formations that include the lower Kuzminskaya which include two beds of phosphorite sandstone, separated by chamosite sands, all of very shallow marine facies (Figure 6). The Svistovskaya Formation in some places overlies the Kuzminskaya Formation with erosion. It is represented by chamosite sands with abundant phosphorite concretions and pebbles in the lower part (Olferiev, 1988).

The Valanginian is absent in most of the Moscow Depression. Thin fragments of Lower Valanginian are found in only two places in the Kostroma province, and in the northern part of the Oka-Don lowland (Ryazan province) where it unconformably overlies the Svistovskaya Formation. Because there is no useful Valanginian section, we do not discuss Valanginian stratigraphy of the Russian Platform. We have instead filled this gap using the more complete northern Siberian sections along the Boyarka River (Zakharov and Judovnyi, 1974).

The overlying Hauterivian section is very well represented in the central part of the Moscow Depression (Moscow and Vladimir provinces) and is divided into six formations. The Rostovskaya Formation (Figure 6) is composed of predominantly fine-grained quartz sands and sandstones that overlie various Cretaceous and Jurassic strata with an erosional unconformity. The thin Krestovskaya Formation is composed of ferruginous sands with characteristic (possibly endemic) ammonite genera: *Pavlovites, Subspeetoniceras, Gorodzovia.* The thin layer of poorly sorted coarse sand indicates shallowing that occurred at the beginning of Krestovskaya time. A subsequent sea level fall resulted in an extensive erosional unconformity throughout the entire Moscow depression at the Lower/Upper Hauterivian boundary.

The overlying four formations reflect the transgression of Late Hauterivian sea. The basal beds are composed of sands of the Sobinskaya Formation that fill depressions and the incised valleys of the eroded surface. The overlying clays and silts of the

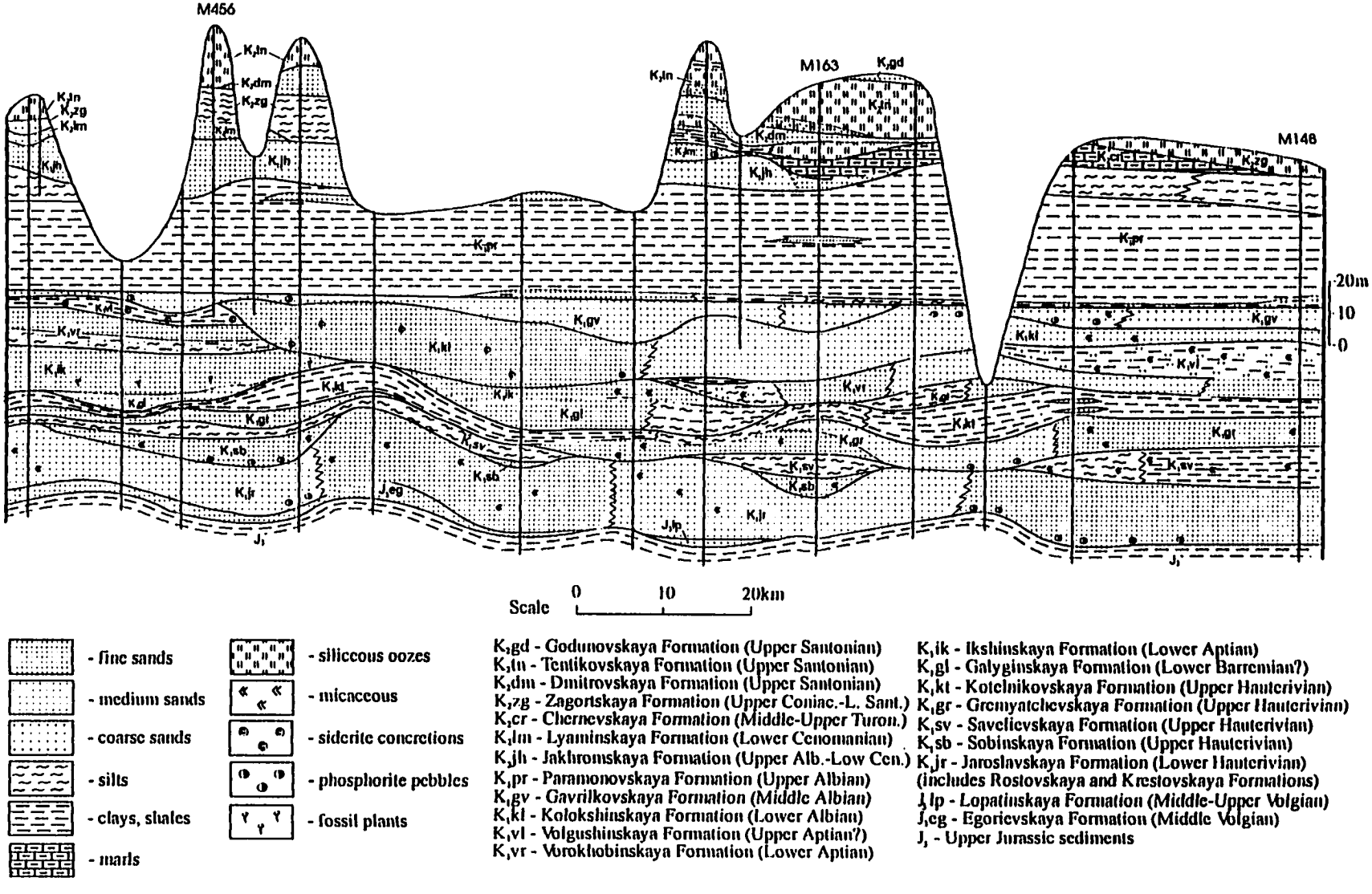

Figure 7. Cross-section of Cretaceous strata of the central part of the Russian Platfrom

Savelievskaya Formation and shoreface sands and silts of the Gremyachevskaya Formation spread more uniformly across the region. The dark-gray clays and silts of the Kotel'nikovskaya Formation are the most widespread, and probably represent the highest sea-level stand in the uppermost Hauterivian. Sands and silts of the lower Barremian Butovskaya Formation conformably overlie the Kotelnikovskaya formation. The Upper Barremian is absent from the Moscow Depression and represents an erosional hiatus throughout the region.

The earliest marine Aptian sediments in the central part of the Russian Platform are documented in the western Ryazan-Saratov trough where unsorted sands and silts fill incised valleys. The Aptian in the Moscow Depression includes three formations. The lowest is the Ikshinskaya which unconformably overlies Carboniferous, Jurassic and Lower Cretaceous strata. It is composed of quartz sands with abundant fossil flora, and grades upward from terrestrial to lagoonal and finally marine sediments. There is a gradual transition from the Ikshynskaya to the Vorokhobinskaya Formation which is composed of offshore marine sands, silts and clays. The overlying Volgushinskaya Formation of Late Aptian Age is composed of shoreface to lagoonal clays and silts with siderite concretions. The Volgushinskaya includes Aptian-Albian spore and pollen assemblages and is assigned to the Upper Aptian based on its position in the section.

Significant regression occurred in the second half of upper Aptian that resulted in erosion of the upper contact of Volgushinskaya Formation. On the entire Russian Platform the marine uppermost Aptian is present only in the Caspian depression and some small areas of the eastern part of Ulyanovsk-Saratov Trough. In the other parts of the Platform this interval is characterized by a significant erosional hiatus (Sazonova, 1958), suggesting one of the most significant sea level falls of the Lower Cretaceous on the Russian Platform.

The lower Albian is represented by the Kolokshinskaya formation of light purple silts and sands with ammonites and palynomorphs (Baraboshkin, 1992). The

unconformably overlying middle Albian Gavrilkovskaya Formation is composed of offshore marine glauconite quartz fine and medium sands with phosphorite nodules (Baraboshkin and Mikhailova, 1987). Shallowing and subaerial exposure occurred in the uppermost Middle Albian which is indicated by an unconformity and mudcracks at the top of Gavrilkovskaya Formation.

The clays of the Paramonovskaya Formation consists of three parts from base to top: 1) intercalations of sands and silts with basal coarse sands; 2) massive silts and black clays; and 3) silts and sands. The Paramonovskaya Formation is the thickest Lower Cretaceous unit preserved in the Moscow depression (up to 57 m) and represents the time of highest Lower Cretaceous sea level. The Late Albian age of the Paramonovskaya is indicated by radiolarians and forams.

The green-gray fine glauconite shoreface sands of the Jakhromskaya Formation overlie the Paramonovskaya clays with an erosional unconformity having relief of up to 20 m. The Lyaminskaya Formation consists of shoreface fine glauconite quartz sands with quartz gravels and phosphorite pebbles. In some places, the Lyaminskaya overlies the Jakhromskaya with some evidence of erosion (Olferiev, 1988).

A large stratigraphic gap includes the Middle Cenomanian to Lower Turonian. The gap is manifest as an erosional unconformity throughout the Moscow Depression, but has been identified as a condensed section on the Voronezh Arch and the eastern Ulyanovsk-Saratov Trough (Naidin, 1981). The Middle-Upper Turonian overlies the unconformity and consists of marls of the Chernevskaya formation. There is another gap in the Lower Coniacian (Figure 6). We have bridged both of these gaps with stratigraphic data (Zakharov et al., 1989a; Zakharov et al., 1989b) from the Ust-Yenisey depression of northern Siberia (Sahagian and Jones, 1993; Sahagian et al., 1994).

The upper Coniacian Zagorskaya Formation unconformably overlies the Albian, Lower Cenomanian, and Middle-Upper Turonian. In the western Moscow Depression (Moscow province), it is composed of intercalated quartz glauconite shoreface sands and

silts with radiolarians. To the east (Vladimir province), it consists of offshore deep marine silicic clays, tripoli, and silts with radiolarians of Late Coniacian and Early Santonian age. The unconformably overlying Dmitrovskaya Formation consists of quartz glauconite shoreface sandstone. The Tentikovskaya Formation also overlies an erosional unconformity, and is composed of offshore to deep marine silts and siliceous oozes. The upper Cretaceous section of the Moscow Depression is capped by the quartz glauconite sands and sandstones of the Godunovskaya Formation, which unconformably overlie the Tentikovskaya Formation. The Godunovskaya Formation is preserved only in the central part of the Moscow Depression. Its age is not clear, but it is conditionally placed in the Upper Santonian based on stratigraphic position. The Campanian and Maastrichtian are absent from the Moscow Depression probably due to subsequent (until present) subaerial erosion.

Northern Siberia

Tectonic setting

The sections specifically analyzed in this part of research are located in a large Mesozoic Yenisei-Lensky Trough. Tectonic development of this structure began in the Early Jurassic and continued to the end of the Cretaceous. The Siberian Craton flanks the Yenisei-Lensky Trough from the south, whereas the northern part of the Trough is bordered by Taimyr Upper Paleozoic folded area (Figure 8). The thick Jurassic-Cretaceous strata, that constrain sedimentary cover of the Yenisei-lensky Trough, overlie an erosional unconformity which caps various generally folded Permian and Triassic rocks. Thus, the overall structure of the region is similar to that of the West Siberian basin (Nalivkin, 1973).

Three large Depressions are separated from each other by basement uplifts and comprise the Trough from west to east. These include: Ust'-Yenisei, Khatanga, and Lena-Anabar Depressions (Figure 8). The two sections that we used for incorporation into the Quantified Eustatic Curve are the Upper Cretaceous of Ust'-Yenisei area and the Valanginian of Boyarka river. They are located in Ust-Yenisei and Khatanga Depressions, respectively. Ust-Yenisei and Khatanga Depressions have undergone different tectonic subsidence as indicated by different thicknesses of the Jurassic-Cretaceous complexes. For example, the general thickness of these rocks reaches 4800 meters in the Ust'-Yenisei Depression, whereas in the Khatanga Depression it does not exceed 2100 meters (Sachs et al., 1965).

Boyarka River Section

The Valanginian section of Boyarka river was specifically taken for incorporation into the Quantified Eustatic Curve because this stratigraphic interval is absent in most of the Moscow Depression. Thin fragments of the Lower Valanginian are found in only two places in the Kostroma province and in the northern part of the Oka-Don lowland (Ryazan province), where they unconformably overly the Berriasian Svistovskaya Formation.

We selected Boyarka as a reference section for its stratigraphic completeness, excellent biostratigraphy at zonal level, and presence of numerous paleodepth indicators. There are some other stratigraphically complete Valanginian sections in Northern Siberia including the mentioned above Nordvik section (Laptev Sea Coast) and Yatria river section of the Subarctic Urals (Golbert et al., 1972; Zakharov and Bogomolov, 1984). Both of them, however, have been formed in relatively deep water environments and, unlike the Boyarka section, do not exhibit cyclicity and do not contain abundant paleodepth indicators such as benthos, sedimentary structures, erosional surfaces, and many others.

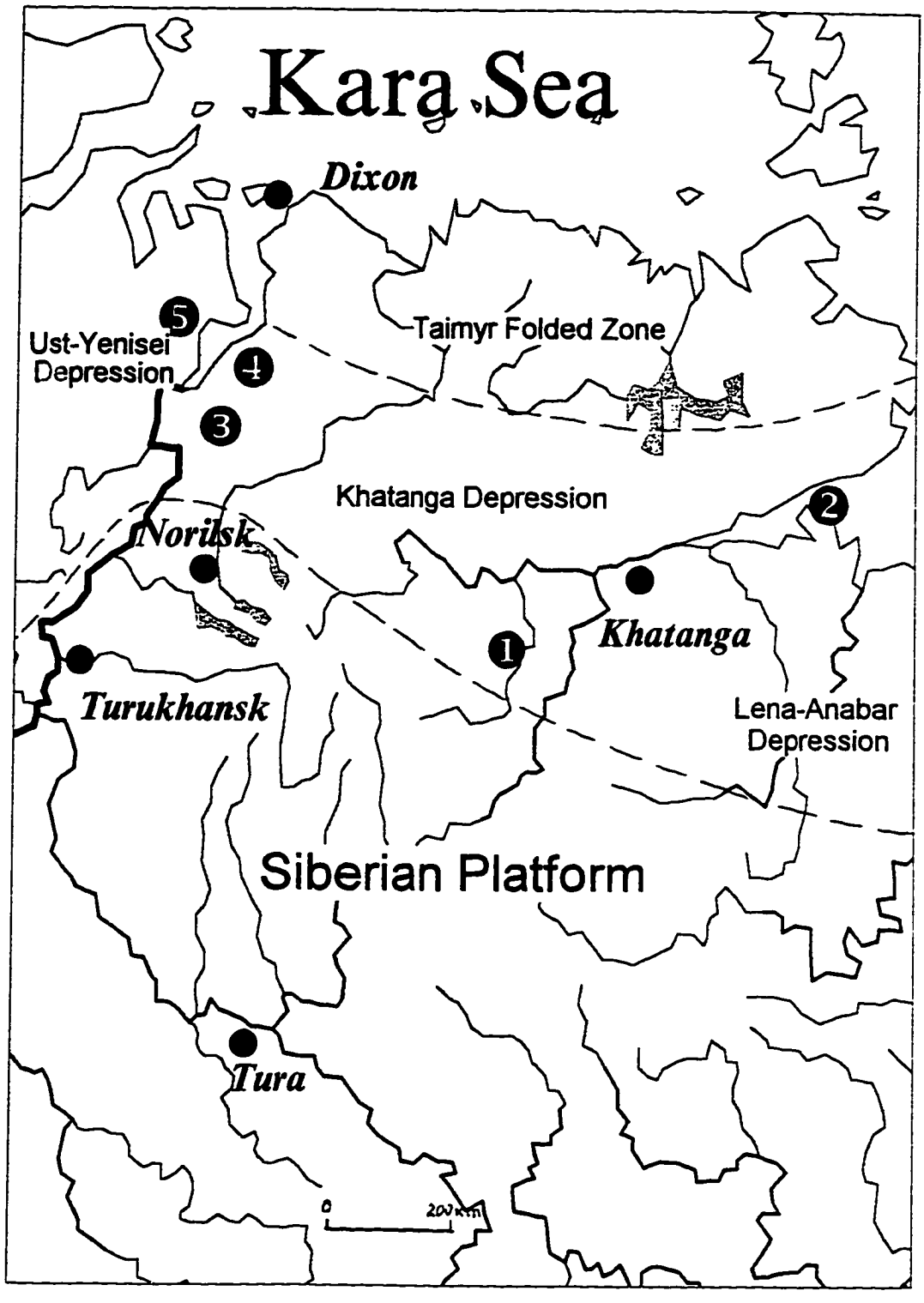

Figure 8. Locations of Study in the northern Siberia.
Lower Cretaceous sections: 1 - Boyarka River, 2 - Nordvik
Upper Cretaceous sections: 3 - Agapa, 4 - Yangoda, 5 - Tanama

General description. The Boyarka river section is located in the southern flank of the Khatanga Depression (Figure 8). It is exposed in several outcrops along the Boyarka river 20-30 kilometers north of the northern edge of the Siberian Craton. The marine section begins from Upper Oxfordian sediments that unconformably overlay Triassic basalts of the Siberian Platform. Marine conditions subsequently dominated through the Upper Jurassic and Neocomian to the Lower Hauterivian (*Homolsomites bojarkensis* Zone). From the Late Hauterivian, continental to lagoonal conditions persisted through the Late Cretaceous. This period of time is characterized by deposition of predominantly fine-grained coal-bearing sediments with plant flora. Marine Upper Jurassic-Neocomian rocks dip in the northern direction with gradient 1-7 °, and thus, the sections of younger age subsequently replace each other downstream, as the river flows to the north.

Marine Upper Jurassic - Neocomian sediments are represented by mostly unlithified terrigenous rocks such as various sands, silts, and clays. The section is characterized by ubiquitous macrofossils with excellent preservation which makes it particularly valuable for biostratigraphical and paleoecological investigations.

The Boyarka river section comprises the most proximal part of the Khatanga basin where deposition occurred in shallow marine conditions. This resulted in explicit cyclicity of the major part of the section as well as a presence of unconformities and stratigraphic hiatuses associated with them. However, the time spans of the hiatuses usually do not exceed one to a few biostratigraphic zones and the whole section is much more stratigraphically complete than that of the central Russian Platform. The deep sea equivalents of the Boyarka sections are exposed northeast on the Nordvik Peninsula of Laptev Sea Coast (Figure 8). In this area the whole section is condensed and is composed of dark marine shales and clays with abundant phosphorite concretions.

Depositional history and facies interpretation. During the Late Jurassic global transgression the marine conditions reached the area of Boyarka river in the Late Oxfordian. During the Late Jurassic time deposition occurred in predominantly quiet relatively deep water (50-100 meters) conditions (Sachs, 1969). During this period of time thick fine-grained strata (mostly clays) were deposited. The process of sedimentation was relatively stable, which is indicated by lack of erosional contacts and other evidence of shallowing. We consider that the depositional environment was deep enough that the Late Jurassic sea-level fluctuations (detected on the central Russian Platform) did not noticeably affect the processes of physical sedimentation. Indeed observations from northern Siberia indicate that during times of shallow water (0-50 m) the facies variations caused by a 20 m eustatic change are clearly recorded, for example, but as water depth increases (50-100 m), these facies variations become damped and are not reflected in observable sediments. We assume that during the Late Jurassic to Berriasian coarse-grained sedimentation was taking place south of the outcrops area as the accommodation space, created by tectonic subsidence and eustasy, was subsequently filled by prograding (possibly) sandy units. As a result, only fine-grained sediments could have reached the distal area of the outcrops. Subsurface geological data may clarify this assumption if a proper analysis (seismic, well-logging) is performed for the area of study.

By the Early Valanginian the accommodation was finally infilled and shallow marine conditions as well as sandy sedimentation reached the area. Deposition is characterized by evident cyclicity for this period of time. Erosional wavy contacts that bracket each cycle most likely resulted from submarine erosion by wave action in shallow marine conditions. At the same time, there is no evidence of subaerial exposure (Zakharov and Judovnyi, 1974). Thin layers of coarse unsorted sand with gravel and, sometimes, oolites comprise the bases of each cycle. These are subsequently overlain by predominantly

massive or horizontally laminated silts or clays that, in turn, are overlain by sands which are cross-bedded in many cases and contain abundant benthic fauna and trace fossils.

During the Valanginian the deposition in the Boyarka river section occurred in a normal shallow marine environment in wave-dominated systems. The oscillations of sea-level change resulted in frequent transgressions and regressions that occurred throughout the area, whereas the overall trend of sedimentation was regressive. We think that the main cause for high frequency sea-level variations was a global eustasy. During Jurassic-Cretaceous time the southern part of Khatanga Sea was a margin of the stable Siberian Craton. There is no evidence of any tectonic activity (rifting, intraplate stresses, etc.) that could potentially result in rapid local uplift or subsidence. This supports our interpretation of steady subsidence during the interval of study which should exhibit a straight-line trend on a relative sea-level curve. As such, after subtraction of tectonic subsidence, the final curve of sea-level change serves as a reliable representation of eustasy and was incorporated into the Russian Platform Curve for filling the Valanginian stratigraphic gap.

By the late Valanginian-earliest Hauterivian the simple land-connected shoreline, that previously dominated, changed to lagoonal-barrier shoreline. This is related to a transgression that occurred during the late Valanginian - initial Hauterivian as well as an increase of sediment supply rate. The Upper Hauterivian section consists of four depositional cycles (see Appendix) that are interpreted as an aggradational (or retrogradational) stack of parasequences. The fine-grained parts of cycles (parasequences) are generally composed of clays or silty clays with massive texture, low diversity benthic fauna, and lack of ammonites. The sandy portions consist of fine to medium sands which are cross-bedded in some parts, and contain abundant trace fossils. According to the interpretation of Zakharov & Judovny (1974) sedimentation occurred in

a system of open shore-parallel lagoons that were protected from the wave action by submarine bars or low barrier islands. This interpretation is supported by: 1) lack of marine cephalopods in clayey units, 2) burial in life position of large shoreface bivalves (*Boreionectes*) in sand layers (in open sea environment the valves would be displaced by wave action), and 3) presence of specific lagoonal fauna and low diversity. Sandy portions of parasequences represent bar and barrier island deposits, whereas fine-grained sediments were deposited further landward in lagoons (Zakharov & Judovny, 1974). This depositional situation is typical for late lowstand - transgressive systems tracts (Emery and Myers, 1996, Figure 2.16). In addition, the relative sea-level curve obtained from backstripping of 1D section shows sea-level rise for the late Valanginian - initial Hauterivian interval (Figure 13) which supports our interpretation of transgression. As a result, we interpret this interval as a latest lowstand to transgressive systems tract that is composed of aggradational to progradational stack of parasequences (cycles).

Summarizing, the Valanginian section of the Boyarka River was deposited in shallow marine environment under conditions of frequent 3rd order fluctuations of eustatic sea-level change. A significant regional transgressive phase began in late Valanginian-initial Hauterivian when a transgressive barrier island-lagoonal depositional system developed. The high order cyclicity of this part of the section probably represents local variations of sedimentation within the depositional system, but may also have resulted from global high order eustatic variations.

For the detailed description of the Boyarka section see Appendix.

Upper Cretaceous Sections.

The best Upper Cretaceous sections that provided data for filling the stratigraphic gaps of the central Russian Platform are located in the Ust-Yenisey depression (Figure 8). The most continuous and useful sections are exposed in the lower Agapa River (Upper

Cenomanian - Loewer Turonian), Yangoda River (Upper Turonian - Coniacian), and Tanama River (Santonian - Maastrichtian) (Zakharov and Khomentovsky, 1989; Zakharov et al., 1989a; Zakharov et al., 1986). Because the Upper Cretaceous section is exposed in several outcrops which contain overlapping portions of the section, a composite section (Figures 9, 10) was used for backstripping and incorporation into the Quantified Eustatic Curve.

A significant tectonic subsidence began in the Ust'-Yenisei Depression in Early Jurassic and continued through the Early Cretaceous. By the Late Cretaceous, however, the whole area was very slowly and uniformly subsiding (subsidence rates can be constrained by facies and stratal thicknesses, which are on the order of a few tens of meters per stage, or 1-5 m/m.y.). In the reference area at the margin of the Ust-Yenisey trough during the Late Cretaceous, subsidence appears to have been very slow and steady (as suggested by the thin and relatively uniform thickness of depositional units throughout the Upper Cretaceous). This is attributed to the influence of the relatively stable Siberian platform to which it is attached (Figure 8). It is thus inferred that stratigraphic architecture was controlled primarily by eustatically-forced transgressions and regressions and their associated facies migrations.

The Upper Cretaceous stratigraphy of the region suggests a terrestrial environment before a prominent transgression which began in the Late Cenomanian, establishing marine conditions. These marine sediments were terrigenous and were generally deposited in shallow water environments. The strata are relatively thin (450 m for the entire section), and very poorly lithified. The section is composed of mostly unconsolidated sediments with occasional lithified horizons which often represent sequence boundaries. In addition, glauconite and other iron and silicate minerals are abundant throughout the section, especially in the Upper Turonian, Coniacian, and

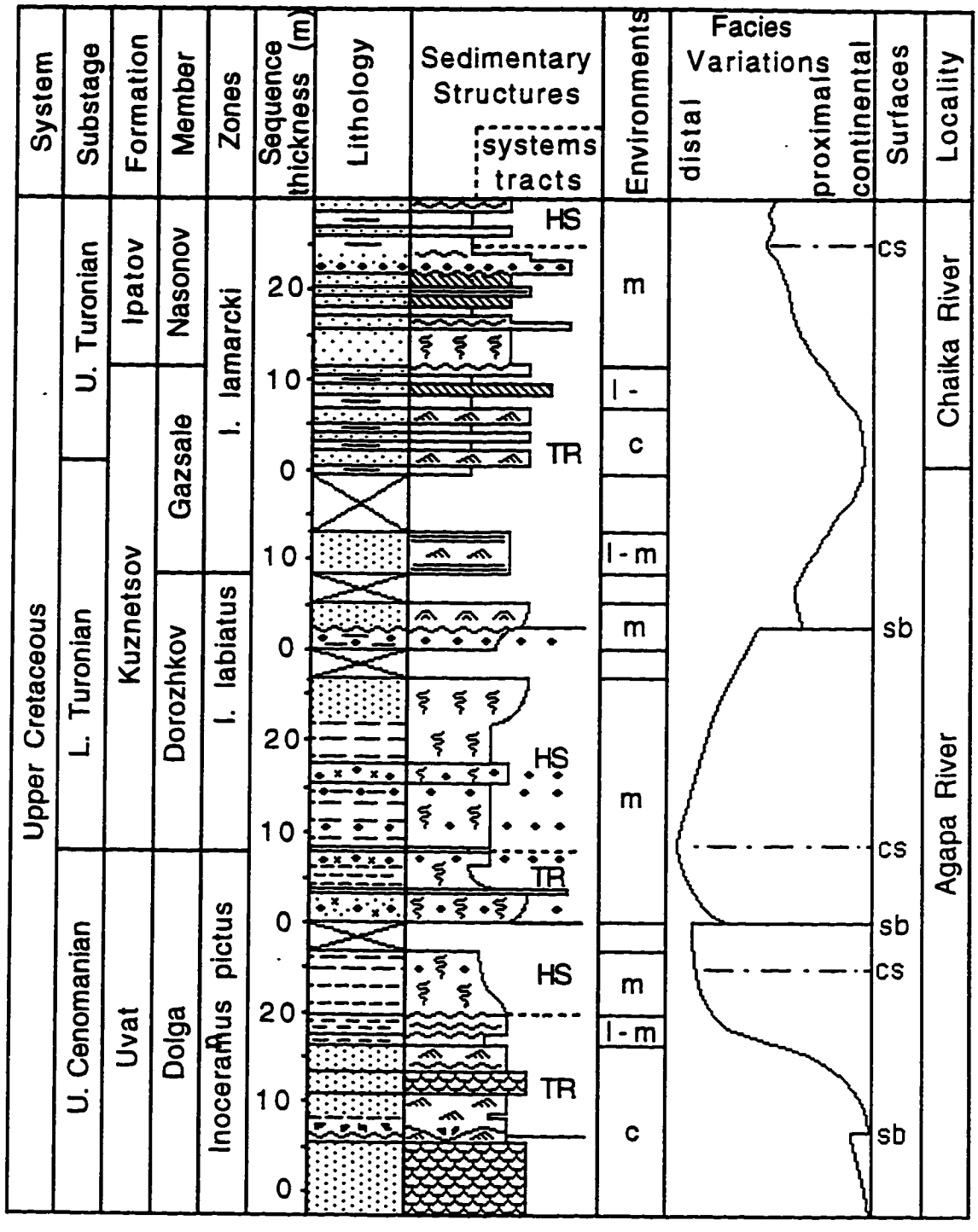

Figure 9. Facies and sequence stratigraphic interpretation of the composite Upper Cretaceous section of North Siberia (Cenomanian-Turonian)

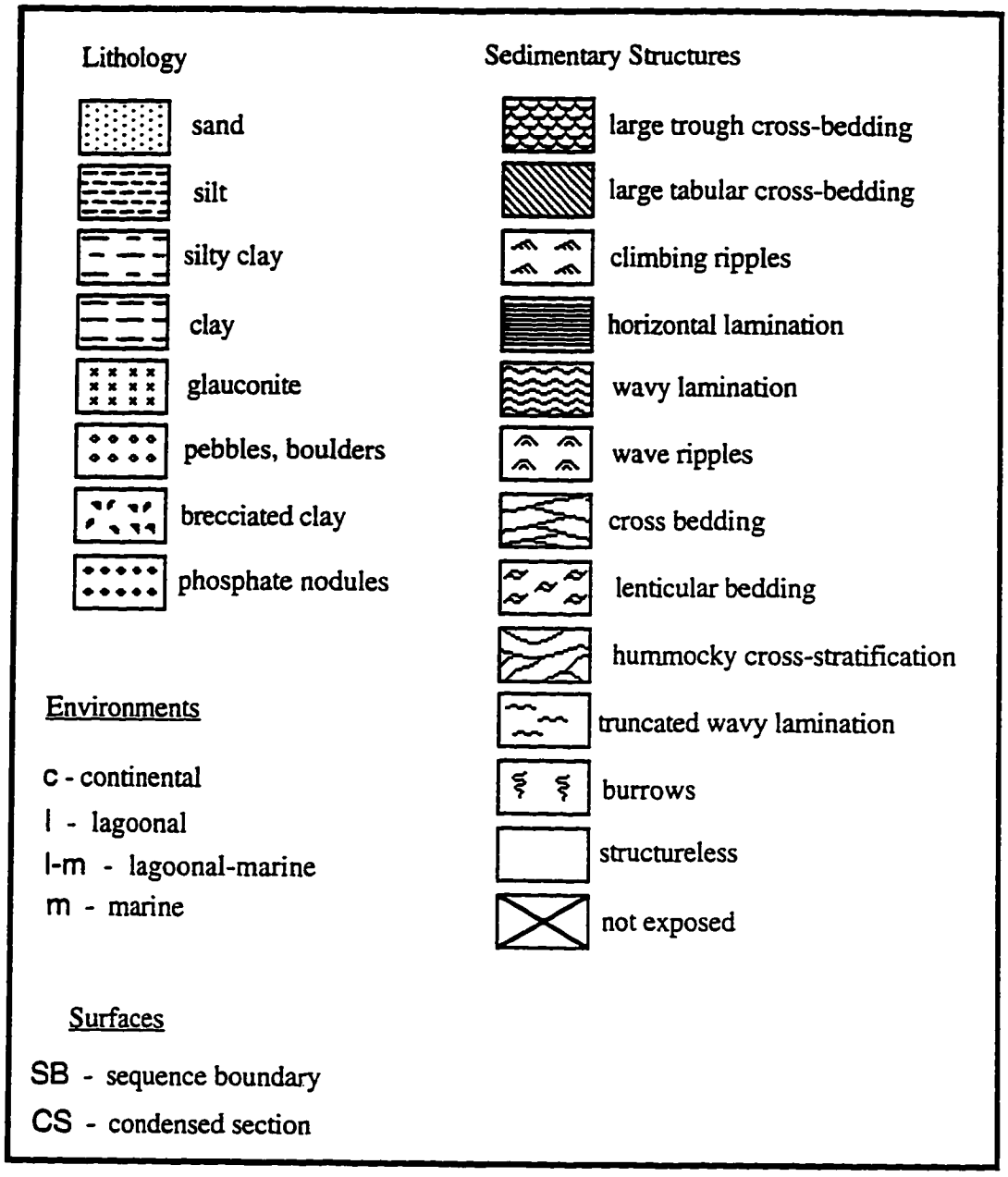

Figure 9. Continued (legend)

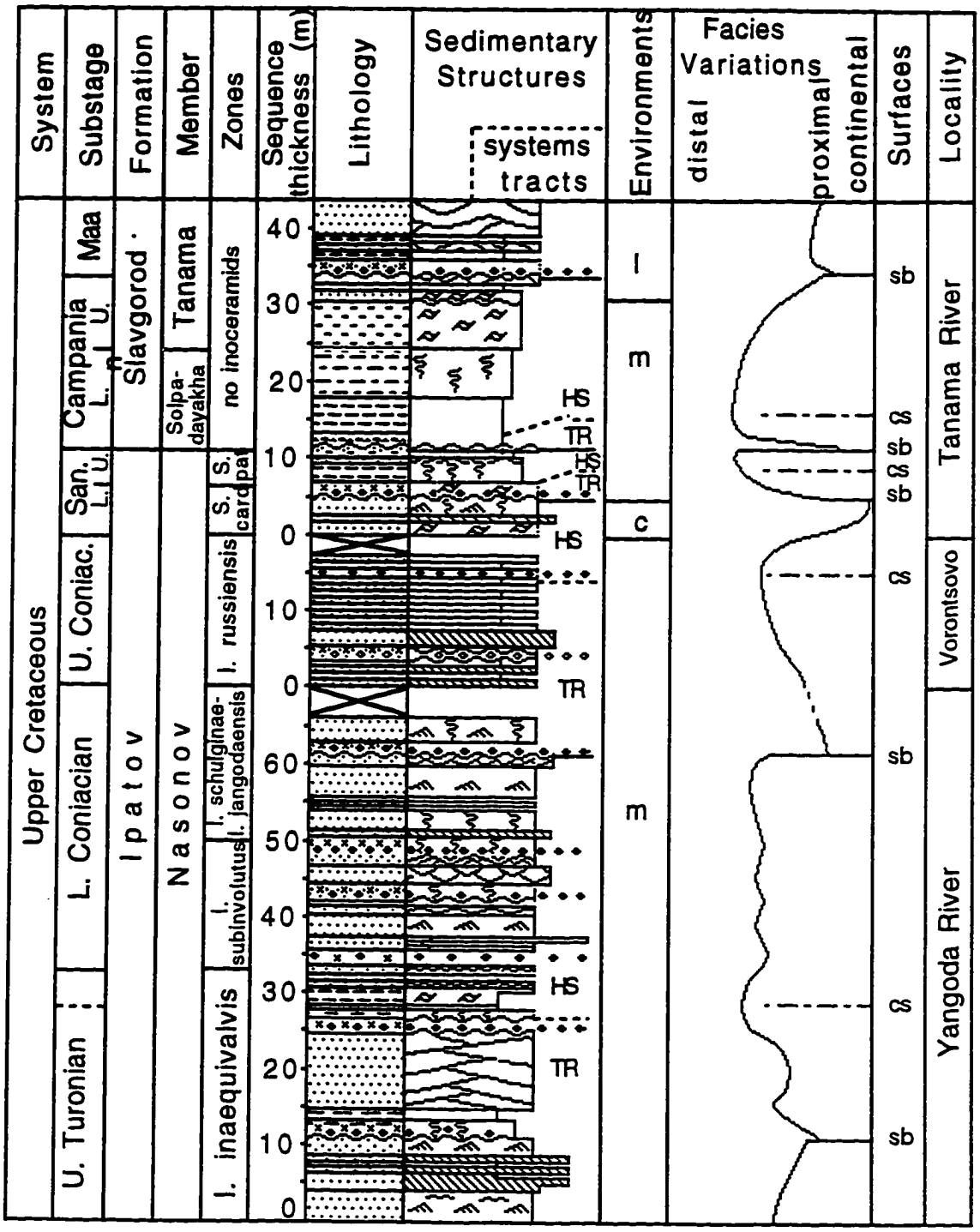

Figure 10. Facies and sequence stratigraphic interpretation of the composite Upper Cretaceous section of North Siberia (Coniacian-Maastrichtian). See Figure 9 for legend.

Santonian. Widespread clay beds are useful for inter-regional correlation of sea-level highstands (Cenomanian/Turonian boundary, uppermost Turonian). Stratigraphic units are areally extensive, and there is no evidence for deltaic sedimentation (above the Lower Cenomanian), valley fill deposits, barrier-lagoonal systems, or other localized depositional features. Consequently we assume that facies variations and sequence boundaries represent the relationship between eustasy and subsidence, but are not controlled by local variations in sedimentation.

Sequence stratigraphic analysis of the Upper Cretaceous sections is summarized in Figures 9 and 10. For the detailed description of the North Siberian sections see Appendix.

Water Depth Scheme

Water depth is an important component in the reconstruction of past sea-level variations, but it is difficult to estimate paleowater depth accurately for backstripping analyses. In the case of extremely slow subsidence and deposition rates, water depth variations may be the sole expression of eustasy. A basis is therefore necessary for the most accurate estimation of water depth possible, particularly when, as is usually the case on the Russian Platform, water depth variations for a given interval are of greater magnitude than sediment thickness of the same interval.

Many different methods have been attempted for paleowater depth reconstruction, but none are universally applicable (Benedict and Walker, 1978; Brett et al., 1993; Clifton, 1988; Eicher, 1969; Hallam, 1967). Most analyses use some form of geologic data (lithological, chemical, paleontological, etc.) and their typically associated water depths in modern marine environments. However, no universal model exists which takes

into account all environmental factors, nor is there a generally accepted scheme for environments of the shallow shelf. Consequently, any attempts to apply water depth schemes based on modern conditions to paleowater depth are limited by the differences in the relationships between water depth and the geologic indicators used for its estimation. In order to accurately determine paleo-water depth, it is necessary to account for all possible local factors including types and rates of sedimentation, climate, bottom geometries, tectonic conditions, etc. on the basis of all available geologic data.

Paleobathymetric model for the Jurassic and Cretaceous seas of the Central part of the Russian Platform. There have been a few attempts to estimate paleodepth on the Russian Platform (e.g. Sazonov and Sazonova, 1967). However, these have involved very low (100 m) depth resolution. For example, Sazonov and Sazonova grouped all Jurassic and Cretaceous facies of the entire Russian Platform into 2 "magnafacies" - shallow water (0-100 m), and deep water (100-200 m). In the present analysis we attempt to obtain the maximum possible depth resolution by developing a consistent quantitative model of water depth for the central Russian Platform.

The paleodepth model for Jurassic and Cretaceous seas of the Russian Platform is summarized in Figure 11. The model is based on the depths which correspond to deposition of different kinds of sediments, formation of sedimentary structures, mineralization, different kinds of taphonomic conditions, trace fossil distribution (ichnofacies), and bottom communities.

Contrasting levels of wave activity due to different geographic conditions in different basins result in significant variations in depth indicators. Wavebase, however, remains at a depth of half the wavelength. On the basis of several factors (e.g. size, shape, depth, etc.), the Mesozoic Russian Platform Sea can be compared to the present Baltic Sea. Observational and theoretical studies indicate that Baltic storm wave base is 20-30 m

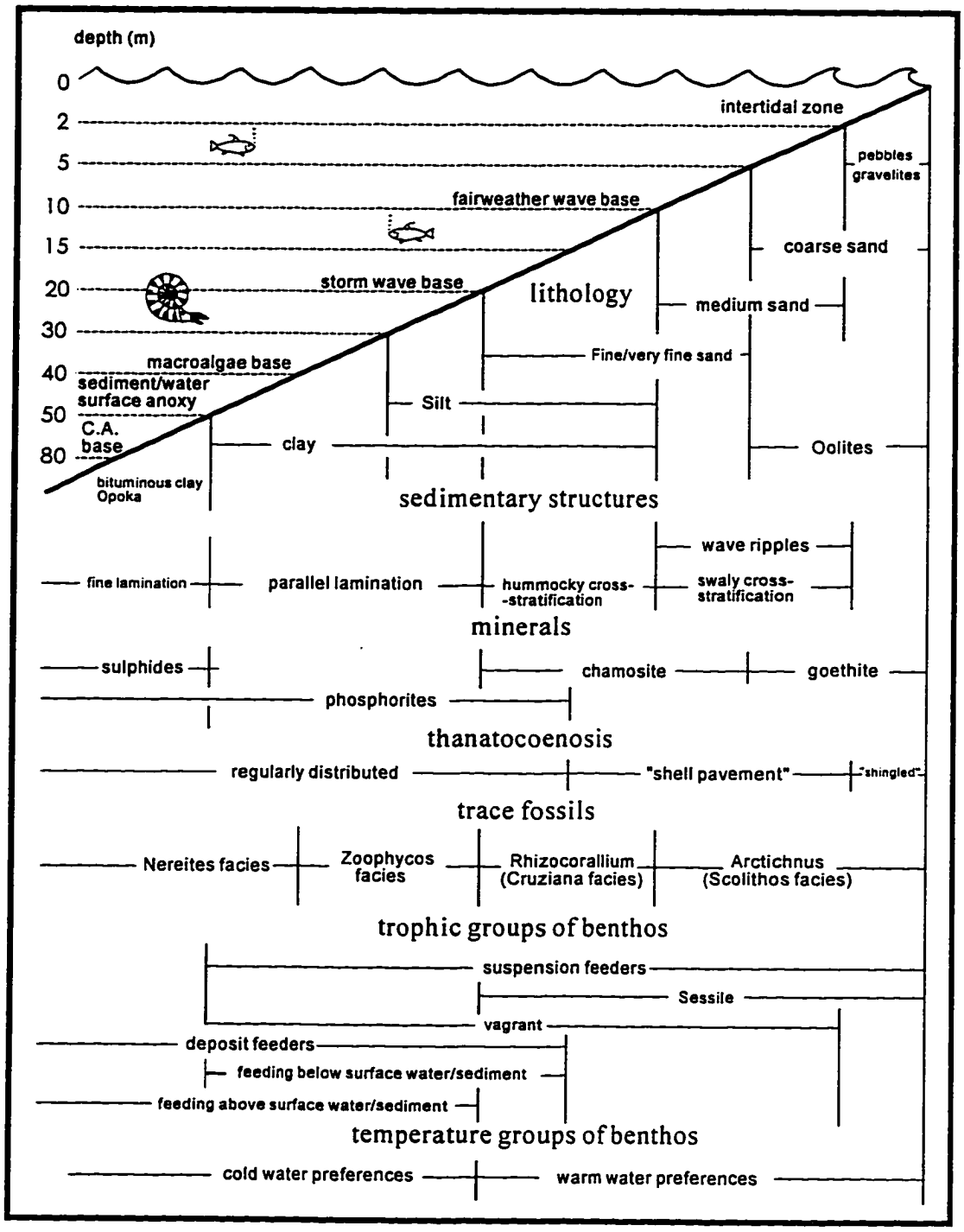

Figure 11. Paleodepth model for Jurassic-Creatceous seas of the central Russian Platform

(Zakharov, 1966). Mild Jurassic and Cretaceous climates may have had winds weaker than present (Hallam, 1985).

Unlike the Upper Cretaceous Seaway of the U.S. Western Interior, which has been interpreted as highly influenced by storms (Ericksen and Slingerland, 1990), the Mesozoic marine strata in the Moscow Depression do not exhibit evidence of significant storm activity (HCS and others). In addition, a computer-generated climatic model for Kimmeridgian-Volgian time (Moore et al., 1992) shows relatively low annual wind activity for the region of the Moscow Depresion. On the other hand, this model shows mid-latitude storm tracks through this area. We strongly doubt the storm-track result of this model mainly because of the presence of fine-laminated black shales in the Middle Volgian (*D.panderi* Zone) section of the Moscow Depression. The interpreted depth of deposition of these black shales does not exceed 60 meters, and therefore the effects of mid-latitude storms would have been evident in the preserved sediments. However, all the sedimentological features of the "panderi shales" suggest extremely quiet deposition. Either, these storms were not as severe as modern ones or the depths of black shale deposition were deeper than we interpreted.

As such, we take Jurassic and Cretaceous fair weather wavelength on the Russian Platform to be 20 m (wave base 10 m). The maximum wavelength for major storms would have been 40 m (wave base 20 m). Fair-weather wave base (5-15 m depending on local conditions), can be considered to divide sand-dominated shoreface sediments from mud-dominated offshore sediments (Walker and Plint, 1992). We thus define a relationship between lithology and water depth in our model.

The three main factors that bear on the distribution of sediments, benthic communities, trace fossils, minerals and chemistry are: 1) wave activity, 2) bottom water temperature, and 3) light.

It is generally accepted that clastic grain size on a shelf tends to get finer with distance from the shoreline, and thus, lithology is depth-dependent. However, the specifics of these relationships depend strongly on environmental factors. Lithology depends on the nature and distance of the clastic source, bottom geometry, climate, and many other factors which can vary widely between different basins. For example, sands may be found in distal parts of submarine fans at a depth of several hundred meters, whereas fine clay sedimentation may occur in lagoons at a depth of less than 1 meter. Despite the complexities, lithologic composition can be used as a form of depth indicator, if the environment is properly identified. The hypsometry of the Central Russian Platform (very low gradient ramp) eliminates any possibility of deposition of coarse sediments in deep water environments such as fan complexes. As such, we infer that no sand deposition occurred below storm-wave base. At the same time, deposition of fine sediments such as clays and silts may have occurred at very shallow depths in paralic environments such as lagoons, bays, and estuaries. In order to avoid possible mistakes, we analyzed paleogeographic position and identified areas of these paralic environments before paleodepth analysis of each stratigraphic section. The depth of deposition of fine sediments (clays and silts) in isolated parts of lagoons, estuaries, and bays was taken to be from 0 to 5 meters.

Sedimentologic evidence may provide important information for paleo-depth reconstruction, especially for shallow marine environments (Clifton, 1988). Sedimentary structures closely connected to wave activity include cross-bedding, swaley cross-stratification, and various types of wave ripples above fair-weather wave base. Parallel laminations and hummocky cross-stratification are predominant below fair-weather wave base, and fine laminations of sediments rich in organic carbon are normally found below storm wave base (Walker, 1984).

Oolites are chemically formed in warm oxygen-saturated turbulent shoreface water above fair weather wave base and are most abundant in depths of less than a few meters

(Kump and Hine, 1986). The abundance of iron oolites and oolitic marls in Jurassic and Cretaceous strata of the Moscow Depression make them an exceptionally useful paleobathymetric indicator.

Authigenic minerals (particularly iron group minerals and phosphates) form at specific depths. Goethite in tropical seas is formed in extremely shallow (0-10 m) water. Chamosite forms in shallow (10- 50m) very warm (up 20 °C) and active water. Glauconite is deposited at the deeper part of the shelf (150-250 m) at temperatures below 15 °C (Porrenga, 1967). Most recent investigators have interpreted a shallow water origin for phosphorites (30 -150 m) (Benedict and Walker, 1978; Bromley, 1967; Bushinski, 1964). Carbon is of particular interest as a paleodepth indicator because it is well preserved in anoxic sediments (Black Sea, Mediterranean Sea depressions, Norway fjords). Carbon is usually reduced with Fe^{+2} (marcasite, pyrite), which is present in sediment and is well preserved in rocks. The presence of sulfides in rocks indicates relatively deep water conditions (below storm wave base).

Benthic communities are useful depth indicators. There are regular patterns in the range of modern marine benthic communities with respect to the alternation of the suspension feeders and deposit feeders throughout the shelf zone (Zenkevitch, 1977). Two zones of suspension feeders can be defined parallel to the shoreline in turbid water along typical continental margins: one in shallow water near the shoreline, and the other in considerably deeper water at the shelf - slope boundary (shelf break). Deposit feeders, however, are concentrated in oxygen-poor water on the deeper shelf and slope (Zenkevitch, 1977). There is no strict bathymetric control on the distribution of modern bottom communities in boreal seas, but suspension feeders are generally found nearshore and deposit feeders offshore.

Trace fossils are used widely for paleodepth interpretation (Ekdale, 1988; Seilacher, 1967). Four ichnofacies are identified from the shoreline seaward, and include *Scolithos, Cruziana, Zoophycos,* and *Nereites*. The only two trace fossil facies which have been

considered depth-constrained are the shallow water *Scolithos* facies and the deeper *Nereites* facies (Seilacher, 1967). Other types of the ichnofacies can be found at different depths. In our model we used the approximation suggested by (Walker and Plint, 1992, Figure 1).

Taphonomic data based on marine invertebrates is useful for quantitative paleobathymetric interpretation for depths from 0 m to fairweather wave base. Depth is indicated by preservation, separation, selection and orientation of hard parts (bivalves, brachiopods, ostracods) (Yanin, 1983). Taphonomic investigation of bivalves in Peter the Great Bay of the Sea of Japan shows the following results: At depths of 0 to 5 m the species from different communities are mixed, the shells are broken, and there are the shell banks. At depths of 5 to 15 m, valves are separated and moved from life position. Occasionally the shells accumulate in spots and lenses. At depths greater than 15 m entire shells are buried in life positions (Evseev, 1981). Two types of accumulations are formed above fairweather wave base. The "Rose-type" or "shingled" is formed at the surf zone above 2.0 m (Zakharov, 1966; Zakharov, 1984). This type consists of a nested and vertically oriented accumulation of large valves. "Shell Pavement" is formed between 2 and 15 m by separate valves of bivalves (or Brachiopods) convex upward and lying in close contact with a cobblestone appearance (Maksimova, 1949).

We assume that the maximum depth of the light penetration to support macro-algae is 40 m and that temperature decreased with depth in the Mesozoic seas. Micro-algae (e.g. calcareous cyanophycean) can reach 80 m. These values are based on low water clarity in the Russian Platform seas interpreted from terrigenous fine grained sedimentation which predominated throughout the Jurassic and most of the Cretaceous.

Subaerial unconformities were assumed to represent at least some time of 0 water depth (exposure), unless further sea level fall could be estimated on the basis of the amplitude of subaerial incision.

Our generalized scheme is adapted for "normal" shallow marine systems and cannot be accurately applied to deltas, lagoons, estuaries, etc., and is subject to the vagaries of bottom relief, currents, and variations in sediment supply. Clearly, all local environmental factors must be taken into account before the model is applied. Because this paleodepth model was specifically constructed for the Moscow Depression epicontinental sea, it should not be applied to other environments and hypsometries, or errors will result. However, the methods by which the model was constructed can be applied to other times and places, and can be used to develop models specific to other basins or platforms.

We applied this model for Cretaceous sections of North Siberian Khatanga Sea (Boyarka, Agapa, and others). These sections were formed in proximal parts of the basin which exhibit very close characteristics (e.g. shape, hypsometry, size, and depths) compared to the Mesozoic sea of the central Russian Platform. As such, we considered that the paleodepth model can be applied unmodified.

Data Analysis

Data analysis consisted of four main parts: geological analysis, backstripping, comparison of the resulting sea-level curves, and error analysis.

Geological analysis

Geological analysis included examination of isopachs, lithology, facies, subsurface geometry, areal distribution, and finally, paleodepth interpretation for each stratigraphic unit. Over 70 wells and outcrops from this region were studied in detail and 32 were specifically used for constructing the composite curve (Figures 4, 12). Five main regional stratigraphic profiles and series of lithologic-paleogeographic maps were carefully

Series	Stage	Substage	Section used	Source
Upper Cretaceous	Santonian	Upper	M163,M47,M1	P121(Lasitsy), M456(Varavino), M45(Skovorodino), M1(Teplyi Stan), M17(Kolomenskaya), M307 (Uglich), M163 (Savelievo), M20 (Tsernskoe), M148 (Shikhobolovo), M15 (Galich), M110 (Paramonovo), M3 (Volgusha), M47 (Yuriev-Polskii), M6 (Yurino), M198 (Boristsevo), M34 (Krest) - - from "CentrGeologia" technical reports (unpublished)
		Lower	M9,M1,M456a	
	Coniacian	Upper	M9,M1,M456a	
		Middle	Yangoda River	
		Lower	Yangoda River	
	Turonian	Upper	M47,M163,M1	
		Middle	M47,M163,M1	
		Lower	Agapa River	
	Cenomanian	Upper	Agapa River	
		Middle	---------	
		Lower	M1,M456a,M163	
Lower Cretaceous	Albian	Upper	M1,M456b,M198,M110	
		Middle	M1,M38,M3,M9	
		Lower	M163,M30,P60,M3	
	Aptian	Upper	M1,M456b,M148	
		Lower	P121,P73,M1,M456b,M20	
	Barremian	Upper	---------	
		Lower	M1,M20	
	Hauterivian	Upper	M163,M1,M456b,M307	
		Lower	M456b,M15,M163,M34,M6	Yangoda River - Zakharov et al., 1989
	Valanginian	Lower	Boyarka river	
		Upper	Boyarka river	Agapa River - Zakharov et al., 1989
	Berriasian		M33,M46	M38 (Gavrilkovo), M3 (Volgusha) - Baraboshkin and Mikhailova, 1989
Upper Jurassic	Volgian	Upper	M33,M19,M26,M17	
		Middle	M4,M456b,M33,M19	M30(Eza),M60(Vorona) - Baraboshkin, 1992
		Lower	---------	
	Kimmeridgian	Upper	M456b,M17,M45	P73 (Lasitskyi ovrag) - Sazonov and Sazonova, 1967
		Lower	M456b,M4,M17	
	Oxfordian	Upper	M456b,M4,M45,M17	M34 (Krest) - Ivanov, 1968
		Middle	M456b,M4,M43,M45	
		Lower	M42,M456b,M4,M43	Boyarka River - Zakharov and Judovnyi, 1974
Middle Jurassic	Callovian	Upper	M64,M42,M456b,M4	M46 (Kuzminskoe) - Mesezhnikov et al., 1978
		Middle	M64,M42,M456b	
		Lower	P121,M64,M4	M33 (Lopatino), M19 (Khodynka) - Gerasimov, 1972
	Bathonian	Upper	P121,P47	
		Middle	P121,P47	M64 (elatma), M42 (Alpatievo), M4 (B.Korovitsa), M43 (Novoselki), P47 (Prosandeevka) - Sazonov,1957
		Lower	P121,P47	
	Bajocian	Upper	P121	

Figure 12. Stratigraphic data sources used for construction of the Quantified Eustatic Curve

examined and subsurface stratal geometries and facies distributions throughout the region were analyzed. Part of the regional profile IV-IV is shown in Figure 7.

For each stratigraphic unit in any given location we identified environment of deposition in order to avoid mistakes during paleodepth analysis. As it was stated above, the paleodepth model can be accurately applied only to normal shallow marine environment or error will arise. Thus, before paleodepth analysis of each stratigraphic section, we identified areas of the development of depositional environment different from normal marine ones. These include paralic environments such as shallow lagoons, estuaries, bays, deltas, and in few cases, coastal plains. The depth of deposition of fine sediments (clays and silts) in lagoons, estuaries, and bays was assumed to be from 0 to 5 meters.

The final result of the geological analysis was a data base for use in backstripping routines which calculates values of sea-level change during time intervals.

Backstripping

In general, stratigraphy of sedimentary basins is controlled by three factors and their mutual interactions: tectonic subsidence, sedimentation, and eustasy. These are related through the backstripping equation.

$$T = \Phi\{(S^*(\rho_m-\rho_s)/(\rho_m-\rho_w)) - \Delta SL(\rho_w/(\rho_m-\rho_w))\} + \Delta Wd - \Delta SL$$

where

T= thermo-tectonic subsidence (water loaded) during some time interval

S* = decompacted sediment thickness deposited in time interval

$\rho_{m, s, w}$ = density of mantle, sediment, water

ΔWd = change in water depth during time interval

ΔSL = eustatic sea-level change during time interval

Φ = basement response function for flexural backstripping. Due to the thin and areally extensive Russian Platform strata, this could be assigned a value of 1 (Sahagian, 1988; Watts, 1989).

In order to solve the backstripping equation for its four variables, S*, T, ΔWD, ΔSL, we must have three additional "equations" or conditions on the variables to reduce the number of unknowns to one. Sediment thickness can be determined by direct measurement and thus specified in the backstripping equation. Water depth can be estimated on the basis of paleobathymetric analysis. This leaves tectonic subsidence and eustasy (ΔSL and T). Because of the tectonic stability of the Russian Platform, we set T to 0, and therefore, the number of unknowns is reduced to one that is eustatic sea-level change (ΔSL).

Summarizing, backstripping involves three primary variables obtained from stratigraphic data: 1) Thickness of each sedimentary unit, 2) reconstructed water depth of deposition, 3) lithology. These variables were used as input data for our simple Airy backstripping routine that accounted for compaction and loading of sediments and water and finally calculated the values of sea-level change (Angevine et al., 1990; Sahagian and Jones, 1993; Watts, 1988).

Coefficients from Angevine et al. (1990) were used for decompaction. A potential error can arise from assigning compaction coefficients to poorly sorted units with variable grain size such as sandy shales or silty sands. However, the thin nature and minimal overburden of Mesozoic strata makes decompaction and associated potential errors relatively small. Because thicknesses of individual depositional units were relatively constant across the stable part of the Russian Platform, a distance greater than the lithospheric flexural wavelength, Airy isostatic response to lithospheric loading is interpreted to be maintained. The compaction of the relatively thicker Paleozoic section is considered to be unaffected by the thin Mesozoic-Cenozoic overburden.

Backstripping resulted in a series of relative sea-level curves. However, we didn't conclude that each one represents a truly eustatic curve because of a potential errors involved. Consequently the final stage of the construction of the Quantified Eustatic Curve was comparison of the resulting curves and error analysis.

The way to fill stratigraphic gaps in the incomplete Russian Platform record is to incorporate data from continuous northern Siberian sections, as mentioned above. In order to accomplish this, we backstripped the appropriate intervals of northern Siberian data to generate relative sea level curves. The resulting curves, however, represent disparate relative sea-level curves, unlike those generated from the central Russian Platform. This is because significant subsidence accompanied deposition in the Northern Siberian sections. The explicitly tilted trend of northern Siberian sea-level curves (compared to the Russian Platform curves) supports the interpretation of tectonic subsidence in those sections (Figure 13). Tectonic subsidence is inferred as a straight line trend superimposed on higher frequency eustatic oscillations (Figure 13).

Curve Comparison and Error Analysis.

The individual relative sea-level curves from each well or section were compared to each other to check for inconsistencies. Most curves coincided with each other indicating close agreement in timing and magnitude of sea-level variations. Nevertheless, some curves exhibited minor deviations for some periods of time. These deviations were examined and the supporting data were scrutinized. Variations between curves were generally caused by uncertain depth interpretations, local erosion, and minor variations of sedimentation rates. Despite the minor differences, general agreement between the wells and outcrop sections analyzed supported the interpretation of a stable region in the Russian Platform, and further validated its use as a reference frame for eustatic quantification.

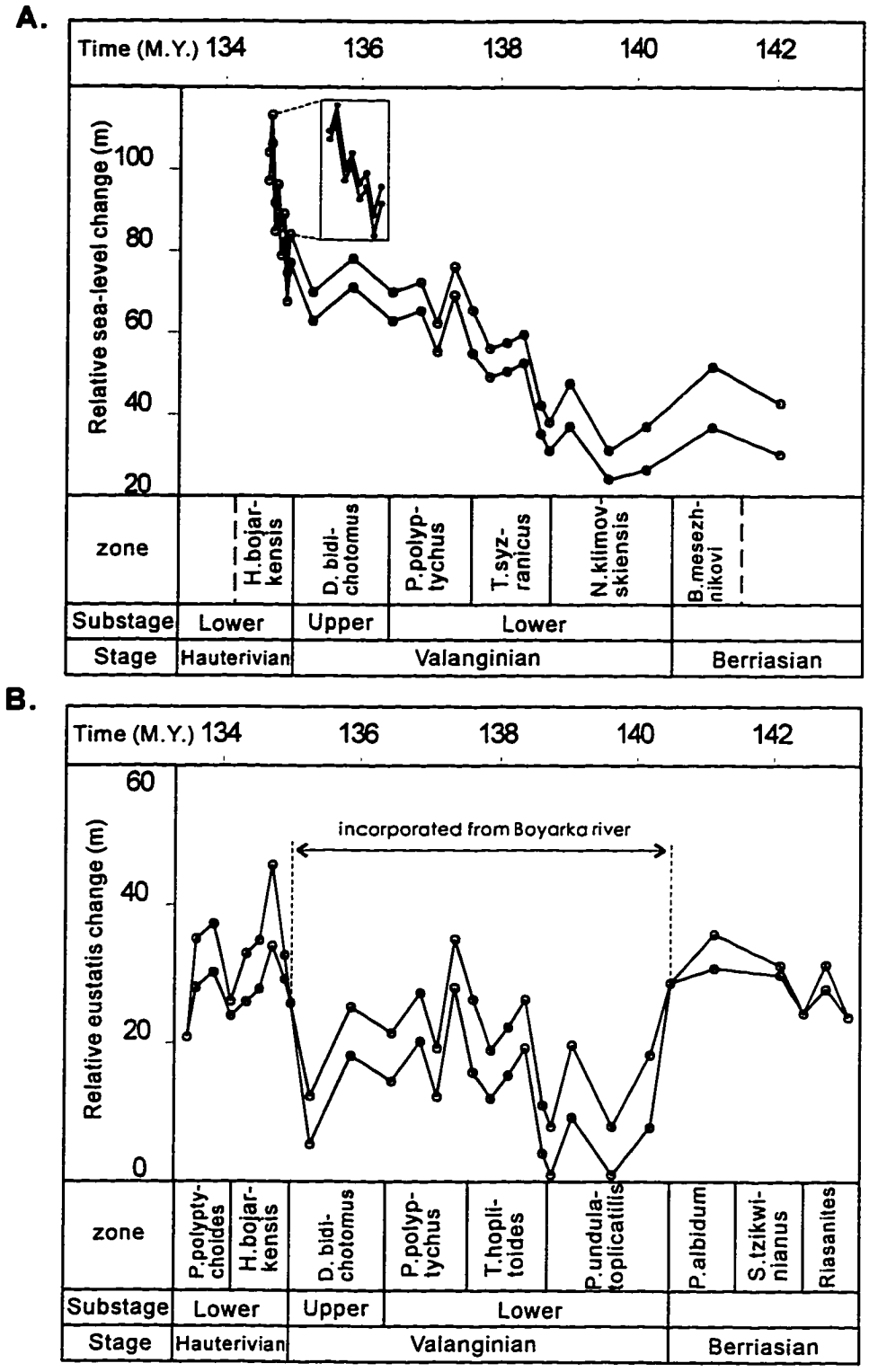

Figure 13. Example of incorporation of Siberian (Boyarka River) stratigraphic data to fill Valanginian unconformity of the central Russian Platform.
A) Relative sea-level curve for Boyarka river section; B) Boyarka river data incorporated into the Russian Platform curve

The Mesozoic strata of the Russian Platform are generally uniform in thickness, but there are variations caused by differential erosion during periods of exposure during eustatic drops, and minor local variations in sedimentation rates (Figure 7). It was impossible on the basis of any pair of individual wells, to distinguish between erosion and depositional variations. However, by examining the entire suite of wells and paleoenvironmental information from each, it is possible to estimate the difference from the pattern of erosion which emerged. It is possible that local erosion could cause variable bathymetry, and that this local variation not be filled during subsequent sea-level cycles. In this case, the eroded area would remain deeper than surrounding areas, and it would be necessary to resolve water depth differences represented by the eroded sediments. This presses the bounds of the resolution of our water depth scheme, and remains a potential source of error in our analysis. However, by constructing a composite curve on the basis of the agreement of relative sea-level curves from many wells and outcrops, this potential source of error is minimized.

The most significant potential error involved in our analysis arose from paleo-water depth analysis. Although our paleodepth model takes into account all available geological information some depth-dependent uncertainties remain. To minimize them we used paleogeographic and subsurface geometry control for paleodepth determination. After identifying paleodepth for each unit, we carefully examined its lateral extent, facies variations within it, thickness differences, extent of erosion, etc. For example, some stratigraphic units with similar paleodepths (as determined by the paleodepth model) exhibited different lateral extent on 3D fence diagrams. In these cases, we assigned greater depths to units with greater areal extent, even though this procedure involves some additional subjectivity into the data analysis. In many cases, paleogeographic control helped improve or correct the initial paleodepth reconstructions.

Sea-Level Curve

Construction of the Quantified Eustatic Curve

A composite relative sea-level curve was constructed using the best preserved sections throughout the stable part of the Russian Platform (Moscow Synclise) (Figure 12). Because of the stability of the Russian Platform, we take the composite curve to represent a global eustatic curve (Figure 14).

On the basis of stratigraphic continuity and reliable geologic age control, the relative sea level curves from two wells, M1 (Teplyi Stan) and M456 (Varavino), were chosen as a foundation for the eustatic curve (Figures 4, 12). Data from the various other well, core, and outcrop sections of the Russian Platform were incorporated both as a check for consistency and as a source for additional stratigraphic detail. The final eustatic curve was constructed as a composite of the individual relative sea-level curves (Figure 14) using the Harland timescale (Harland et al., 1990). The thickness of the error band reflects uncertainties in water depth analysis as well as other smaller factors.

Data Incorporation (filling stratigraphic gaps)

The data for Upper Bajocian-Bathonian as well as two zones of the basal Aptian were taken from the western Ryazan-Saratov trough region of the Russian Platform (Figure 1). These data were incorporated directly, because the similarity of these sections to those from the Moscow Synclise indicates stability during the incorporated intervals.

The gaps caused by the most prominent unconformities (Valanginian, Upper Cenomanian-Lower Turonian, Lower Coniacian) were filled with northern Siberian stratigraphic data. We incorporated these data by matching highstands in the two regions immediately before and after each Russian Platform unconformity. In order to accomplish

this, we backstripped the appropriate intervals of northern Siberian data to generate relative sea level curves. This procedure accounted for sediment fill, compaction, and loading as well as water depth variations and loading, and resulted in the sum of tectonic subsidence and eustasy (Angevine, 1989; Steckler and Watts, 1978). The relatively short durations of the intervals made it possible to assume that Siberian subsidence rates were constant within the intervals (usually <5 m.y.). Thus the tectonic subsidence defined a straight-line trend, the deviations from which could be attributed to eustatic variations. In order to merge Russian Platform and Siberian data, we chose highstand tie points in the Russian Platform eustatic curve immediately before and after each hiatus to be filled, and correlated them to their northern Siberian equivalents. The correlations were based on biostratigraphic control at biostratigraphic zonal resolution. For example, for the Valanginian hiatus, we correlated highstands in the upper Berriasian ammonite zone *P. albidum/B. mesezhnikovi* and lower Hauterivian zone *H. bojarkensis* (Figure 13). The difference in sea level rise in this interval between the two curves was attributed to northern Siberian subsidence, and the slope defined by this difference was subtracted from the northern Siberian stratigraphic data. This procedure resulted in a subsidence-corrected northern Siberian sea level curve for the interval. Once this was obtained, it was possible to simply use the northern Siberian adjusted data to fill the gap in the stratigraphy of the Moscow Depression completing the missing intervals in the eustatic curve (Figure 13).

Upper Barremian and upper Aptian sediments are absent throughout most of the Russian Platform (Sazonov and Sazonova, 1967) and are also poorly controlled biostratigraphically and/or completely absent in Siberian sections. These intervals, in addition to the Lower Volgian and Mid-Cenomanian, are shown with dashed lines on the Quantified Eustatic Curve (Figure 14).

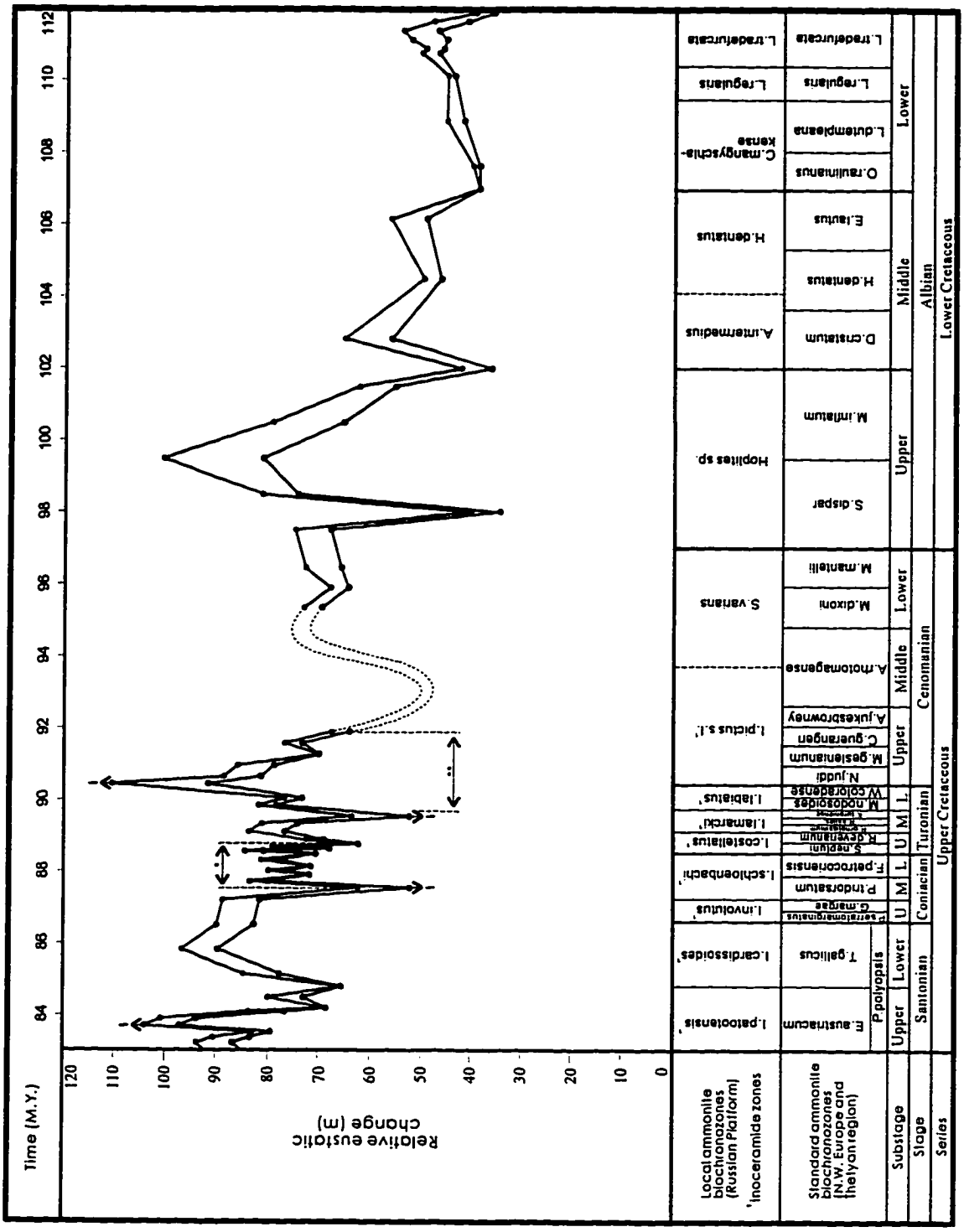

Figure 14. Quantified Eustatic Curve for late Bajocian - Santonian time. The time scale is from Harland (1990). The elevation scale is arbitrary, with 0 set on the lowest point on the curve.

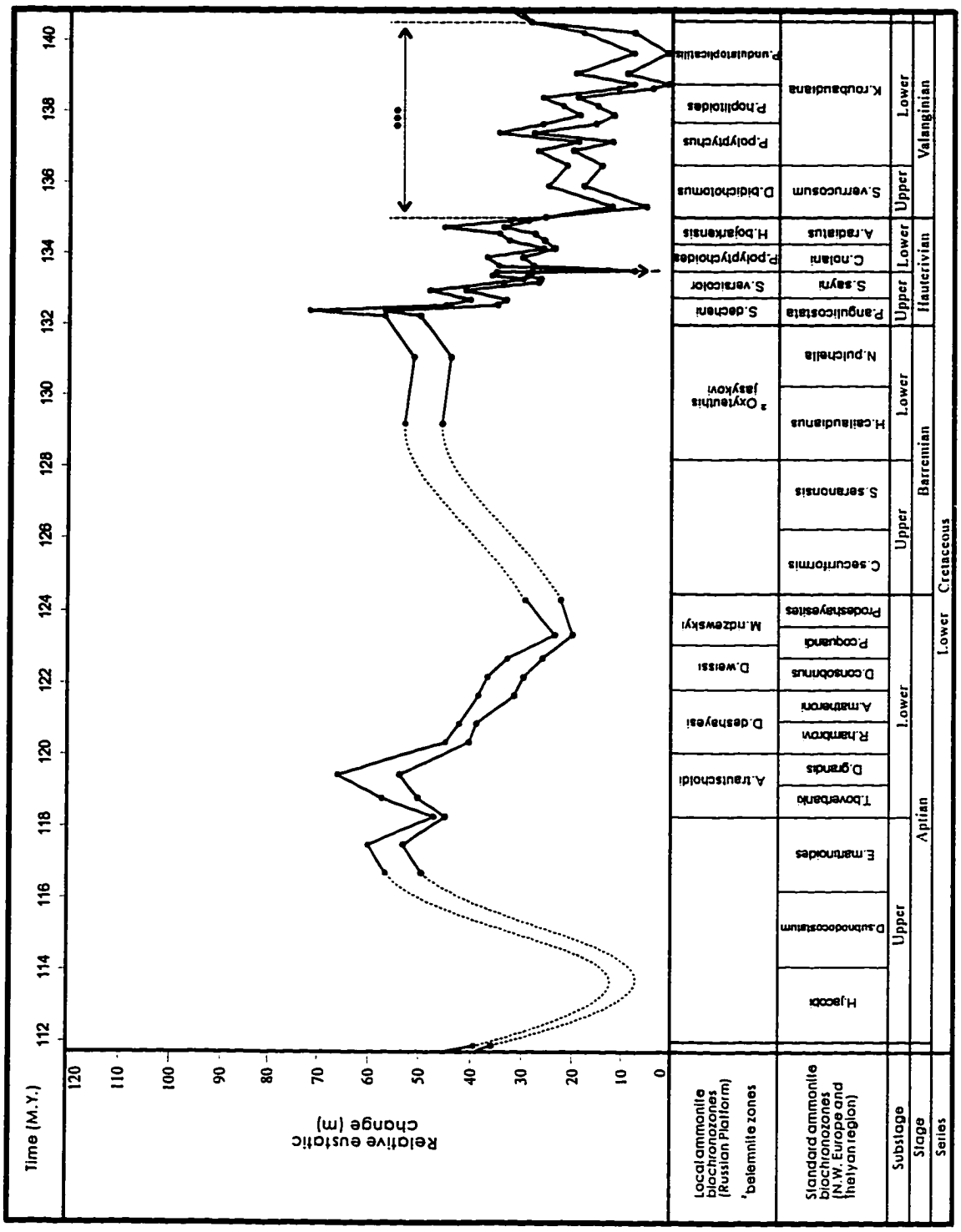

Figure 14. Quantified Eustatic Curve, continued.

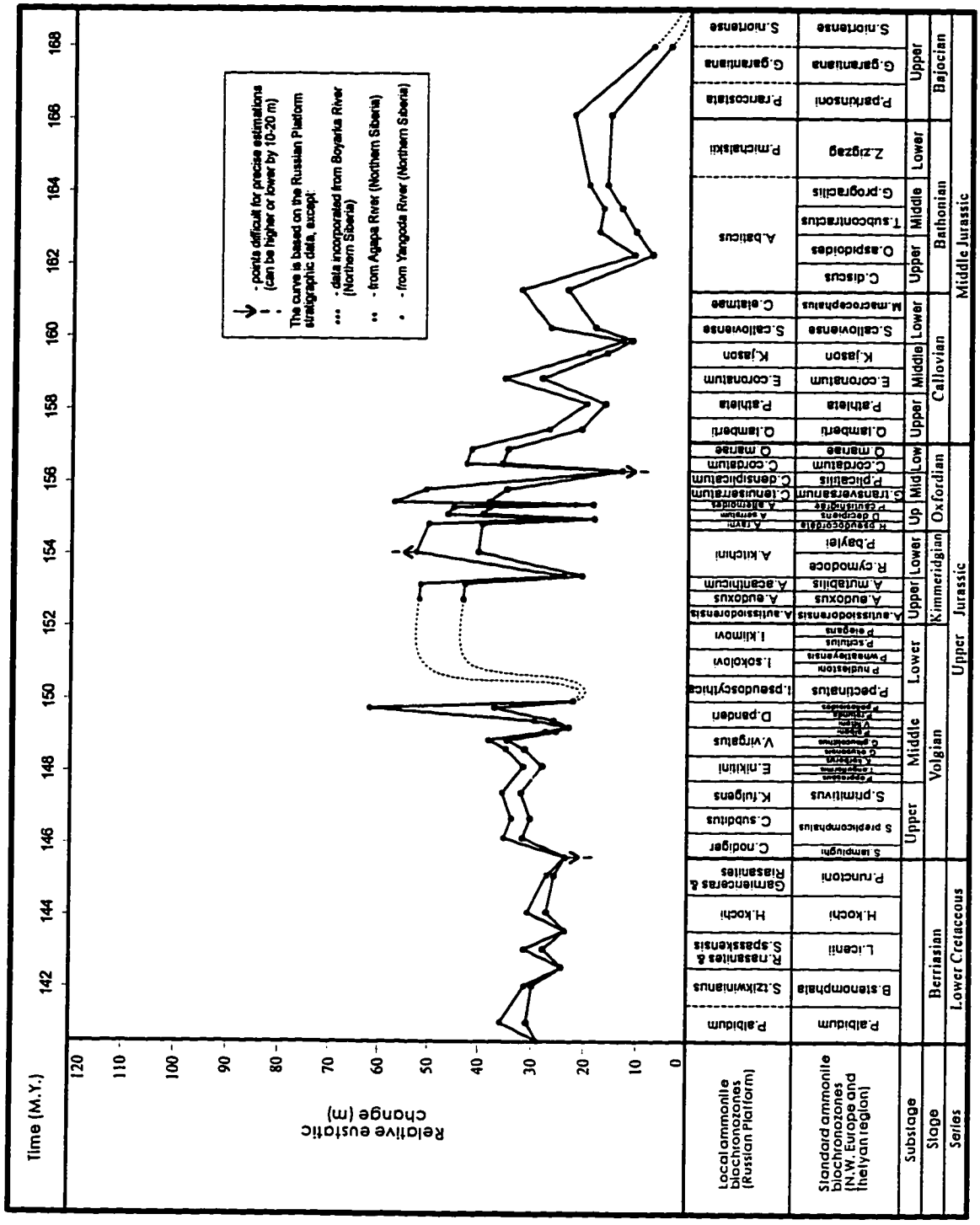

Figure 14. Quantified Eustatic Curve, continued.

Curve description

The final composite eustatic curve depicts numerous small scale sea-level oscillations superimposed on a long-term trend. In general, sea level was continuously rising throughout Mid - Late Jurassic time. This resulted in continuous expansion of the area of marine sedimentation over the Russian Platform and West Siberia. In the Jurassic portion of the curve, the Upper Oxfordian - Lower Kimmeridgian interval and the lower part of the Middle Volgian can be regarded as most prominent transgressive events, while major sea-level falls occurred at the Lower/Middle Oxfordian boundary and at the base of the Middle Volgian. The upper part of the Volgian is regressive and the Jurassic - Cretaceous boundary exhibits a significant unconformity throughout the Russian Platform. In the Middle Volgian the long-term trend changed to gradual fall until the beginning of the Hauterivian. The Berriasian and Valanginian stages were a time of relatively low sea level during which a series of high-frequency sea-level oscillations took place. The highest rates and amplitudes of sea-level fluctuations occurred in the Hauterivian. During a period of a few million years in the Late Hauterivian, sea level rose by a total of 60-80 meters in three transgressive cycles. The Barremian interval is generally regressive. From the beginning of the Aptian, the overall trend shows long-term sea-level rise until the end of the Santonian. A significant sea-level fall followed a Late Albian transgression and resulted in an unconformity at the top of Upper Albian on the Russian Platform and West Siberia. The Middle to Upper Cenomanian and Lower Turonian are absent from the Russian Platform, but are generally regarded to have been a time of eustatic highstand based on the stratigraphy of West Siberia and elsewhere in the world. The absence of sediments from this interval cannot be regarded as indicating non-deposition. Instead, we suggest that the thin distal Cenomanian and Lower Turonian sediments were eroded from the platform during a major Mid-Turonian regression (Sahagian and Jones, 1993). A second eustatic highstand is evident in the Late

Cretaceous, in the Late Santonian. The stratigraphy of the Campanian and Maastrichtian are absent from the Moscow Synclise, presumably due to subsequent erosion.

Relation of the Eustatic Curve to Present Sea Level

Although there is stratigraphic evidence for stability of the Moscow Depression throughout Mesozoic deposition, there is also evidence of significant post-Santonian rejuvenation of pre-Mesozoic structures. Consequently, we do not use the present elevation of the central Russian Platform strata as an absolute measure of eustatic change after the Mesozoic, but restrict its use to the variations within the Mesozoic. In order to tie the Mesozoic curve to present sea level, and set the elevation scale in Figure 14, it is necessary to choose a point which can be considered stable through Cenozoic time. On the Paleozoic Voronezh Arch (Figure 1), the top of Cenomanian is flat-lying and lies at 214 to 225 m above present sea level across a region spanning 250 km lying on a trend of NW-SE (Blank et al., 1992). However, to the south of the Voronezh Arch is the Dnepr-Donetsk depression in which the Cenomanian has subsided by 500-600 m, and to the north of the Voronezh Arch, the base of the Aptian lies at an elevation of 260-270 m, indicating significant uplift which caused erosion of the Cenomanian strata. This setting compromises the reliability of the Voronezh Arch for tying Mesozoic to present sea level.

There is a region in Minnesota which also has flat-lying Cenomanian-Turonian strata, and which has been inferred to be tectonically stable since that time (Sahagian, 1987; Sleep, 1976; Sloan, 1964). The region extends through Minnesota and into Iowa, and may have extended across an eroded or non-deposited region as far as Tennessee (Marcher and Stearns, 1962). There is no evidence for any epeirogenic activity in the region aside from glacial rebound and regional erosion (Sahagian, 1987). However, the limited stratigraphic range of these deposits (only Cenomanian-Turonian) does not allow construction of a continuous Mesozoic sea level curve. If the elevation of the Minnesotan strata are used as a baseline, with the elevation of the Cenomanian-Turonian highstand at

270 m above present sea level (Sahagian, 1987) 160 m should be added to the arbitrary elevation scale in Figure 14. It is important to emphasize that the shape and magnitude of variations within the eustatic curve in Figure 14 was determined solely on the basis of Russian Platform stratigraphy (with some short sections from Siberia). The Minnesota horizon can only be used for placing the zero point of the elevation scale (vertical axis) relative to present sea level.

Discussion

The relationship between eustatic variations and sedimentation is quite different on cratonic areas than it is on passive margins. This is a result of contrasting geometries (hypsometries), sedimentation rates, and tectonics. High rates of subsidence and sediment supply on passive margins result in relatively continuous deposition of thick (>100 meters) sedimentary units. Shoreline shifts are primarily caused by variations of ***rates*** of eustatic change and relative sea-level change can be interpreted through change of coastal onlap. However, even though eustatic change is generally considered as the main forcing factor which drives coastal onlap shifts, transgressions and regressions on passive margins remain very sensitive to subsidence and sedimentation rates. For example, Pitman (1978) demonstrated that on passive margins, transgressions as well as regressions may occur as a result of variations in the rate of sea level fall. This may result in potential error in reconstructions of eustasy on the basis of changes in coastal onlap unless the time and space distribution of tectonic subsidence is known a priori. This problem does not arise in cratonic regions like the Moscow Depression which lack discernible syn-depositional tectonics and have extremely slow sedimentation rates. In these environments, transgressions and regressions are driven only by eustatic rise and fall, respectively.

An important difference in the phase relationship between eustasy and shoreline shifts (transgressions-regressions) exists between passive margins and cratonic basins. Angevine et al. (1990) showed that maximum regression may occur anywhere from the point of maximum rate of eustatic fall to lowstand depending on tectonics and geometry. This results in different timing of shoreline shift episodes in different basins caused by the same eustatic change. Angevine et al. (1990) calculated that for third order eustatic variations, transgressive/regressive episodes may vary in timing by as much as 2.5 Ma in different basins. This results in uncertainties of dating of eustatic events inferred from subsiding basins which are avoidable only in the unusual case in which the time and space distribution of tectonic subsidence rate is well documented for the period of deposition. It has been argued that the most meaningful way to view subsidence, eustasy, and sedimentation on passive margins is on the basis of rates rather than amounts (Christie-Blick, 1990; Jervey, 1988; Pitman, 1978). However, if the rate of subsidence is zero and the rate of sedimentation is very small, as on the Russian Platform, it may be useful to consider amounts of eustatic change instead.

The tectonic stability and very slow sedimentation rates of the Moscow depression make a phase relationship such that eustasy and shoreline shifts change in parallel. Thus, the assignment of eustatic events to stratigraphic elements observed on the Russian Platform is much more precise than would be possible on passive margins. Another advantage of the Russian Platform is its well documented ammonite biostratigraphy (for most of the section), which provides the most reliable correlation possible.

Potential errors in eustatic reconstructions arise from different sources on passive margins and stable cratons (e.g. Moscow Depression). On passive margins, there are large potential errors from subsidence, sedimentation, and water depth (all terms of the backstripping equation), whereas erosion is a negligible factor compared to sedimentary thicknesses. On the Russian Platform there are potential errors from water depth

estimation and erosion, with smaller errors arising from minor variations of sedimentation. These errors can be minimized by the use of multiply redundant stratigraphic data.

The greatest potential source of error for eustatic reconstruction based on the stratigraphy of the Moscow Depression arises from paleodepth interpretations. This is a universal problem, but compared to other basins, the Moscow depression is well suited for paleodepth analysis as a result of shallow water and thus relatively precisely estimable paleodepths. Unlike previous sea-level analyses based on passive margins in which potential errors from estimation of thermo-tectonic subsidence is so great that water depth variations are small in comparison and thus are ignored, in our analysis these same water depth variations are the largest potential sources of error, and have been carefully accounted for to achieve the greatest eustatic interpretive reliability.

Erosion in the Moscow Depression resulted in very limited distribution of certain stratigraphic units. This makes it more difficult to constrain paleodepth estimations on the basis of paleogeography and stratal geometry. The areal extent of younger sediments on the Russian Platform is more limited than that of older sediments due to extensive post-depositional (including Quaternary) erosion. For example, upper Cretaceous strata are only locally preserved, although there is ample evidence that indicates that there was deposition throughout most of the Late Cretaceous. Thus, our facies analysis and sea-level curve based on the Russian Platform are more precise for earlier times than for later. The lack of proximal margins (shoreline deposits) of many units due to erosion also results in difficulties with paleogeographic control for those deposited during highstands of sea level. During significant regressions, the Russian Platform was completely exposed, resulting in unconformities due to erosion and/or non-deposition. Thus, the least accurate depth estimates are for times of extremely high or extremely low sea level. During highstands, there is deep water which is difficult to quantify, and the proximal

margins of highstand deposits are generally eroded. During lowstands, previously deposited sediments may be eroded. Incorporation of intervals from Siberian basins can fill the gaps, but represent an additional potential source of error. Nevertheless, the magnitude of this error is only a few meters, whereas the error for eustatic reconstructions from passive margins or subsiding basins (with kms of subsidence and sedimentation) can be considerably greater.

The quantification of eustatic variations on timescales of less than 1 m.y. bears on the issue of rates and causes of eustatic changes. Because we use stratigraphic techniques, deposition rates must be considered minimum estimates. Thus, rates of sea-level rise are minima. During the Late Hauterivian event, sea level rose by at least 60 m in at most 2 m.y. This rate of greater than 30 m/m.y. is normally considered greater than that attributable to the mechanisms accepted for causing sea-level variations during the Mesozoic. In the absence of major continental ice sheets (Barron, 1985; Barron et al., 1981), the mechanisms for large, rapid eustatic variations are poorly understood. Some explanations have been offered which may bear on the problem (Cloetingh, 1988; Jacobs and Sahagian, 1993; Karner, 1986), but no single mechanism is yet accepted which can account for the inferred magnitudes and rates.

Conclusions

The Russian Platform provides a stable frame of reference for the quantification of Mesozoic eustatic changes. The Quantified Eustatic Curve so constructed should be more reliable than curves inferred from passive margin and subsiding basin stratigraphies because of better tectonic control. In our analysis, our largest source of error is paleodepth, which is relatively well constrained due to shallow water depths. Other, larger sources of error such as thermal subsidence or sedimentation rate variability are

eliminated by the stable tectonic environment of the Russian Platform. A well established biostratigraphic framework based for the most part on ammonites and good correlation with Western Europe makes it possible to accurately assign ages to the interpreted eustatic events. The relatively small potential errors result mainly from paleodepth interpretations and erosion.

The fortuitous hypsometry and elevation of the Russian Platform during the Mesozoic led to shallow marine deposition which was useful for accurate paleowater depth determination. However, these same conditions also led to the development of many unconformities throughout the Jurassic and Cretaceous section. The largest of these stratigraphic gaps (zone to substage duration) have been filled with stratigraphic data from adjacent subsiding regions with more continuous sections.

The Quantified Eustatic Curve shows a general eustatic rise from the middle Jurassic through the Late Cretaceous, punctuated by many higher order events. The highest sea level was reached in the basal Turonian at an elevation of 270 m above present sea level (using Minnesota as a datum). Comparison of the Quantified Eustatic Curve with other published sea level curves shows low-order similarities, but many differences at higher order. In many cases, events can be correlated between curves, but magnitudes are different.

The Quantified Eustatic Curve may be a useful tool which is applicable to any basin globally. The West Siberian Basin may be a particularly well-suited case for initial application because of its well established interregional biostratigraphic correlation with the Russian Platform. The eustatic curve (Figure 14) can be applied to problems of basin subsidence and basin modelling where eustatic input is necessary. It thus may potentially be used as a tool to 1) estimate the influence of local factors (subsidence and sedimentation rates) by removing the eustatic signal from stratigraphic data; 2) improve geological correlation (where there is poor biostratigraphic control); and 3) constrain the eustatic parameter for computer models of basin sedimentation. By subtracting the

eustatic signal from backstripping results from any basin, tectonics and sedimentation can be quantified at a resolution and reliability previously unattainable. This may lead to a better understanding of depositional and thermal histories of specific sedimentary basins.

CHAPTER II

CRITICAL COMPARISON OF THE QUANTIFIED EUSTATIC CURVE

Test of validity

In order to establish any sea-level curve as a eustatic curve, it is necessary to test it against relative sea level curves derived from basins with contrasting tectonic environments. There is no method demonstrated to date to prove the validity of any eustatic curve in terms of representation of the relative volumes of ocean basins and ocean water. However, most authors (Hallam, 1992; Lawrence, 1993; Miall, 1992) agree that eustasy can be inferred if age equivalency of sea-level events (within limits of biostratigraphic resolution) is demonstrated in separate tectonically unrelated basins. Chronostratigraphic precision is of critical importance for such a test. However, even truly eustatic variations may be manifest in stratigraphic sequences at different times in different basins due to differences in tectonic subsidence rates (Angevine et al., 1990; Lawrence, 1993). It is therefore important to choose test areas for critical comparison to the QEC whose subsidence is known to be slow so that the phase shift is within narrow biostratigraphic correlation resolution limits.

Several sea-level curves have been published in recent decades, mainly based on the stratigraphy of passive margins or otherwise subsiding basins (Gygi, 1986; Hallam, 1988; Haq et al., 1988; Norris and Hallam, 1995). As such they are subject to flaws inherent to

influence of the regional factors such as tectonics and sedimentation. Nevertheless, they provide useful materials for comparison to the QEC and confirming eustatic origin of the inferred events of sea-level change.

In order to conduct the test, we compared our QEC to the often cited eustatic curves of Haq (1988) and Hallam (1988). I also reviewed several works on Jurassic-Lower Cretaceous eustatic reconstructions from European sections. Finally, I compared the Upper Cretaceous part of QEC to transgressive regressive history of the U.S. midcontinent.

Exxon's sea-level curve

One of the most cited eustatic curves is that of Haq et al. (1987, 1988). This curve, however, has been criticized by some (Miall, 1992; Sloss, 1991) for not taking sufficient account of the tectonic and sedimentary processes which dominate the mainly passive margin environments upon which it was based. Nevertheless, it was based on a large body of stratigraphic and biostratigraphic data, and provides an interesting comparison for our eustatic curve.

The most obvious result of this comparison is that both curves have similar long-term trends. Haq et al. (1988) indicate a general sea-level rise from the Bathonian (Middle Jurassic) to the Volgian (Late Jurassic) punctuated by several sea-level falls. I have obtained a similar pattern (Figure 15) although the magnitude of the long-term rise is less than that indicated by the Haq et al. curve. Both curves indicate a long-term lowstand in the Berriasian and Valanginian and sea-level rise in the Hauterivian that continued to a maximum in the Early Turonian.

There are also similarities and some significant differences between the curves at finer scale, particularly with respect to magnitude of eustatic events. The Bathonian

portions of both curves are almost identical, showing slow eustatic fall. The similarity continues through the Late Jurassic. While the number of small-scale eustatic events is similar in the two curves, there are some discrepancies in timing of events at the biostratigraphic zonal level, possibly owing to biostratigraphic correlation uncertainties.

There are significant discrepancies in the Berriasian - Valanginian interval. There is a sea-level fall at the Jurassic-Cretaceous boundary which caused a regional erosional unconformity throughout the Moscow Depression. However, the Haq et al., curve shows a sea-level highstand at this time. Further, there is no evidence for the major sea-level drops of more than 100 meters indicated by Haq et al. at 128.5 and 126 Ma on either the Russian Platform or the more continuous record of West Siberia (note different timescales on the Quantified Eustatic and Haq et al. curves).

Despite the differences at the short-term resolution level, both our eustatic curve and that of Haq et al. (1988) show a general lowstand of the long-term trend in the Valanginian. On the Quantified Eustatic curve (Figure 16), the Valanginian lowstand is followed by Early Hauterivian eustatic rise with a magnitude of at least 30 m. After a sea level fall at the end of the Early Hauterivian, there is another rise of at least 60 m in a time interval of at most 2 m.y. The total magnitude of sea-level change during Hauterivian time is estimated to have been at least 60 m between a low in the uppermost Valanginian to a high in the basal Barremian. This generally agrees with the results of Haq et al. (1988) who place a lowstand in the Valanginian and a high in the basal Barremian, but is different in detail.

There is little agreement between the two curves for the Barremian-Aptian interval. For Albian time both Haq et al's. (1988) and our curves indicate an overall sea-level rise with a highstand in the Upper Albian. In the Upper Cretaceous, both curves agree with respect to a few important events, but again show different amplitudes. These include mid-Cenomanian and mid-Turonian sea-level falls, and a maximum highstand just after the Cenomanian-Turonian boundary.

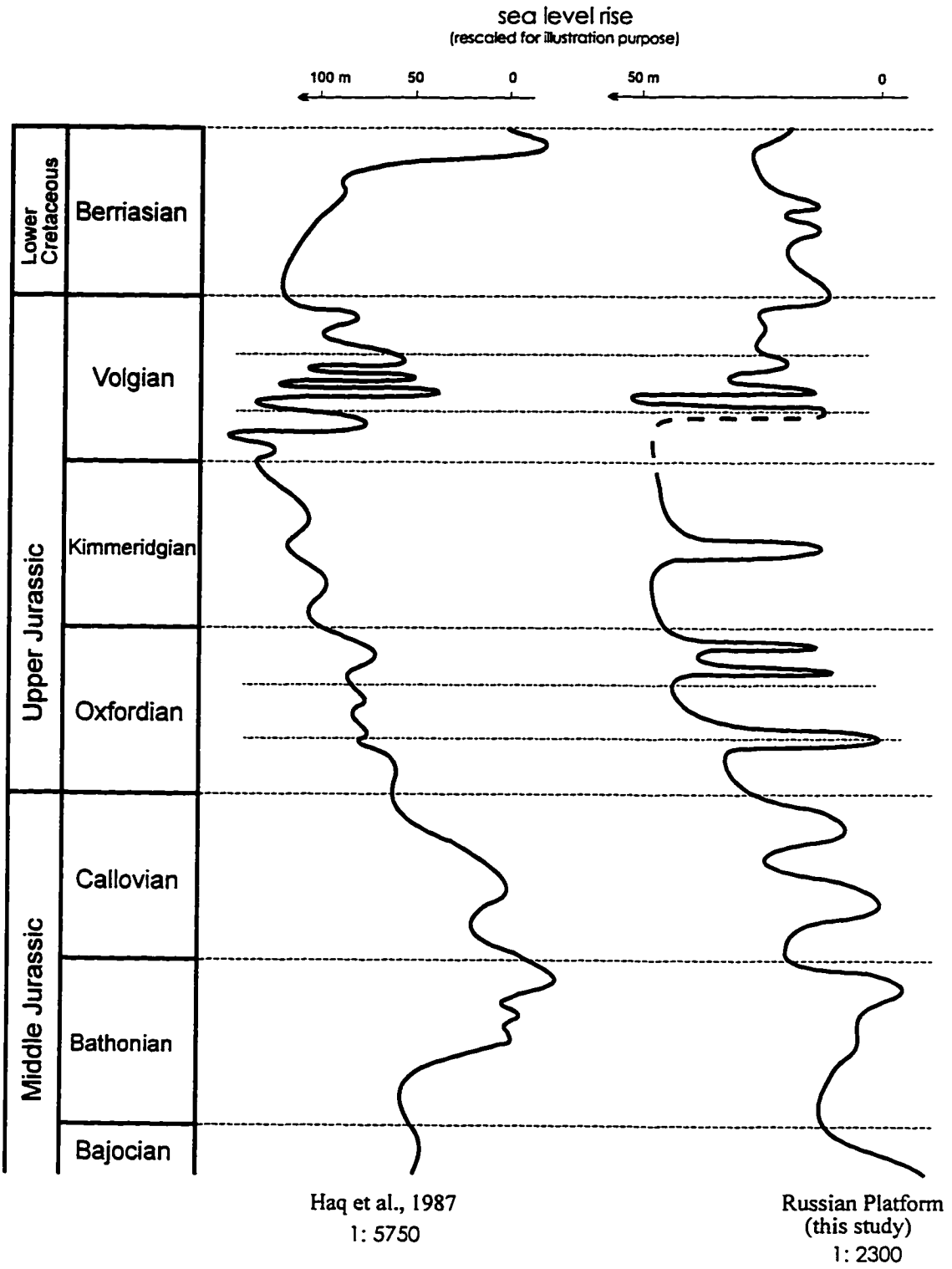

Figure 15. Comparison of Jurassic results of the present study with those of Haq et al. (1988)

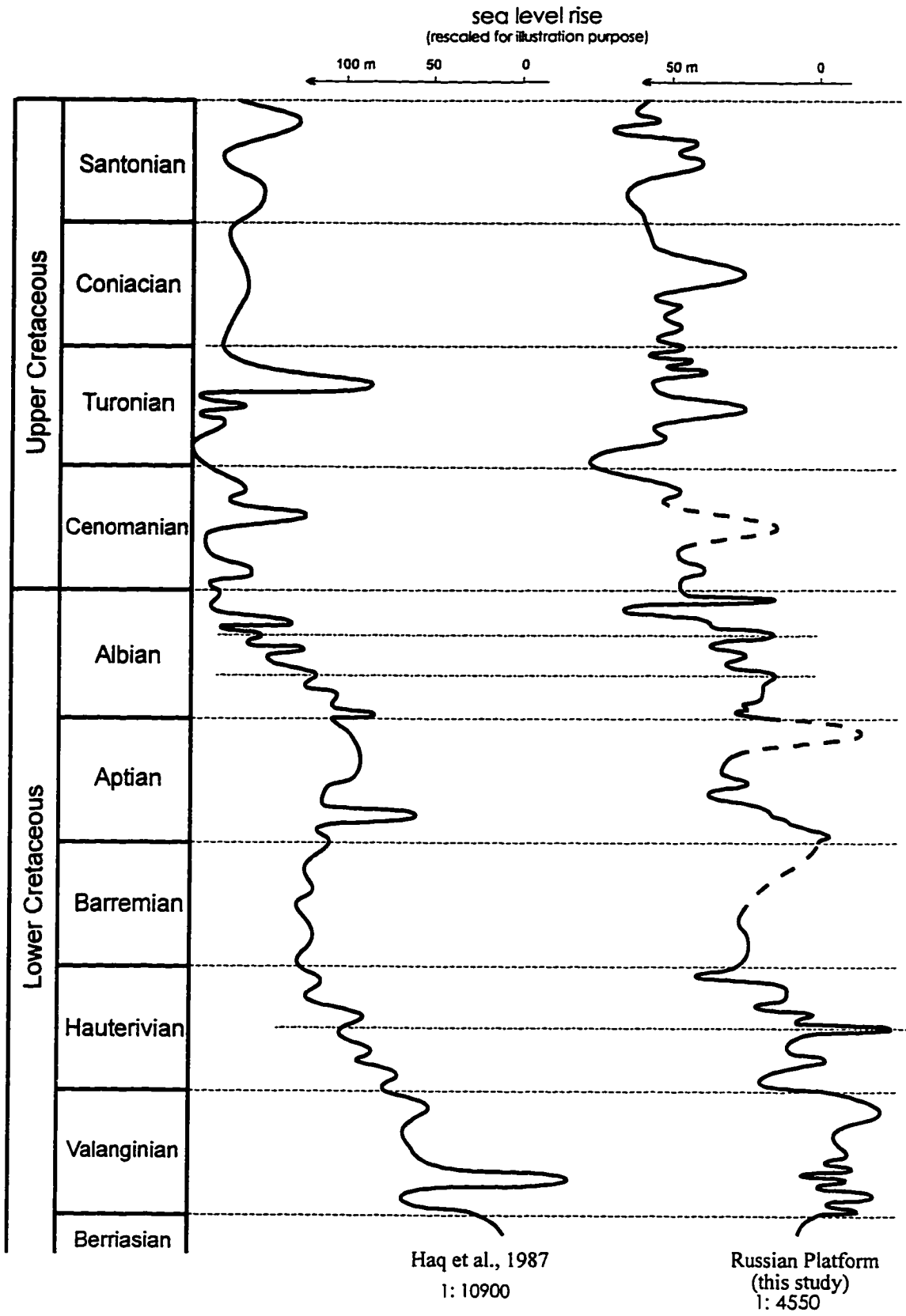

Figure 16. Comparison of Cretaceous results of the present study with those of Haq et al. (1988)

Summarizing, I conclude that Exxon's curve providing reasonably good picture of long-term eustatic change, fails at the level of higher-order resolution (3rd and higher order eustatic cycles). While, some intervals such as Bathonian-Oxfordian, Hauterivian-Barremian, and Albian-Turonian reveal reasonably good correspondence to the QEC, the others display a total lack of agreement at the short-term resolution level.

At this point it is worth noting that the intervals of agreement such as Bathonian-Oxfordian and Albian-Turonian are inferred from southern England and the U.S. Western Interior sections, respectively for construction of the Exxon curve. These two regions both represent cases of deposition with limited tectonic activity in shallow epicontinental cratonic seas. This, once again, shows that cratonic sections provide much more valuable data for eustatic reconstructions than those inferred from passive margins.

Upper Jurassic (Callovian-Kimmeridgian)

The Callovian-Kimmeridgian time interval has a well established ammonite biostratigraphy that provides the excellent means for regional as well as intercontinental correlation. In addition, during this time vast continental areas were covered by epicontinental seas as a result of a major global transgression. Consequently, Callovian-Kimmeridgian marine strata have great areal extent and are encountered in numerous outcrops and subcrops throughout the world. As a result, numerous studies related to sea-level change have been undertaken for this stratigraphic interval, rendering it a prime interval to test.

Publication of the sequence stratigraphic concept (Loutit et al., 1988; Posamentier et al., 1988; Van Wagoner et al., 1988) and Global Cycle Chart (Haq et al., 1988) stimulated a large number of publications with critical evaluations of sequence stratigraphic patterns

and attempts to extract eustatic signal from relative sea-level change. Most work on Jurassic eustasy focused on Western Europe because of the presence of numerous marine sections exposed in outcrops many of which are classic type-sections. In addition, petroleum exploration in Jurassic-Cretaceous strata of the North Sea shelf stimulated sequence stratigraphic studies and analyses of sea-level change throughout the region.

Significant tectonic activity accompanied Jurassic-Cretaceous sedimentation in the North Sea and many other basins of Western Europe (Underhill, 1991; Wignall, 1991). Consequently, one should be very careful interpreting any sea-level change of the region as eustatically caused or influenced. For example, Underhill and Partington (1993) demonstrated that the mid-Cimmerian unconformity, which is interpreted as one of the most significant sea-level falls on the Exxon Chart, was formed as a result of periferal tectonic uplift related to North Sea rifting. Some Western European sections, however, were formed during periods of relative tectonic stability, and thus may provide useful information for reconstruction of eustasy.

Hallam's events of sea-level change

Hallam (1963) was a pioneer who suggested a eustatic origin of major Jurassic sedimentary cycles of Western Europe. In a series of publications he presented several versions of a Jurassic eustatic curve (Hallam, 1978; Hallam, 1988; Hallam, 1992). While realizing that the curve constructed only from European sections may not represent a global picture, he analyzed sections from the other continents as well. As a result, he identified transgressive/deepening events recognizable in more than one continent and regressive/shallowing events of regional importance in Europe (Hallam, 1988; Hallam, 1992). Comparison to the Quantified Eustatic Curve showed that many of them (not all) correspond to those of the central Russian Platform on which the QEC is based. These include transgressive episodes: 1) Late Bajocian; 2) Late Bathonian; 3) Early Oxfordian; 4) Mid-Oxfordian; 5) Late Oxfordian; 6) Early Kimmeridgian; 7) Mid-Volgian, and

regressive events: 1) latest Early Callovian (sub-coronatum Zone); 2) latest Early Oxfordian; 3) latest Mid-Oxfordian; 4) Early Kimmeridgian (sub-mutabilis Zone). In the same publication Hallam (1988) puts Russian Platform and the West Siberia among the regions where a significant transgressive event occurred in the Early Callovian. In some older literature (Gerasimov, 1962; Nezhdanov et al., 1992; Sazonov and Sazonova, 1967) this major episode was described as an "Early Callovian" transgression during which marine regime started to dominate in both regions. However, later on, the age of this event was redetermined as Late Bathonian (Meledina, 1994). At this point we should keep in mind that Hallam (1988) noted that his record of the eustatic events might be modified in the future, and some of the events reinterpreted as being caused by regional factors. Reinterpretation of the timing of the initial Late Bathonian transgression in West Siberia and the Russian Platform is a good example of such a modification.

Callovian

The first marine sediments on the Russian Platform and West Siberian Basin were deposited as valley fill during the latest Bathonian. This marks the first extensive marine transgressions on these regions during Jurassic. This event is co-eval with Late Bathonian transgression of Hallam (1988). Subsequently, marine sedimentation spread uniformly over the regions in Early to Middle Callovian time. The Lower/Middle Callovian boundary of the central Russian Platform is characterized by sea-level fall which is followed by sea-level rise with a maximum highstand in the latest Middle Callovian. Sea level fall at the beginning of the Late Callovian is determined by clear evidence of shallowing (see "Stratigraphy" of the Russian Platform). It is followed by significant sea-level rise that reached its maximum in the Early Oxfordian (upper mariae Zone).

Great Britain. The most detailed analysis of sea-level change during the Callovian-Early Oxfordian was published by Norris and Hallam (1995). In this study they analyzed

numerous sections throughout western Europe and other parts of the world, focusing on the Callovian-Oxfordian transition. Some events such as the Latest Callovian sea-level fall of Hallam (1988) were redefined as sea-level rise. As a final result, they proposed a eustatic curve for the Mid Callovian- Early Oxfordian interval (Figure 17). The authors claim that the eustatic nature of the interpreted sea-level events is demonstrated by good correlation of those within Western Europe on the intercontinental level. The main conclusions of the paper can be summarized as follows: 1) The Middle Callovian eustatic sea level rise began in latest Early Callovian or Middle Callovian and continued through the Late Callovian; 2) The latest Callovian (lamberti Zone) was a period of maximum rate of sea-level rise; and 3) The Early Oxfordian was a period of sea-level highstand conditions and subsequent sea-level fall. These results, being one of the most sophisticated and comprehensive reconstructions of eustasy to date, represent an extremely useful case for comparison with our Quantified Eustatic Curve.

In order to confirm the eustatic nature of the sea-level events interpreted from this study and the Russian Platform we compared it to the QEC. Quantified Eustatic Curve shows very similar patterns to that of Norris and Hallam's (1995), except in a few details. According to the QEC, the upper part of Early Callovian was characterized by sea-level fall that reached a minimum at the Middle/Upper Callovian boundary and was immediately followed by a middle Callovian sea-level rise (Figure 14). During the Middle Callovian, sea-level rose to a maximum in the coronatum Zone and then fell to a lowstand at the Middle/Upper Callovian boundary. The entire Late Callovian interval exhibits a continuous rapid sea-level rise. The important difference between the QEC and the Norris & Hallam curve (1995) is the lack of eustatic falls at the Early/Middle and Middle/Late Callovian boundaries in the latter. While these events are certainly real on the central Russian Platform, their amplitudes could have been smaller than we interpreted. The basal Middle Callovian beds of the central Russian Platform contain clear evidence of shallowing and erosion including hardground surfaces, shallow marine

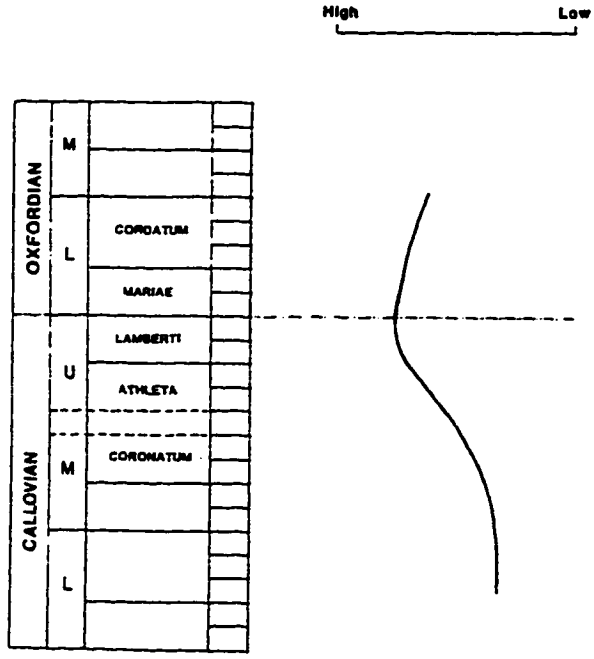

Figure 17. Proposed eustatic curve for the Callovian-Lower Oxfordian interval (Norris & Hallam, 1995).

fauna, oolitic beds, and many others (Gerasimov, 1971; Olferiev, 1986). The sea-level fall at the Middle/Late Callovian contact was of lower amplitude and is represented by evidence of shallowing such as partial erosion and abundant oolites. Despite these differences, the Quantified Eustatic Curve demonstrates excellent agreement with the 2nd and 3rd conclusions of Norris & Hallam (1995) including rapid sea-level rise in the Late Callovian and highstand with subsequent sea-level fall in the Early Oxfordian. The only minor disagreement involves the interpretation of precise timing of the peak of sea-level highstand. While Norris & Hallam (1995) place it in latest Callovian (Figure 17), we interpret it to have occurred in Early Oxfordian (mariae Zone) (Figure 14).

western European sections, Norris & Hallam (1995) analyzed numerous sections throughout the world. Surprisingly, most sections exhibit evidence of sea-level rise or highstand at the Callovian/Oxfordian boundary, which is also in agreement with the QEC. For example, in southern England this boundary is in the Oxfordian Clay unit, in Normandian sections it is a junction of two clay formations, and in the central Russian Platform it is in the middle part of the Podosinkovskaya clay Formation.

Summarizing, I conclude that sea-level rise during the Late Callovian to its highstand in earliest Oxfordian is a globally recognizable eustatic event.

Oxfordian

Oxfordian marine strata are areally extensive and are encountered in numerous outcrops and subcrops throughout the world as a result of global marine transgression and highstand during this time. In addition, the Oxfordian represents a time interval among the finest biostratigraphic resolution in the Mesozoic due to its well-developed ammonite zonal scales. This provides excellent opportunities for precise correlation within extensive regions as well as for intercontinental correlation.

During the last decade considerable attention was paid to the study and interpretation of Oxfordian strata in terms of sequence stratigraphy and sea-level change. This was

mainly stimulated by cyclic nature of the many Oxfordian section throughout the world as well as their good biostratigraphic resolution.

Corallian sections (Southern England). Classic Corallian (Oxfordian to Kimmeridgian) sections of the Dorset coast (Southern England) represent one of the most interesting cases for examining eustasy during this period of time. Arkell (1933) was the first to recognize the cyclic nature of these sections and interpreted it as three shallowing upward cycles (clays through sands to limestones). Subsequently, many different authors examined these sites and published various interpretations (Sun, 1989; Talbot, 1973; Wright, 1986). The most comprehensive and up-to-date of these is the one of Sun (1989).

Sun (1989) identified 4 regressive-transgressive cycles that are separated from each other by sharp erosional surfaces of transgression (Figure 18). The Corallian group of sections is located in the Wessex basin that covers a significant part of southern England. The most representative outcrops are exposed along the Dorset Coast which is in the transitional zone between Wessex and Channel Basins. During Permian-Cretaceous the sedimentation in the Wessex Basin was primarily influenced by episodic extensional tectonic movements that produced a series of grabens and fault block highs. However, a regime of slow flexural subsidence had become established by the beginning of Oxfordian and continued until the end of the stage. Based on this, as well as on an apparent consistency of his sea-level interpretation with that of Haq et al. (1988), Sun (1989) suggested that Corallian cycles were formed as a result of eustatic fluctuations.

The lower portion of the Corallian section consists of the upper part of Oxford Clays that are overlain by sands of Nothe Grit (Figure 18). This part of the section is assigned to the upper part of Lower Oxfordian (cordatum Zone). According to Sun's (1989) interpretation, the Oxford Clay Formation was deposited during sea-level highstand, while the Nothe Grit represents a regressive part during which sea-level fell to its

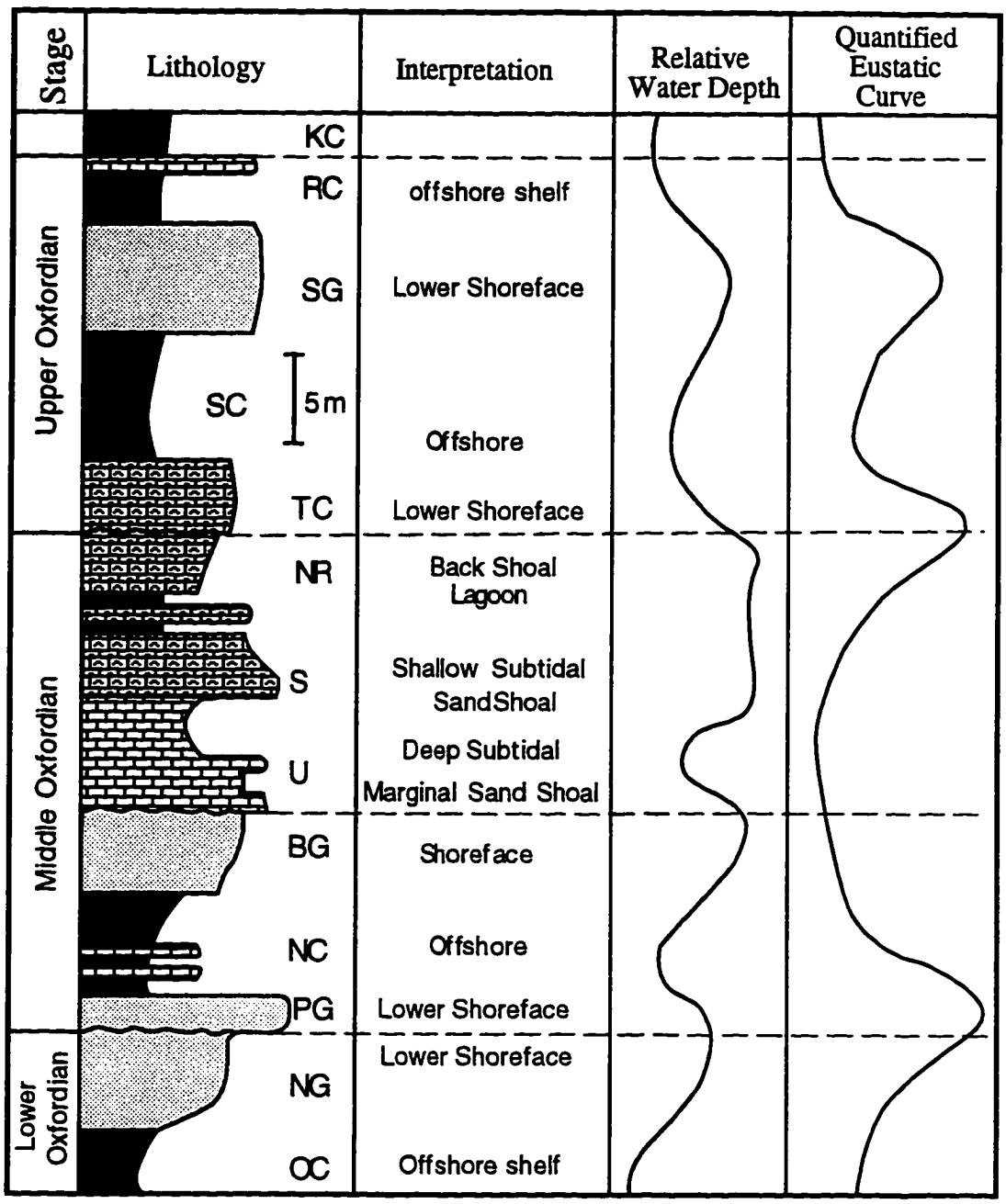

OC - Oxford Clay, NG - Nothe Grit, PG - Preston Grit, NC - Nothe Clay
BG - Bencliff Grit, U - Upton, S - Shortlake, NR - Nodular Rubble,
SC - Sandsfoot Clay, SG - Sandsfoot Grit, RC - Ringstead Clay,
KC - Kimmeridge Clay

Figure 18. Composite section and facies interpretation of the classic Corallian cycles of the Dorset Coast, England. After Sun (1989) and Hallam (1992).

minimum at Nothe/Preston Grits contact that marks the Lower/Middle Oxfordian boundary. This is in agreement with the data of the QEC which also demonstrates significant eustatic drop during the upper part of Lower Oxfordian to the Lower/Middle Oxfordian boundary. This observation is particularly important because the Lower/Middle Oxfordian boundary is a period of time during which a sea-level drop occurred in most localities worldwide (see previous chapter and Hallam (1988)). On the central Russian Platform this is the most significant regressive event in Jurassic time. It is also observed in southeastern West Siberia (See Nyurolskaya Depression and viccinity chapter). As such, I conclude that after the highstand in the beginning of Early Oxfordian, eustatic sea-level started to fall and subsequently dropped to it's minimum at the Early/Middle Oxfordian Boundary. This event of the eustatic drop was one of the most important in Jurassic history.

Lying on the sharply eroded surface of Nothe Grit member, the Preston Grit represents a transgressive phase and consists of unsorted sediments with abundant reworked particles and a highly diverse fauna. Overlying is Nothe Clay member which is composed of strongly bioturbated clays and was deposited during sea-level highstand. The Bencliff Grit member consists mainly of very fine sandstone and contains abundant cross-bedding and swaley cross-stratification structures that sometimes laterally pass into hummocky cross-stratification. This part of the section is interpreted as being deposited in a shallow high-energy environment above fair-wave base and represents a period of sea-level lowstand.

During the late Middle Oxfordian carbonate deposition dominated over clastic sedimentation. This resulted in deposition of the calcareous Osmington Oolite Formation that includes Bencliff Grit, Upton, Shortlake, and Nodular rubble members. The Upton member overlays the top of the Bencliff Grit with a sharp erosional contact. Talbot (1973) argued that Corallian cycles formed as a result of eustatic oscillations that occurred as a series of sea-level rise episodes interrupted by periods of standstill during

which progradation of terrigenous sediments occurred. A similar scenario of eustasy with periods of standstill followed by sea-level rise (no fall) was suggested by (Gygi, 1986) who examined a series of Oxfordian sections in the North Switzerland (Figure 19). However, Hallam (1988) showed that the unconformity at the base of the Osmington Oolite Formation exhibits erosional truncation of calcareous concretions from the underlying layer. According to Hallam (1988), this implies that at least one meter of sediments was removed due to sea-level fall. On the contrary, Sun (1989) interpreted this unconformity as a transgressive surface formed by wave action during rising sea-level. This is supported by the obvious transgressive nature of the overlying beds of Upton member such as abundant oolites, bioclasts, intraclasts, and high faunal diversity. The Bencliff Grit member was deposited above the fair-weather wave base and therefore the wave activity could have been strong enough to erode one meter of sediments in some places at the beginning of transgression. As such, it is possible to assume that Talbot's (1973) interpretation (Nothe Clay formed as a result of sea-level rise followed by period of standstill (no fall) during which sandy sediments of Bencliff Grit prograded over the area) may be a reasonable approximation. This is consistent with data of Gygi (1986) who shows pause (standstill) at the stratigraphic level that presumably corresponds to that of Nothe-Bencliff members (Figure 19). On the central Russian Platform this "pause" during Middle Oxfordian sea-level rise may have not been recorded because of the great distances to the clastic sources.

The lowest part of the Upton member is a transgressive bed which represents a transition from clastic dominated to carbonate-dominated sedimentation. It was deposited in a shallow marine environment which is indicated by abundant ooids, vertical burrows, and fauna. Upward increase of fine sediments and horizontal trace fossils suggests a continuous deepening. The upper part of the Upton member, being composed of strongly bioturbated nodular limestone, most likely characterizes a relatively deep marine environment and culmination of sea-level rise. This part of the section may represent a

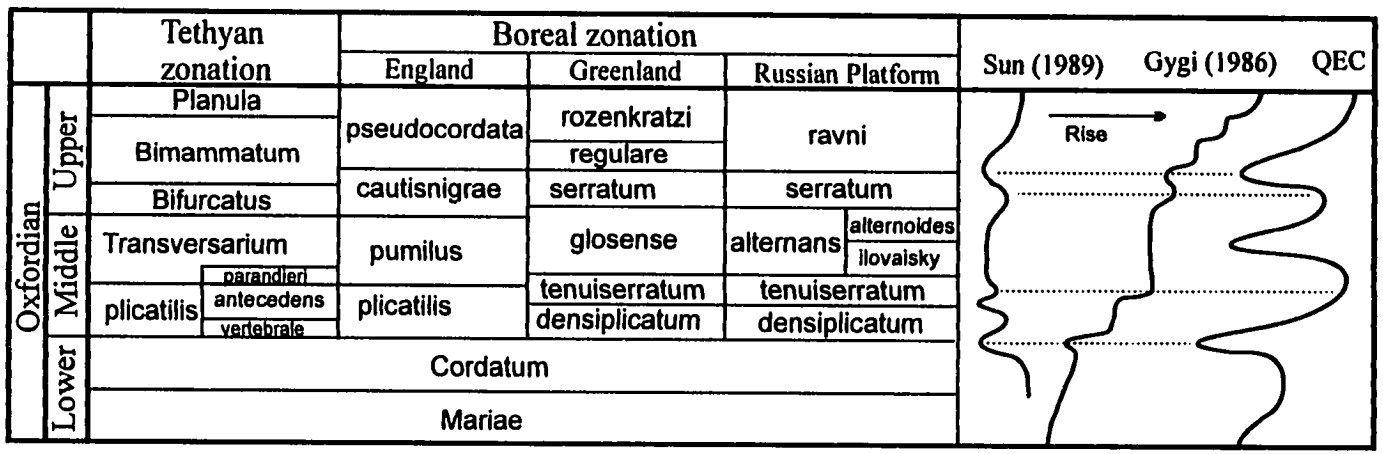

Figure 19. Comparison of the Oxfordian sea-level curves of Sun (1989) and Gygi (1986) with the Quantified Eustatic Curve .

maximum eustatic highstand during the Middle Oxfordian which is in agreement with the QEC and Gygi's (1986) sea-level curve (Figure 19).

The lower Shortlake member generally consists of cross-bedded oolites overlain by bioturbated oolites, interpreted by Sun (1989) to reflect a shallow water high energy environment produced by sea-level fall. The upper part of the Shortlake as well as overlying Nodular Rubble member were apparently deposited in a low energy, possibly deeper, environment. However, some distinct features such as restricted fauna, abundant bioturbation, and widespread micritization suggest that deposition occurred in a restricted backshoal lagoon environment rather than in a deep water system. Thus, the upper Shortlake and Nodular Rubble most likely represent a continuous sea-level lowstand (Figure 18).

Upper Oxfordian sedimentation in the Corallian sections began with transgression that resulted in deposition of basal lag with abundant intraclasts, ooids, and bioclasts at the base of Trigonia Clavellata. The overlying clays of the Sandsfoot Clay and sandstones of Sandsfoot Grit indicate a phase of sea-level highstand which was followed by sea-level fall. This sea-level fall generally corresponds to those in the Late Oxfordian of the QEC and Gygi (1986) curves, that supports its eustatic interpretation (Figure 19). The sandsfoot Grit member is overlain by the Ringstead and then Kimmeridgian clays that represent the onset of latest Oxfordian-Early Kimmeridgian sea-level rise.

Swiss Jura. The eustatic sea-level history of the Oxfordian was published by Gygi (1986). This study was based on analysis of depositional sequences, subsidence, and paleobathymetry of the platform to basin transition of northern Switzerland. The eustatic curve represents a series of sea-level rise episodes interrupted by periods of stillstand (no sea-level falls) (Figure 19). There are, however, significant discrepancies in correlation between Swiss Jura and Tethyan province on subzonal level (Jenkyns, 1996). In Gygi's (1986) scheme, the transversarium Zone consists of two subzones including lower

antecedens and upper parandieri. In contrast, Jenkyns (1996) shows the antecendens as the upper part of plicatilis Zone and parandieri is at the base of transversarium Zone (Figure 19). Attempting to correlate Swiss sea-level events with those of Corallian and the QEC I used the scheme from Jenkyns (1996).

Evidence from carbon isotopes. Jenkyns (1996) analyzed carbon isotopes from Middle Oxfordian carbonate sections of two locations in southern France and northern Italy. He detected that a clear positive excursion of $\delta^{13}C$ is present in the transversarium Zone. Similar results were reported from other studies from different European locations and Gulf of Mexico (Bill et al., 1995; Heydari and Wade, 1993; Hoffman et al., 1991).

During the last decade several papers were published that demonstrated correspondence between positive deviations of $\delta^{13}C$ and periods of significant transgressions (Arthur et al., 1987; Weissert and Lini, 1991). There is a relationship between synthesized carbon volumes and areal extent of the shelf seas because the bulk of organic carbon is deposited in shelf environments where plankton productivity is highest. Thus, a global areal increase of shelf seas will cause an increase of the amount of carbon buried in sediments. As the isotopic ratio of C13 to C12 in organic matter is considerably lower than that in the carbon dioxide-carbonate reservoir, sequestration of organic matter is one of the prime control on the C13 to C12 ratio. In other words, the greater rate of organic carbon burial, the higher the $\delta^{13}C$ in sea water will be (Jenkyns, 1996).

Jenkyns (1996) examined evidence of sea-level rise in the Middle Oxfordian (transversarium Zone) of Europe and other regions and discerned that most localities demonstrate regional overstepping and/or evidence of shoreline retreat and/or evidence bathymetric deepening. Correspondence of these events in the transversarium Zone to noticeable $\delta^{13}C$ excursions indicates that a significant sea-level rise took place at this stratigraphic interval. Consistency of these data with those of the QEC, as well as the sea-

level change in Corallian and Swiss sections described above (Figure 19), clearly indicates that the Middle Oxfordian sea-level rise represents a global eustatic event. The peak of this rise occurred most likely at the base of the transversarium (parandieri Subzone).

In many cases, faunal provinciality makes it difficult to correlate the timing of facies evolution and interpreted events of sea-level change dated on the basis of biostratigraphy. Particularly, Boreal-Tethyan correlation has long been a major problem in biostratigraphy, especially for the Late Jurassic.

There is a reasonably good correlation established between Submediterranian, Subboreal (NW European), and Boreal provinces for the Callovian to Early Oxfordian interval because of the presence of the same ammonite taxa. However, after the Early Oxfordian, the ammonite zonations become very different because of significant increase of provincialism of the ammonite groups. For example, there are three parallel Mid Oxfordian ammonite zonal schemes for Boreal, Subboreal, and Tethyan regions (Figure 19). In addition, there are different correlations suggested in different publications. Mesezhnikov (in Krymholts et al., 1988) takes the alternoides zone of the Russian Platform as correlative to the boreal glosense Zone (Sykes and Surlyk, 1976) which, in turn, correlates to the British cautisnigrae Zone. However, in later publications Jenkyns (1996) shows that only the uppermost part of glosense Zone corresponds to cautisnigrae and the major lower part is correlative to the transversarium/pumilus Zone of Subboreal and Tethyan provinces. As such, the major part of alternance Zone of the Russian Platform may be in the Middle Oxfordian. Note that use of the zonal/subzonal scale from Jenkyns (1996) resulted in closest correlation of the sea-level events from the QEC, Corallian sections (Sun, 1989), and Swiss Jura (Gygi, 1986). This suggests that this version of interregional correlation for Mid Oxfordian is the best to date. It also provides an example of the application of eustasy to enhance interregional correlation.

Summarizing the review of Oxfordian sea-level change I conclude the following:

1) A significant eustatic fall occurred at the Early/Middle Oxfordian boundary;

2) Middle Oxfordian interval marks a period of eustatic rise and subsequent highstand. Some minor eustatic fall occurred in latest Middle Oxfordian and was followed by another eustatic rise;

3) Eustatic fall took place in the Late Oxfordian at the base of the upper zone (pseudocordata/ravni) and was followed by the late Oxfordian-Early Kimmeridgian eustatic rise.

Kimmeridgian

Wignall (1991) analyzed mud-dominated Kimmeridgian sections of England and Northern France in order to test the concept of sequence stratigraphy and Global Cycle Chart of Exxon (Haq et al., 1988). As a result he identified five depositional sequences within the Lower Kimmeridgian portion (Figure 20). At this point it is important to note that the British Lower Kimmeridgian is correlative to the entire Kimmeridgian of the boreal sections, whereas the Upper Kimmeridgian is an equivalent of boreal Lower Volgian with panderi Zone of Middle Volgian, respectively. The depositional sequences consist of a coarsening upward succession of clay/mud to silt and are separated from each other by basal erosion surfaces marked by basal layers of phosphatic pebbles or shell beds. All these surfaces are laterally extensive and do not vary in character from proximal zones to the central basin. This suggests that the unconformities formed from widespread synchronous tectonic movements or global eustatic variations. Another important point is that in the eudoxus Zone the distribution of black shales expanded throughout most of Southern England, indicating a widespread deepening event (Figure 20).

As Wignall (1991) noted, the only one of the interpreted surfaces which is unconformity (K3) within cymodoce Zone of Lower Kimmeridgian has a correlative in the Haq's (1988) curve (143 sequence boundary). Comparison of the Wignall's sequences

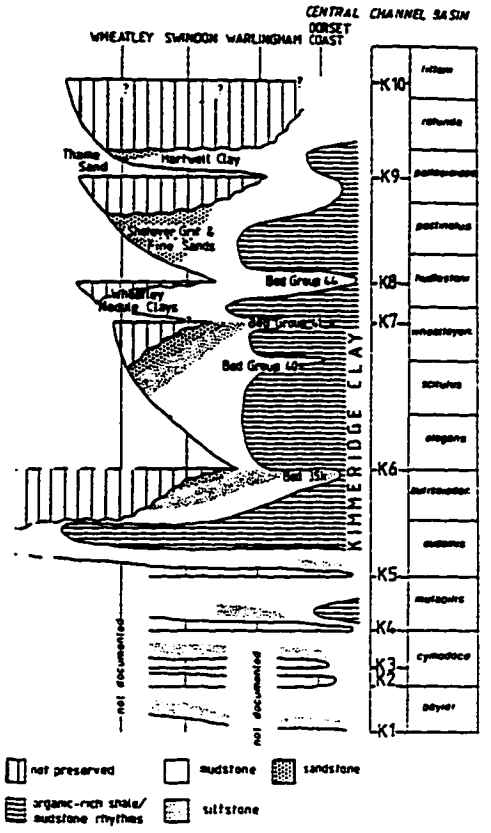

Figure 20. Coastal onlap patterns of Kimmeridgian strata of the southern England sections, (from Wignall, 1991).

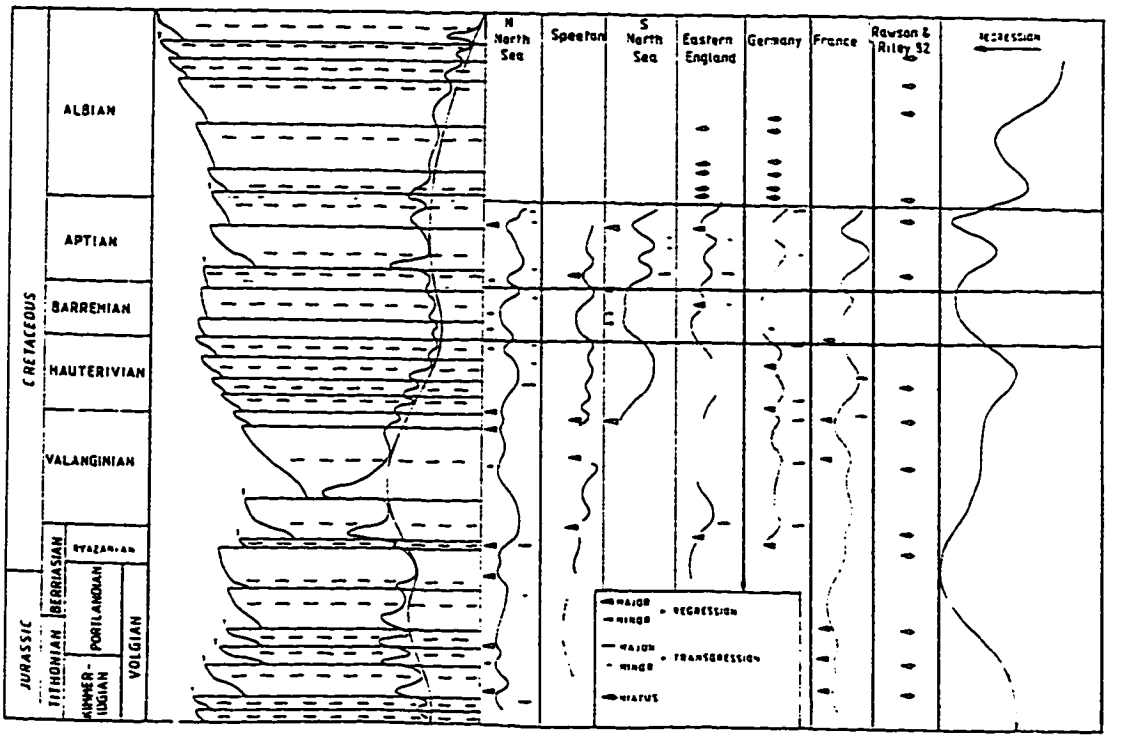

Figure 21. Summary diagram of the Lower Cretaceous sea-level change in the Western Europe, (from Ruffel, 1991)

to the QEC also revealed a correspondence for only one event which is a sea-level fall at the Lower/Upper Kimmeridgian boundary (corresponds to K5 SB). Upper Kimmeridgian on the Russian Platform is usually incomplete and areally limited due to significant post-depositional erosion. The gray clays of the Gorkinskaya Formation are usually assigned to eudoxus zone and only in few places they exhibit ammonites of the mutabilis Zone in their basal parts (Olferiev per comm.). This suggests that the peak of sea-level rise occurred during the eudoxus Zone which is consistent with the timing of black shale expansion in Southern England.

Summarizing, I conclude that the sequence boundaries (except K5) identified by Wignall (1991) were formed as a result of widespread uniform tectonic movements that occurred in the basins of England and Northern France in the Kimmeridgian. Unconformity K5 at the Lower/Upper Kimmeridgian boundary corresponds to sea-level fall on the QEC, and therefore, is interpreted to have been eustatically forced. The peak of the eustatic rise in Kimmeridgian most likely occurred during eudoxus Zone which is supported by black shale expansion in Southern England.

Lower Cretaceous

Ruffell (1991) compared Lower Cretaceous sedimentary successions from many regions of Western Europe in order to evaluate sequence stratigraphic patterns and examine relative sea-level change. The area of study included: North Sea basins, Southern England, Paris Basin, Atlantic margin basins, and Tethyan regions of southern France. He summarized West European sea-level change as a transgression/regression curve (Figure 21), which provides an interesting comparison for testing the QEC.

For the Valanginian interval Ruffel assumes that the presence of so-called non-sequences in many areas may result from climatic changes or a series of transgressive-regressive events reworking sediments for a long period. The latter is in accordance with the QEC that shows a series of five cycles of eustatic oscillations. This fact may be evidence for justification of the Valanginian portion of the QEC.

Hauterivian portion of the Ruffel's curve shows no agreement to the QEC. This interval primarily reflects relative sea-level change on France and North Sea region which is different from that of the Speeton sections of Yorkshire (Figure 10 in Ruffell, 1991). On the other hand, transgressive-regressive trends of the Speeton show similar patterns to those of the QEC. These include sea-level rise at the basal part, maximum sea-level fall in the middle part of the stage, and continuous rise during the Late Hauterivian to the peak at the Hauterivian/Barremian boundary. Thus, the Speeton sections may have been formed under the dominant influence of eustasy, while France and the North Sea experienced significant tectonic activity during the Hauterivian.

There is a remarkable correspondence between the QEC and the "European curve" of Ruffel (1991) for Barremian through Lower Albian interval (Figure 21). Although the minor-scale variations are beyond the resolution of the Ruffel's curve, the agreement for the long-term change is virtually one-to-one. The both curves exhibit general sea-level lowering during the Barremian. The Upper Barremian interval of the QEC is shown with dashed line because no sediments of this age are preserved in the central Russian Platform due to extensive post-depositional erosion resulting from significant sea-level fall. The close agreement with the "European curve" supports our interpretation. In the Aptian both curves indicate continuous sea-level rise to a peak in the latest Early Aptian with subsequent high-amplitude fall to the end of the stage. It is followed by sea-level rise in Early Albian. For this event the QEC shows a considerably lower amplitude. This may result from some inaccuracy involved in paleobathymetric analysis of Lower Albian sediments of the Russian Platform. The amplitude of the sea-level rise could have been

higher (than QEC shows) because of the extensive marine transgression detected in the West Siberian basin for the Lower Albian interval (Nezhdanov et al., 1992). I conclude that despite minor differences in amplitudes and low-scale events, agreement between the QEC and the European curve of Ruffel (1991) suggests that the QEC represents the correct eustatic history for the Early Cretaceous.

Comparison of the Ruffel's curve to the Exxon's one revealed a considerably less agreement (Ruffell, 1991) (Figure 21) which, once again, argues in favor of the QEC.

Upper Cretaceous

In its general trend, the Quantified Eustatic Curve agrees particularly well with those of Weimer (1984) (using the Obradovich & Cobban timescale) for the Upper Cretaceous of the U.S. Western Interior. Our Quantified Eustatic Curve includes some high frequency oscillations which do not appear on the Wiemer curve, but at the level of major events, the agreement is excellent (Figure 22). In addition, the latest data of absolute chronostratigraphy from the Albian interval of the Western Interior Seaway confirm sinchroniety of events such as the Late Albian sea-level rise and pre-Cenomanian fall on the central Russian Platform and U.S. Interior (Obradovich per. comm.).

It is particularly noteworthy that both the Russian Platform and the U.S. Western Interior were covered by shallow cratonic seas during the Late Cretaceous. This is another confirmation of our interpretation that in epeiric cratonic seas eustasy plays more important role for controlling sedimentation patterns than it does in passive margin settings.

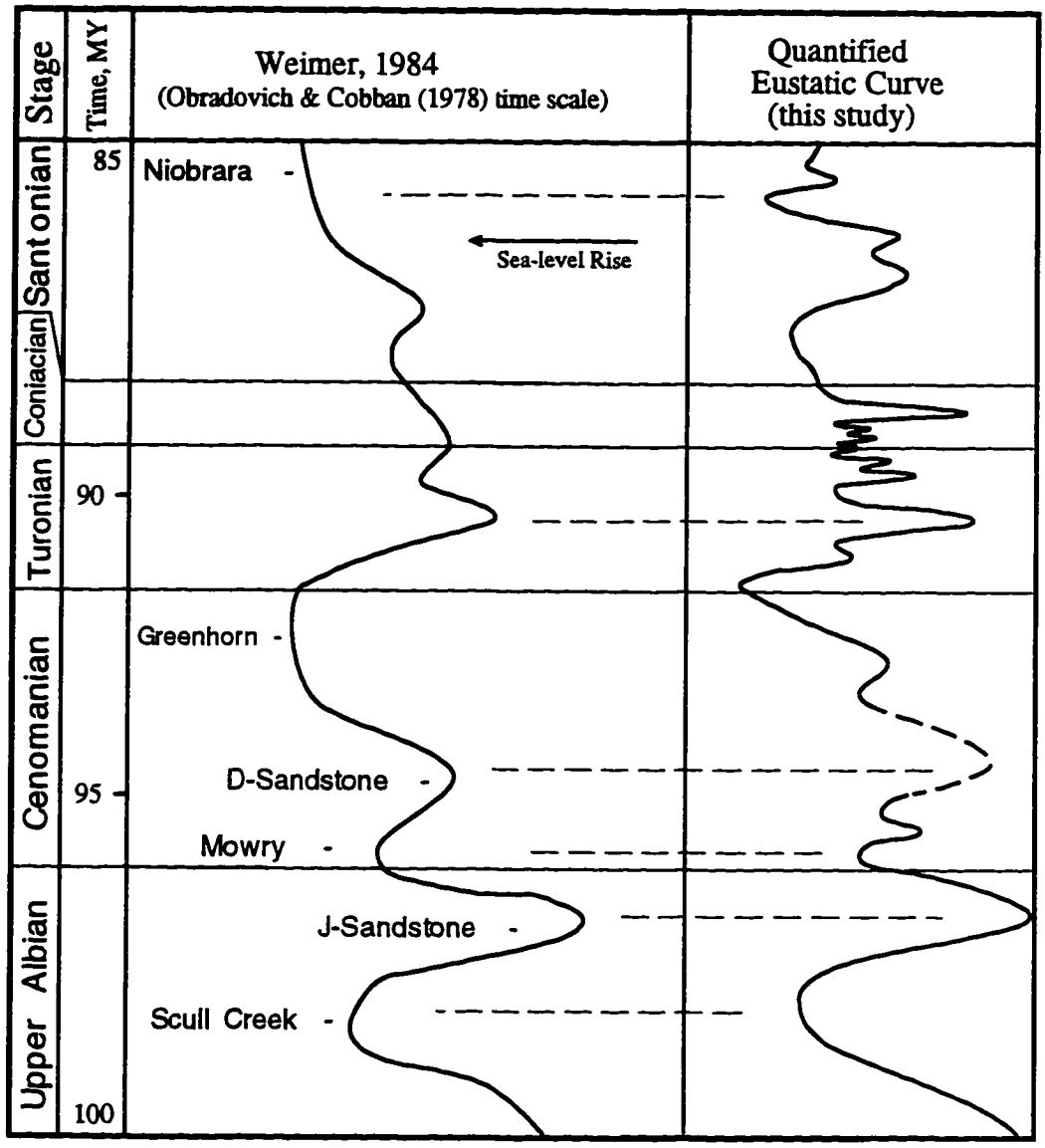

Figure 22. Sea-level curve for the Late Albian - Santonian of the U.S. Western Interior. After Weimer (1984).

Conclusion

Results of comparison of the Quantified Eustatic Curve with sea-level curves from other regions can be summarized as follows:

1) Exxon's curve, providing a reasonably good picture for long-term eustatic change, fails at the level of higher-order resolution (3-rd and higher order eustatic cycles);

2) The eustatic origin is confirmed (based on their global occurrence) for the following events:

- Eustatic rise in the Late Bathonian
- Late Callovian eustatic rise and subsequent highstand during the Earliest Oxfordian
- Eustatic fall during the late Early Oxfordian to the minimum at the Early/Middle Oxfordian boundary
- Significant eustatic rise in the Middle Oxfordian with maximum highstand in transversarium (=ilovaisky) Zone
- Eustatic fall in the Late Oxfordian (uppermost serratum Zone)
- Significant sea-level rise in the Late Oxfordian (base of pseudocordata/ravni Zone) continued to Early Kimmeridgian;

3) Subsequent more extensive testing is needed for the following intervals that demonstrate good agreement between the curve but include some minor discrepancies:

- Early to Middle Callovian
- Kimmeridgian
- Hauterivian
- Aptian
- Late Albian - Turonian

CHAPTER III

WEST SIBERIAN BASIN: SEQUENCE STRATIGRAPHIC ANALYSIS AND TESTING THE QUANTIFIED EUSTATIC CURVE

Introduction

West Siberian Basin is an ideal place to test the applicability of the Quantified Eustatic Curve because of its contrasting tectonic setting and its well-defined high-resolution biostratigraphic correlation with the Russian Platform. Testing against other basins with well established biostratigraphy (such as boreal sections of Western Europe) may not be as rigorous a test as that provided by West Siberia because of faunal provincialism for some periods of time (see the previous chapter).

The West Siberian Basin (Figure 23) is one of the largest Mesozoic sedimentary basins in the world (second only to the Persian Gulf), with an area of 1.4×10^6 km^2 (Tamrazian, 1990). Mesozoic strata lie at 1-3 km depths in the central part of the basin and partially crop out at the margins. As the largest petroleum province in Russia, the West Siberian basin has been extensively explored (Ulmishek and Masters, 1993). Since the late 50's, large highly productive oil fields have been discovered in Jurassic, Neocomian, and Upper Cretaceous sediments (Rovenskaya and Nemchenko, 1992). Detailed exploration has resulted in tens of thousands of wells in the basin in addition to detailed seismic and well-log data.

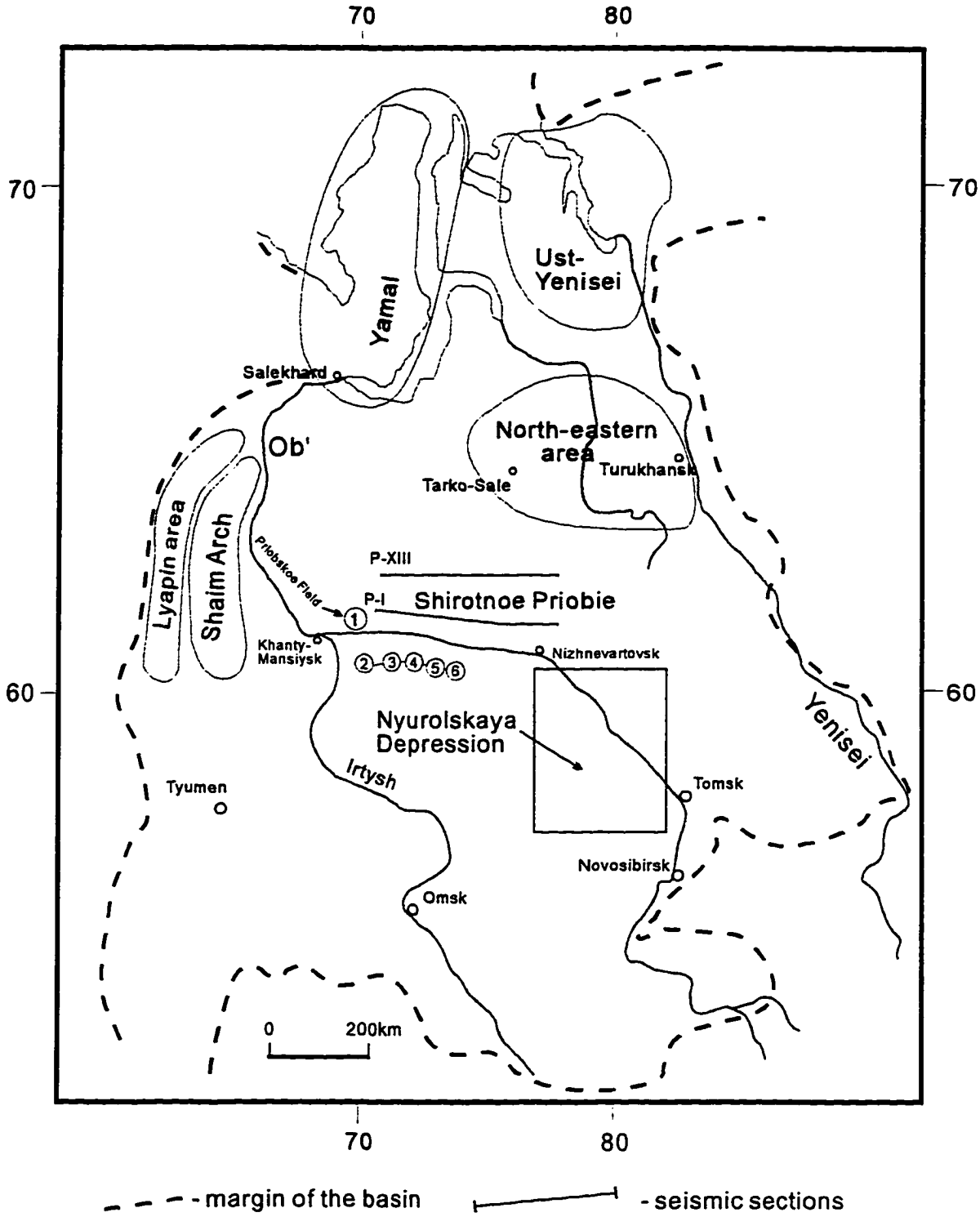

Figure 23 . Locations of Study in the West Siberian Basin

The geological/geophysical studies of West Siberia have been performed mainly by local governmental organizations concerned with specific oil fields within the basin. These studies have largely focused on geophysical methods of subsurface stratigraphic analysis. Less attention has been paid to other methods such as biostratigraphy, sedimentology, and facies analysis. This has resulted in major problems in intra-basin correlation and general synthesis at basin scale (Mesezhnikov, 1989). More comprehensive academic studies of the West Siberian Basin, conducted by various organizations in Moscow, St. Petersburg, Tyumen, and Novosibirsk have led to some understanding of the large-scale basin structure and history (Kunin et al., 1993; Nezhdanov et al., 1992; Vyachkileva et al., 1990). However, their stratigraphic interpretations have often strongly disagreed with each other because of different operating assumptions and stratigraphic conceptualizations as well as different regional biases caused by the previous Soviet structure of data distribution and propriety. This indirectly resulted in decrease of hydrocarbon production for the region in general.

The largest anticline petroleum reservoirs with simple structures (including giants such as the Samotlor and Salym reservoirs) have been significantly depleted, and exploration priorities are being reoriented toward smaller traps which collectively represent a significant total volume (Ulmishek and Masters, 1993). However, exploration of these reservoirs requires very detailed stratigraphic data and models because of their complicated structure and zoning. For example, during exploratory drilling in Upper Jurassic of the Shaim region in 1980s, each third well was dry (Kliger, 1994). This waste of time and resources may have arisen from insufficient attention to the quality of stratigraphic interpretations. The integration of various types of stratigraphic data and formulation a self-consistent basin-scale model of sedimentation is presently one of the most important problems for oil exploration in West Siberia. In recent years, new detailed data have been obtained by extensive seismic exploration and increased drilling activities

in new areas and stratigraphic intervals, but an appropriate basin-scale synthesis is still lacking.

During the last decade, application of the sequence stratigraphic concept in stratigraphic analysis has become an essential tool in geology, e.g. (Weimer and Posamentier, 1993). A useful aspect of sequence stratigraphy is that it makes it possible to integrate all available multidisciplinary information into a self consistent geologic model. Sequence stratigraphic analysis has never been performed at basin scale in West Siberia, but would help solve various problems in stratigraphic interpretation, and for resolving discrepancies between local interpretations. This was highlighted at the symposium on the Sequence Stratigraphy of Russian Basins at VNIGRI in St. Petersburg (May 15-19, 1995).

Consequently, in this work I present one of the first sequence stratigraphic analyses of the Mesozoic strata of several regions in West Siberia. The application of the Quantified Eustatic Curve will greatly improve the final interpretations and may set a stage to further development of sequence stratigraphic concept.

West Siberian Basin - general review

Basin formation and fill

The basement underlying the West Siberia consists of folded Paleozoic and Precambrian rocks and was generally consolidated by the Middle Triassic (Milanovsky, 1987). During the Middle and Late Triassic, the basin formed by rifting and aulacogen formation, followed by deposition of flat-lying clastic and volcanic rocks. These are overlain by predominantly siliciclastic sediments of Jurassic, Cretaceous, Paleogene,

Neogene, and Quaternary age (Ulmishek, 1993). The thickness of Mesozoic-Cenozoic sedimentary cover increases northward from an average 2-3 km in the south up to 4-6 km along the coast of the Kara Sea (Nalivkin, 1973). The total sedimentary volume provided to West Siberia in Meso-Cenozoic time by the East Siberian Highlands, Kazakhstan, and the Urals has been estimated as equivalent to erosion of 20-30 Caucasus ranges (Nalivkin, 1973).

Summary of West Siberian Jurassic-Neocomian Sedimentation.

Lower-Middle Jurassic (Hettangian-Mid Bathonian). During the Early and Middle Jurassic (Hettangian-Bathonian), West Siberia was a low plain with predominantly fluvial and lacustrine sedimentation (Peters et al., 1993), with marine conditions only in the north (Yamal and Ust-Yenisei, Figure 23). The marine sections are characterized by cyclicity which Nezhdanov (1990) attributed to eustatic variations. During the most prominent transgressive events, marine sedimentation temporarily expanded southward to the Shaim-Krasnoleninsk region, producing uniform shales containing marine faunas in the central basin (such as the Toarcian Togur Member).

Upper Jurassic (Late Bathonian-Volgian). A major Late Bathonian transgression brought marine conditions to most of the basin which persisted until the Early Barremian. The transgression produced considerable accommodation throughout the basin which was later filled with Callovian-Neocomian sediments (Figure 24) derived primarily from the East Siberian Highlands and also from the Urals (Milanovsky, 1987). During Callovian-Kimmeridgian time prograding clinoformal units were deposited in the marginal parts of the basin (Nezhdanov, 1990). The clinoforms generally consist of thick sands and silts

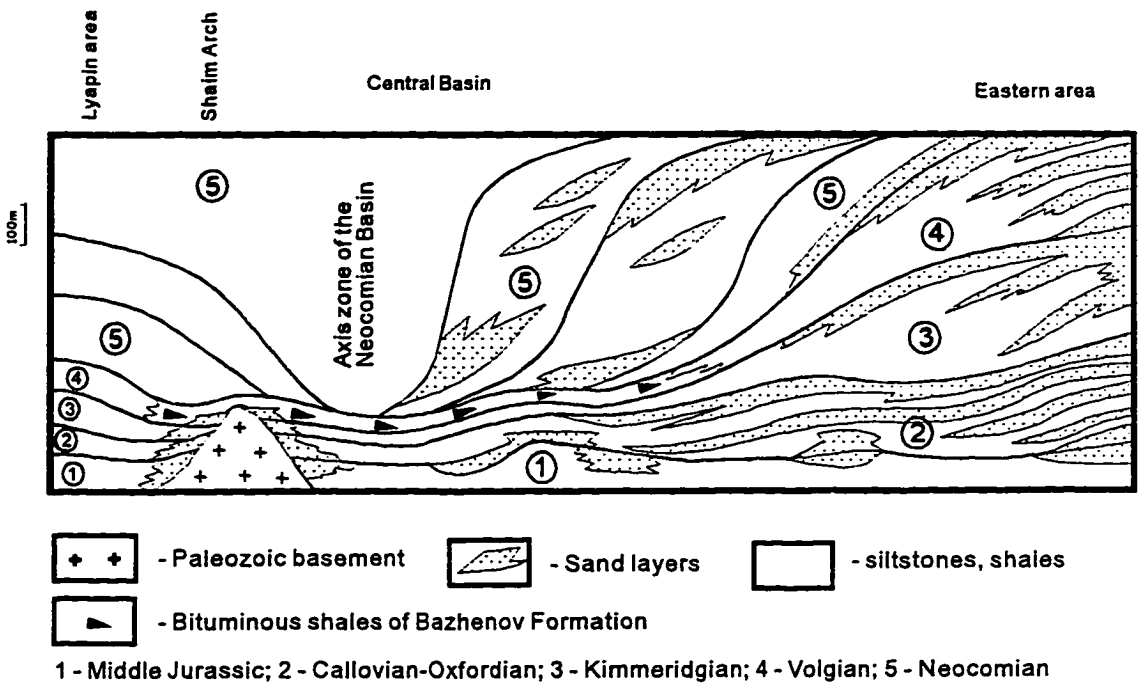

Figure 24. Simplified latitudinal stratigraphic cross-section of the Bajocian to Neocomian of the West Siberia. Adapted from Nezhdanov et al. (1992)

(100-200m) separated by thin shales (Nezhdanov, 1990), suggesting a series of marine transgressions throughout Callovian-Kimmeridgian time. The clinoforms grade to thinner shales toward the west (central basin) (Figure 24). The central basin maintained deep marine conditions throughout this time resulting in the deposition of the thin (10-30 m), shales of the Abalakskaya formation (Nezhdanov, 1990).

The character of sedimentation on the western flank of the basin contrasted with that of the east. During most of Mesozoic deposition, the Urals provided predominantly fine (muddy and silty) material which accumulated mostly in the Lyapin sub-basin (Figures 23, 24). The Berezovo and Shaim arches represent a paleo-island chain which divided the Lyapin depression from the central basin. Significant erosion of the island coasts (Nezhdanov, 1990) during subsequent marine transgressions resulted in deposition of coarse grained sediments that grade basinward (east and west) to finer grained silty and shaly units.

In the Early to Middle Volgian a major subsidence phase (Kunin et al., 1993), coincided with a eustatic highstand. As a result, the area of marine sedimentation expanded greatly and a single, deep-water basin formed. All previously existing islands (Shaim and Berezovo regions) were submerged and the organic-rich Bazhenov Formation was deposited (Figure 24). The Bazhenov Formation is the main oil bearer of West Siberia (accounts for more than 85% of West Siberian oil) and is one of the largest oil-generating systems in the world (Peters et al., 1993).

Cretaceous. During the Neocomian, a series of clinoforms prograded and eventually filled the accommodation when eastern and western clinoforms met in the axial part of the basin (Figure 24) in the Late Hauterivian-Early Barremian (Milanovsky, 1987). The sedimentary complex formed during this time (termed "Clinoform Neocomian") contains the richest petroleum reservoir of West Siberia. During the Barremian, marine sedimentation occurred in long (about 2000 km) and narrow (50-150 km) sub-meridianal

strip in the central part of the basin. This zone has been termed the "remnant channel zone" by local geologists (e.g. Kunin et al., 1993).

The Aptian-Cenomanian interval is represented by continental deposits intercalated with occasional shaly marine beds. The uniform shale unit that formed during the Late Albian eustatic highstand is a prominent example of these, and can be traced throughout most of the basin. The Cenomanian sediments of West Siberia consist primarily of sandy continental facies. In the Early Turonian, the largest transgression since the Volgian (when the Bazhenov Formation was deposited) led to development of a marine basin throughout West Siberia (Braduchan et al., 1986; Nezhdanov et al., 1992). During Late Turonian to Maastrichtian time, deposition of prograding clinoformal units filled the available accommodation in a scenario comparable to Neocomian deposition.

Review of existing stratigraphic models

Copious stratigraphic data are available for the West Siberian Basin. However, the regional interpretations disagree because of: a) different and incomplete data including local biases; b) limited interpretation methods; and c) the complex architecture of some West Siberian depositional units. The resulting depositional models of West Siberian Mesozoic stratigraphy have not benefited from modern sequence stratigraphic conceptualization. This shortcoming was recently addressed during a symposium on the Sequence Stratigraphy of Russian Basins at VNIGRI in St. Petersburg (May 15-19, 1995).

In this section we focus on the Neocomian section as an example of the discrepancies in stratigraphic modelling that may be reconciled through sequence stratigraphic methods. The stratigraphic analyses in West Siberia in the 1960's and 70's were conducted primarily on the basis of geophysical (well log and seismic) methods. For example, seismic investigation of the Neocomian complex during that time was restricted to tracing the most continuous reflecting shale units such as the Bazhenov (Upper

Jurassic), Alym (Lower Aptian), and Kuznetsov (Upper Cenomanian-Lower Turonian) Formations. The correlation of strata within the complex was primarily performed by well logging methods with lithostratigraphic control from cores. However, biostratigraphic methods were not generally utilized, and biostratigraphic data were commonly used only for age dating of the units defined by geophysical methods, but not for linking biofacies to chronostratigraphic units.

One of the stratigraphic models that synthesized the results of the stratigraphic studies of the 60's to early 80's was developed by researchers from ZapSibNIGNI (Tyumen city). Based on this model, they also constructed a regional stratigraphic scheme of the Mesozoic which was approved by International Stratigraphic Commission in 1978. The ZapSibNIGNI model of geologic structure was based on the assumption that the Neocomian complex and other sedimentary units were uniformly deposited on flat lying depositional surfaces. According to this model, the Neocomian complex, for example, consists of generally flat-lying subparallel strata (Kunin et al., 1993). In latitudinal cross-section, sand layers grade westward to shales, and antiform-type structures act as petroleum traps. All non-horizontal structure was attributed to post-depositional tectonic activities. Thus, this model assumed that most sediments were deposited on the shelf, and does not allow for slope processes or progradation. While some alternative stratigraphic models without "flat" deposition were suggested (Naumov et al., 1977), most West Siberian geologists accepted this flat model during the 70's and early 80's because of its simplicity and its apparently successful application to oil accumulations in simple structures.

In the early 1980's, highly-productive stratigraphically trapped petroleum reservoirs were discovered in the deltaic Neocomian complexes of the Priobskoe and Prirazlomnoe fields. The first attempts to correlate sand strata in these complexes by traditional

methods of "flat" geology failed in those cases (Kunin et al., 1993). At the same time, improvements in seismic resolution brought out much smaller-scale features of subsurface geometry. The fine-resolution seismic modelling of the Neocomian and other intervals revealed clinoform structures. In addition, additional biostratigraphic data collected by that time showed numerous fundamental contradictions in the flat "ZapSibNIGNI model". As a result, some alternative stratigraphic models were suggested, based primarily on 2-D seismic interpretations (Kunin et al., 1993; Mkrtchyan et al., 1990; Sosedkov et al., 1987). These approaches consisted of identifying seismic facies based upon reflection configurations and terminations, and geometrical shapes of units (traditional "first sight" seismostratigraphic approach). Seismic units were suggested as the basis for stratigraphic subdivision and correlation. For example, (Kunin et al., 1993) subdivided the Neocomian section of the Shirotnoe Priobie area into a series of formal seismostratigraphic units - "seismopackets" corresponding to laterally progressive clinoforms. Each "seismopacket" in its turn was subdivided into smaller scale units - "seismoquants". These seismic units are classified according to their external geometry and distribution of depositional systems into "extremely transgressive, moderately transgressive, regressive", and other types. Although useful for rough estimation of regional variations, in many cases this approach does not provide reliable reconstructions of sedimentation history because it is based on only a single class of information (seismic).

A popular alternative approach is "lithmo" or cycle stratigraphy (Karagodin and Nezhdanov, 1988; Nezhdanov, 1990), based on the assertion that any sedimentary section can be subdivided into universal units ("cyclites") that form during transgression-regression cycles. According to this concept, the Mesozoic section of the West Siberia is subdivided into 12 regional "cyclites", each of which is in turn subdivided into smaller scale zonal cyclites. The model was successfully applied to the Priobskoe and numerous

other petroleum fields (Karagodin et al., 1996; Karagodin et al., 1991). Karagodin and Armentrout (1996) conducted a comparative analysis of definitions and terms of lithmostratigraphy with those of sequence stratigraphy. The conclusion of this paper is that the main difference between the two concepts stems from the fact that unlike lithmology, sequence stratigraphy is based on genetic relationship of stratal units as a result of dynamic development of depositional systems within a basin. The basis of lithmostratigraphy is a time relationship of certain lithologic features in a vertical section (Karagodin and Nezhdanov, 1988). In other words, lithmostratigraphy is an approach that makes it possible to subdivide stratigraphic sections into formal units (cyclites) on a basis of change of certain parameters (usually grain size) in the vertical direction. Therefore, unlike sequence stratigraphy that provides explanation for dynamic development of sedimentary patterns in 2D to 3D systems, lithmologic concept implies a restrictive 1D approach. This directly results in the lack of classification for unconformable surfaces (such as transgressive surface, maximum flooding surface, and sequence boundaries of sequence stratigraphy) in the lithmostratigraphy. In addition, Karagodin and Armentrout (1996) mentioned that the relationship of cyclites to facies models and dynamics of depositional systems is a very important, but entirely undeveloped aspect of lithmostratigraphy. And finally, it should be noted that the lack of genetic basis in lithmostratigraphic concept renders it impossible to predict stratal geometries and development of depositional systems which is one of the most attractive utilities of sequence stratigraphy (Weimer and Posamentier, 1993).

Summarizing, there have been three main approaches in the basin stratigraphy and depositional history of West Siberian Mesozoic section: 1) traditional approach of interpretation of the entire section as a stack of sub-parallel, generally flat-lying units (ZapSibNIGNI); 2) seismostratigraphic reconstruction based mainly on seismic facies (Kunin et al., 1993; Mkrtchyan et al., 1990); and 3) "lithmostratigraphic" concept based on the postulate of universal cyclicity (Karagodin and Nezhdanov, 1988; Nezhdanov,

1990). Each has only limited value for multidisciplinary basin-scale stratigraphic analysis because they rely either on particular assumptions or are based on a single type of data and thus lead to inconsistencies when applied to units other than those for which they were specifically designed.

Sequence stratigraphy is one of the most powerful tools in stratigraphic analysis and makes it possible to integrate all available multidisciplinary information into a geologically sound model (Weimer and Posamentier, 1993). The application of sequence stratigraphic methods to the West Siberian Basin should make it possible to integrate the various types of available stratigraphic data and formulate a consistent model of basin sedimentation for the second largest Mesozoic basin in the world.

Data Availability.

West Siberia is spanned by a series of regional seismic profiles that cover the basin latitudinally and longitudinally. Two of them were specifically used in this study (Figure 23). Thousands of exploratory and productive wells have been drilled throughout the basin. On the basis of available cores, wells may be classified as: 1) regional key wells (full cores from surface to basement); 2) specialized key wells which are reference wells for local second order structural elements (depressions, swells, troughs, etc.) or oil fields from which full cores are available from productive intervals (e.g. entire Neocomian, Upper Jurassic, etc.). There are 20 to 120 such wells in each oil field; 3) regular wells from which short cores are available only from productive beds or traps (e.g. Bazhenov Fm.).

Geophysical data (seismic and well log) are usually of good quality and were used directly, but a significant part (30-50%) of the sedimentologic interpretations and descriptions are from old sources (1960's - 70's), and will require significant effort in the future to bring "up-to-date". In addition, there are few interpretations regarding

sedimentary structures, and no detailed facies analyses have been performed for most available cores. Thus, a significant future task for West Siberian geologists will be reexamination of the sedimentologic data and facies modeling.

Biostratigraphy/paleoecology provide "up-to-date" high quality, detailed information. Some biostratigraphic interpretations are out of date, but most have been recently reexamined in the Lab of Mesozoic Stratigraphy, Russian Acad. Sci., Siberian Branch. The biostratigraphy of all Mesozoic marine strata in West Siberia is based on reference fossils such as ammonites, bivalves, and belemnites, as well as microfossils and palynomorphs (Vyachkileva et al., 1990). The Middle Jurassic to Lower Cretaceous of W. Siberia includes some of the most fossiliferous rocks in the Boreal realm. Detailed zonal scales have been developed for this time interval based on numerous sections throughout W. Siberia and good correlation has been established with Western European chronostratigraphic standards (Krymholts et al., 1988). The presence of abundant ammonites in Middle Jurassic-Neocomian cores provides a rare opportunity to establish reliable age determinations and correlation. For paleodepth reconstructions there is a well established model based on macrobenthos and linked to micropaleontologic data (Zakharov et al., 1983).

Nyurolskaya Depression and vicinity

Introduction

The Nyurolskaya depression is located in the south-eastern part of West Siberia and covers western and northwestern parts of Tomsk and Novosibirsk Provinces, respectively. There has been extensive drilling and exploration due to the productivity of some stratigraphic intervals including marine Upper Jurassic-Neocomian, and continental Low-Middle Jurassic. A large proportion of the petroleum accumulations discovered in this

region is concentrated in Callovian-Oxfordian deposits of the Vasyugan Formation (Belozerov et al., 1989b).

The Southeast margin of West Siberia was a low shelf to low elevation coastal plain during the Bajocian-Kimmeridgian interval of time. The depositional setting was a low ramp that was periodically flooded and exposed due to frequent sea-level changes. As a result, it contains a good record of transgressions/regressions in proximal facies. Individual producing zones represent a variety of facies and locally demonstrate interruptions and internal heterogeneity.

The productive sandstone units range in thickness from 3 to 20 meters which is beyond the usual resolution of the seismic stratigraphic methods which have been applied to the region (Slavkin et al., 1996). However, high resolution sequence stratigraphic analysis based on examination of well logs and cores that are abundant for productive areas may help greatly for understanding the depositional histories and preserved facies architecture as well as sea-level reconstructions. We analyzed the data of the interpretations of about 150 well logs and 60 cores, focusing on the sections from Kaimysov Arch (Tomsk Province) and Mezhov Arch (Novosibirsk Province), from which four distinct depositional sequences were identified including transgressive systems tracts, lowstand complexes, incised valley fills, and highstand deposits.

Tectonic structure

The modern tectonic structure of the southeastern part of West Siberian basin can be described as a series of positive structures (arches and swells) that are separated from each other by zones of depressions or troughs (Figure 25). This is a direct result of vertical block movements of the basement that occurred mostly during the Lower-Middle Jurassic time (Belozerov, 1989). Nyurolskaya Depression was developed over the extinct Koltogorsky rift complex. Most Jurassic oil accumulations are concentrated in the Nyurolskaya Depression and surrounding positive structures including the Kaimysov

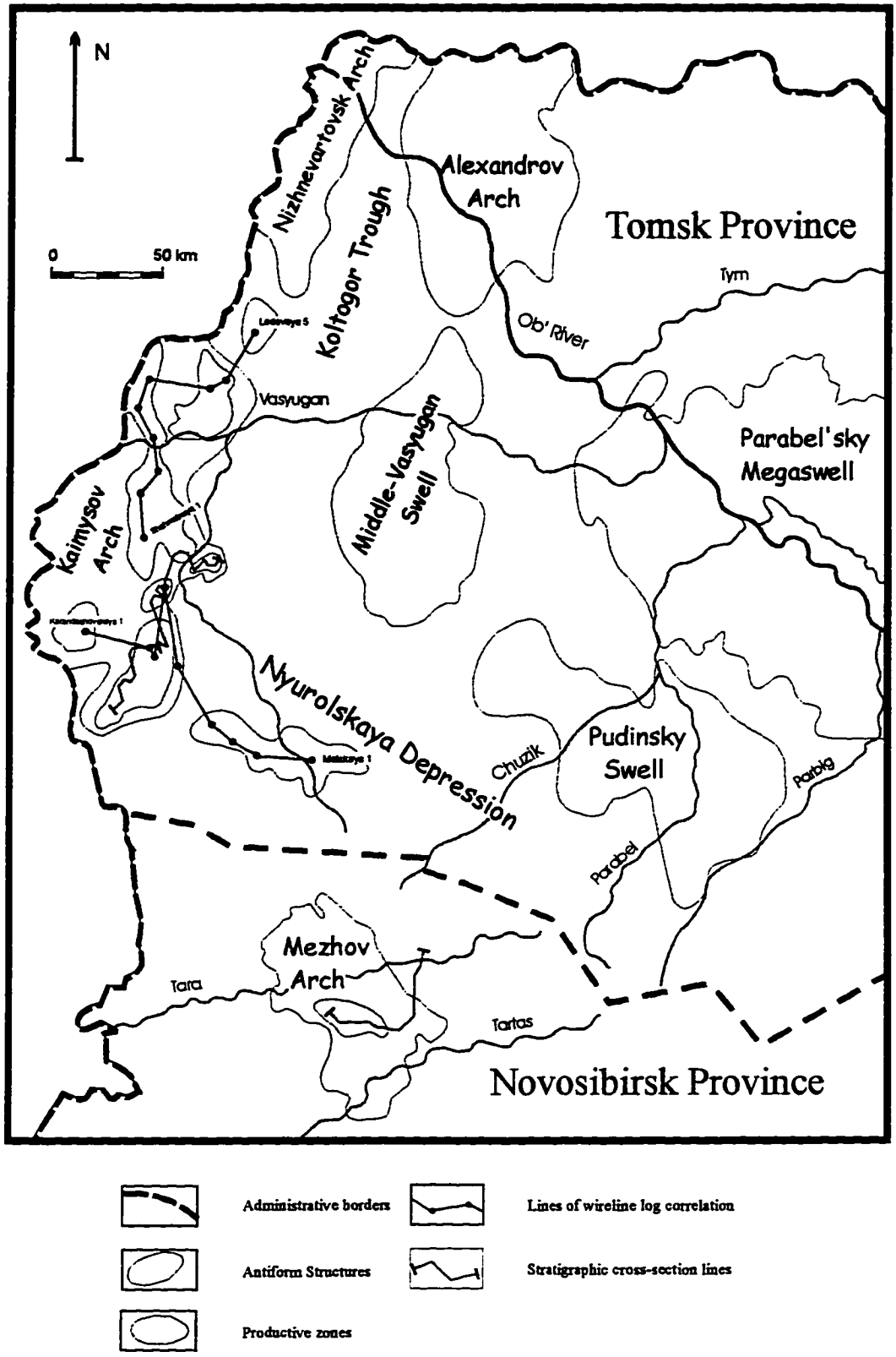

Figure 25. Locations of study in southeastern West Siberia

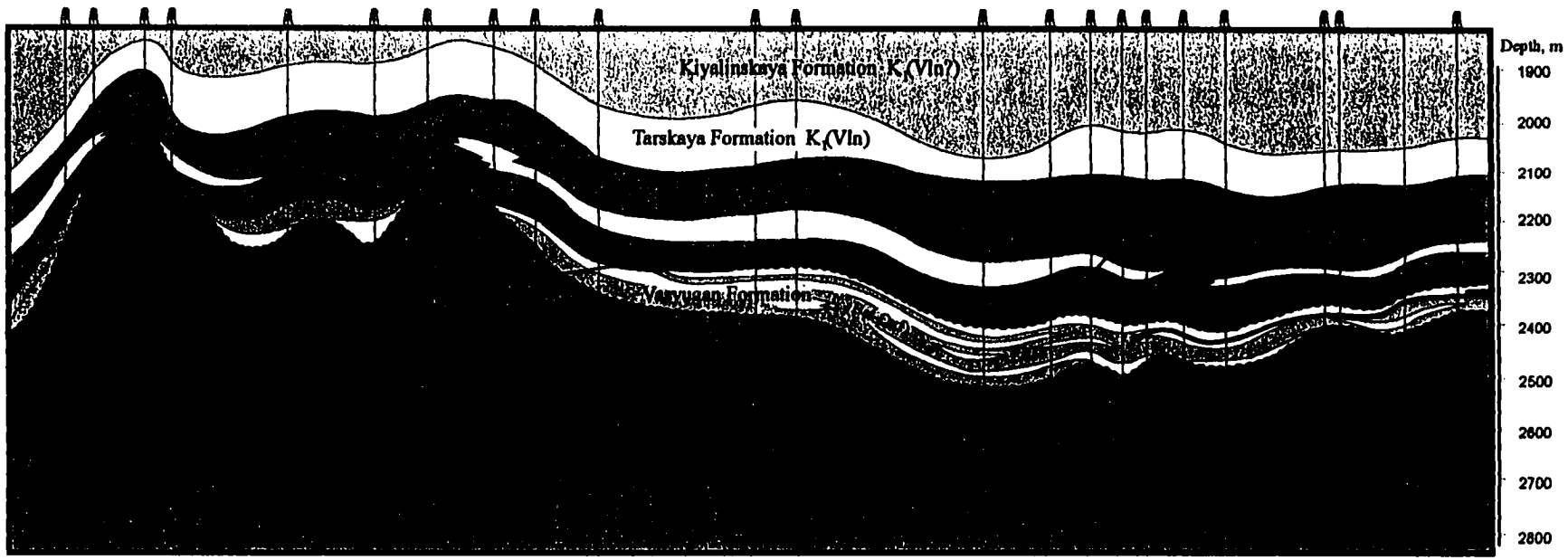

Legend:

- Continental deposits of the Kiyalinskaya Formation
- Marine shales of Tarskaya and Kulomzinskaya Formations
- Marine sandstones of Tarskaya and Kulomzinskaya Formations
- Sandstones of Vasyugan Formation, shallow marine and coastal plain facies
- Bituminous shales of Bazhenov Formation deep marine facies
- Shales and siltstones of Vasyugan Formation, shallow marine and coastal plain facies
- Continental sediments of Tyumenskaya Formation, various continental facies
- Paleozoic basement
- Coal beds
- unconformities

Figure 26. Generalized Stratigraphic Cross-Section of Jurassic-Neocomian of the Mezhov Arch Area

Arch, Alexandrov Arch, Nizhnevartovsk Arch, Mezhovsky Swell, Middle Vasyugan Swell, and Pudinsky swell (Figures 25, 26). From these, the richest oil fields are in the structural traps of the Nizhnevartovsk and Kaimysov arches that confine the Nyurolskaya depression from the north and west, respectively.

Depositional features

During Early Jurassic to Bathonian time the southeastern margin of the West Siberian Basin was a continental plain with a minor relief where mostly fluvial and lacustrine sedimentation occurred. The first extensive marine transgression occurred in Latest Bathonian time. Subsequently, deposition took place under dominating marine conditions except for the interval near the Early/Middle Oxfordian boundary when the entire area was subaerially exposed (Figure 27).

Paleotectonic reconstructions show that present antiform structures such as Kaimysov, Mezhov arches (and others) represented positive relief during deposition in Jurassic time (Figure 26). The remote position of the main clastic sources resulted in slow rates of sediment supply. In addition, very slow tectonic subsidence during the deposition significantly limited accommodational potential. As a result, these factors led to deposition of very thin stratigraphic patterns throughout the area. For example, the thickness of the whole Vasyugan Formation generally varies from 30 to 90 meters.

The deposition of Vasyugan Formation is characterized by frequent regional transgressions/regressions. During the relative sea-level falls the most elevated parts of the positive structures were subaerially exposed as islands (Figure 27). This resulted in a highly dissected geometry of the paleoshorelines that was constantly changing through time (Brylina and Danenberg, 1989). The stratigraphic patterns exhibit significant internal heterogenity due to facies variation and extensive local erosion.

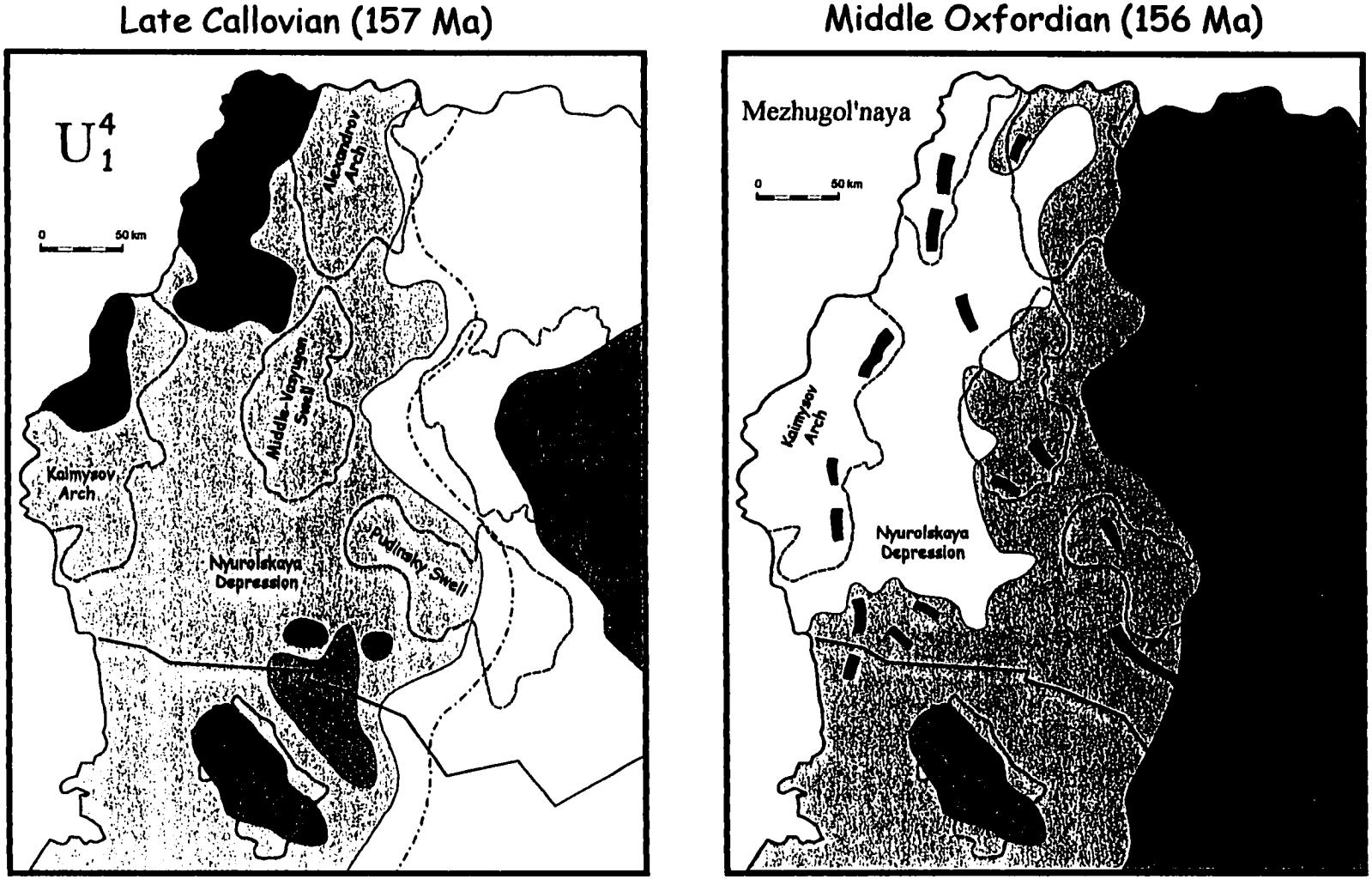

Figure 27. Callovian-Oxfordian Paleogeography of the Nyurolskaya Depression and viccinity (Adapted from unpublished technical reports)

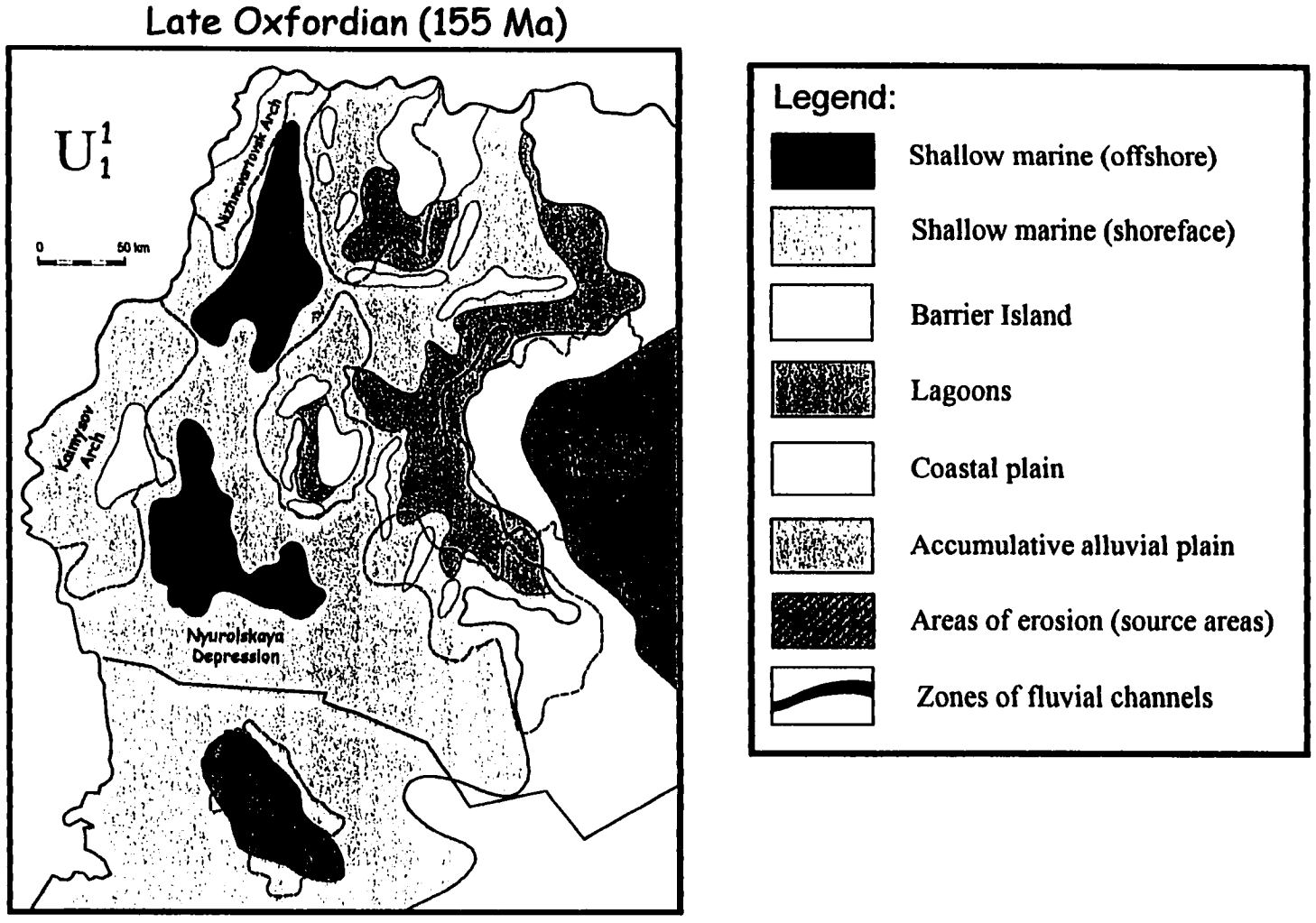

Figure 27. Paleogeography, continued.

Stratigraphic description

The Vasyugan Formation is conventionally subdivided into two subunits- the Lower Vasyugan (Shaly) Group and Upper Vasyugan (productive) Group (Belozerov et al., 1989a). The Lower Vasyugan Group includes the basal transgressive U1-0 bed and the upper Shaly Part. The Upper Vasyugan interval of section contains the main productive units including the indexed sandstone beds U1-1 through U1-4 (Tatianin and Volkov, 1982). It is subdivided into two parts by the continental Mezhugol'naya (Inter-coal) member. The lower part of the Upper Vasyugan Group is conventionally called the Podugol'naya (Sub-coal) Member and includes the U1-4 and U1-3 beds, whereas the U1-2 and U1-1 sandstone beds comprise the Upper Nadugol'naya (Above-coal) Member (Belozerov et al., 1989a).

Lower Vasyugan Group

The U2-0 unit at the base of Vasyugan Formation represents a basal bed of the Late Bathonian marine transgression. Varying in thickness from 0.5 to 5 meters, U2-0 consists of poorly sorted sandstones to siltstones with abundant siderite oolites and marine microfauna. It onlaps the sharp erosional unconformity developed over the top of continental sediments of the Tyumenskaya Formation (Figures 26, 28, 29).

The overlying Shaly Part of Lower Vasyugan Group consists of predominantly fine-grained sediments and reaches up to 55 meters in thickness. In the most complete sections it can be subdivided into three members (Belozerov et al., 1989a). The upper and lower members consist of shales with minor siltstones and sandstones and exhibit significant lateral variations. In contrast, the middle member is a mostly uniform and laterally extensive shale horizon. The age of the Lower Vasyugan Formation is determined as Early to Late Callovian, based on ammonite biostratigraphy, micropaleontology, and palynology.

Analysis of stratigraphic patterns and paleogeography suggest that Lower Vasyugan Formation was formed during relative sea-level rise and subsequent highstand (with a maximum during the deposition of the Middle member) (Belozerov et al., 1989a). There are no evidences of sea-level falls at the Lower/Middle and Middle/Upper Callovian boundaries, as suggested by the QEC. Among possible explanations, is an onset of a major regional subsidence phase in the southeastern West Siberia during the Callovian. Remote position of clastic sources resulted in a lack of coarse-grained materials, and fine-grained sedimentation of Lower Vasyugan was not affected during the eustatic falls.

Upper Vasyugan Group

Podugol'naya Member. Podugol'naya part of the section was formed during Middle Callovian to Early Oxfordian and generally displays a regressive trend. The thickness of the Podugol'naya unit varies from 4-5 meters at the central most elevated parts of the arches to 15-20 meters in the marginal parts (Slavkin et al., 1996) (Figure 28). The marginal sections are usually stratigraphically complete and exhibit clear differentiation of U1-4 from U1-3 by a layer of sandy shales between. The both sandstone beds are composed of coarsening upward medium to fine sandstones deposited in the upper shoreface facies. However, the sandstones of the upper U1-3 bed are usually better sorted and, at the same time, are less areally extensive. For example, U1-4 is present throughout the entire Kaimysov Arch, while U1-3 is absent in the most elevated areas due to post-depositional erosion (Slavkin et al., 1996).

Mezhugol'naya Member. Mezhugol'naya Member was deposited under continental conditions during the maximum of regional regression. Varying in thickness from 0 to 30 meters, it consists of intercalations of generally thin layers of shales, siltstones, and sandstones (Belozerov et al., 1989a). The most characteristic distinctive feature of the

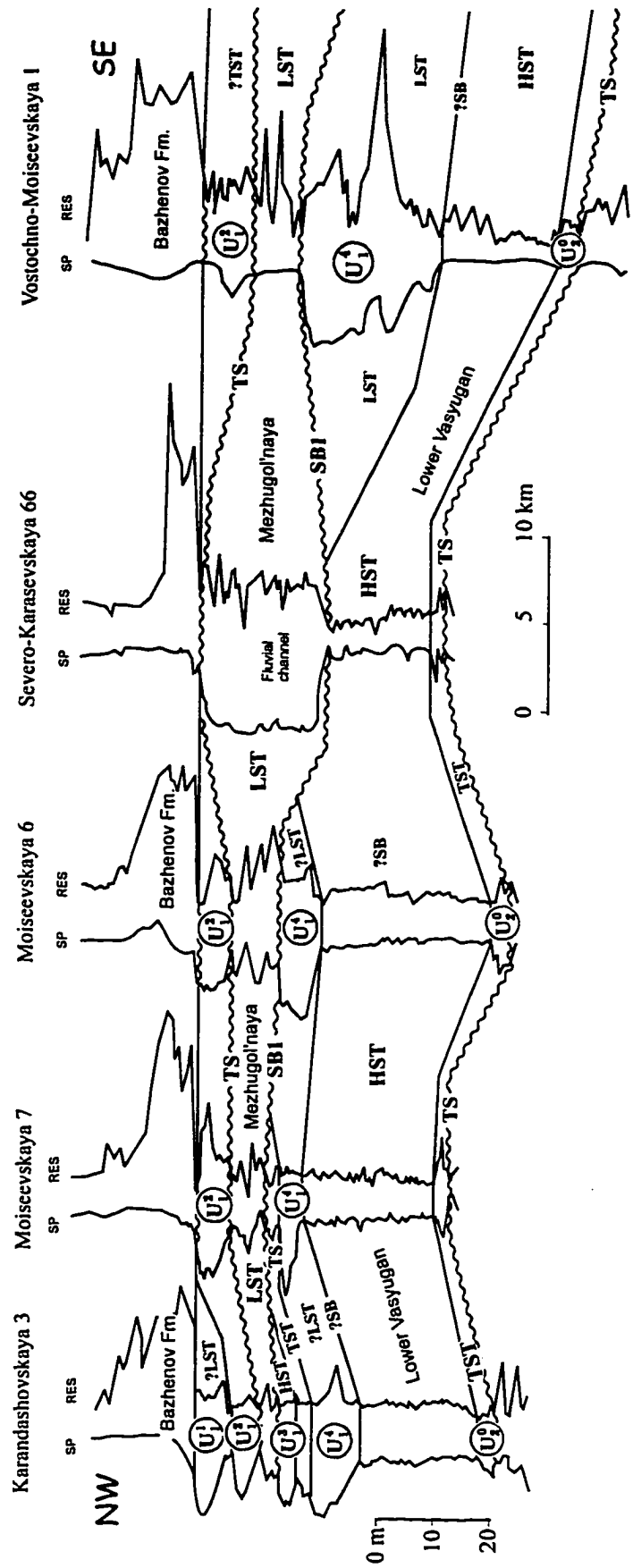

Figure 28. Wireline log correlation and sequence stratigraphic interpretation of the southern Kaimysov Arch and northern Nyurolskaya Depression

LST - Lowstand systems tract; TST - transgressive systems tract; HST - highstand systems tract
SB (1) - sequence boundary (type 1); TS - transgressive surface

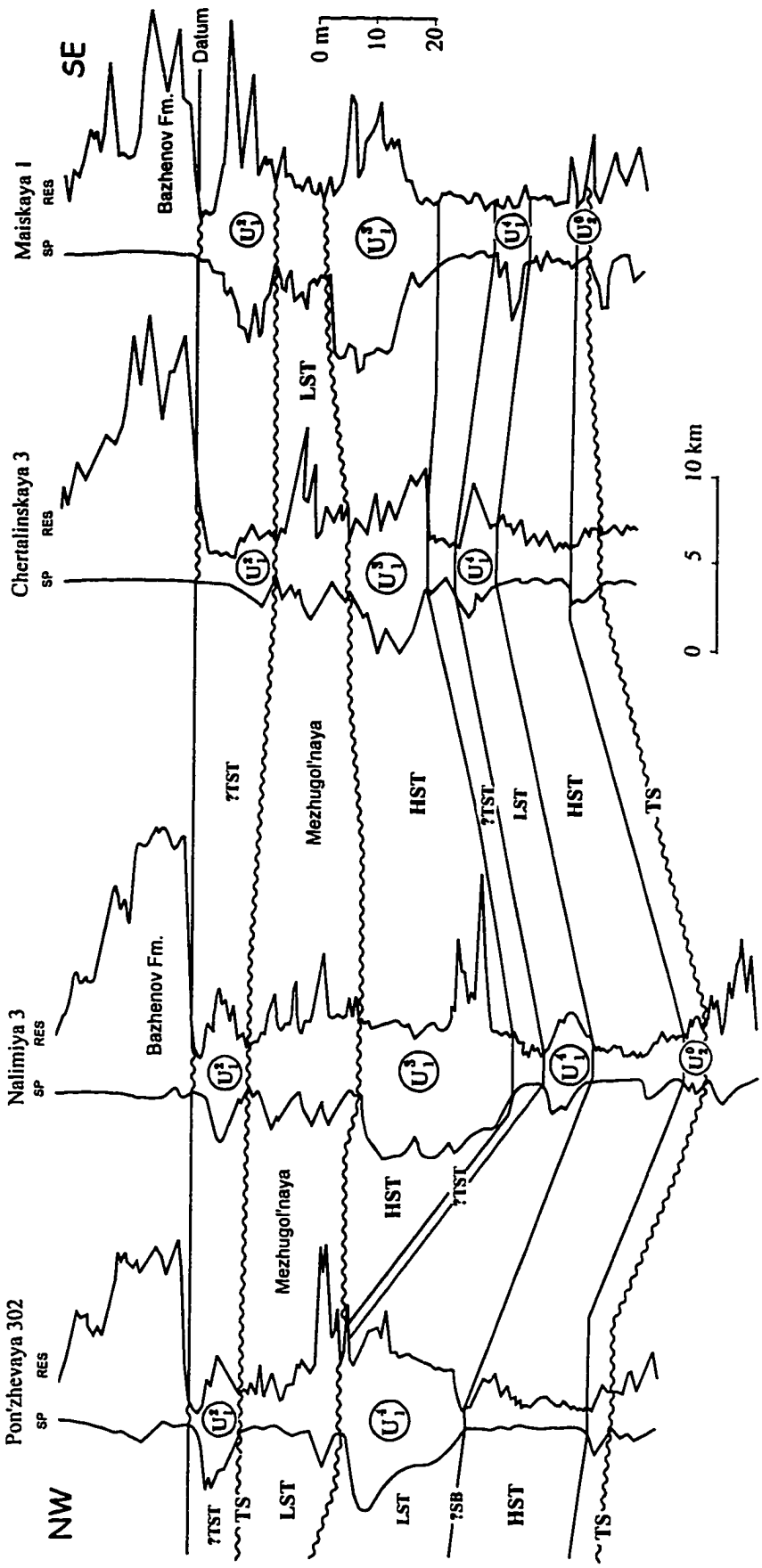

Figure 28. Wireline log correlation and sequence stratigraphic interpretation, continued

section is the presence of numerous lenses and layers of coals or lignitic shales, as well as a great abundance of coaly detritus. Some sections contain relatively thick fining upward sand bodies that consist of coarse to medium (or medium to fine) sandstones with abundant gravels and even pebbles. These units overly the older sediments of Lower Vasyugan Group, U1-4, and U1-3 beds with a sharp erosional contact, and transit laterally to various sandstones, shales and coals of terrestrial origin (Slavkin et al., 1996). It is clear that these sand bodies were deposited in channel facies of fluvial depositional systems, whereas other parts of Mezhugol'naya section represent various interfluvial and lacustrine facies.

Nadugol'naya Member. The onset of Nadugol'naya deposition is related to the start of the significant marine transgression during which marine conditions spread again throughout the area of study. The lower part of U1-2 is characterized by typical features of basal transgressive deposits including poor sorting and the presence of gravel, shell lags and glauconite. The most complete sections are comprised of distinct U1-2 and U1-1 beds that are separated by shale layer or erosional surface. In many cases, however, the Nadugol'naya Member lacks either U1-2 or U1-1 as a result of erosional events that occurred at the U1-1/U1-2 boundary and at the top of U1-1 (Figure 29). Being deposited in normal shallow marine depositional systems, U1-1 and U1-2 are composed of predominantly sandy sediments of beach and shoreface facies (Brylina and Danenberg, 1989). The beach zones represent the best oil reservoirs.

Sequence stratigraphy

The Vasyugan Formation in the area of study consists of a stack of third-order sequences (Figure 28). The thin nature of the stratigraphic units does not allow identification of parasequence sets. As a result, the recognition of individual systems

tracts is not straightforward. Nevertheless, the key-depositional surfaces such as sequence boundaries and transgressive surfaces are clearly distinguishable in many cases (Figure 28).

Lower Vasyugan Group. The basal U2-0 bed is a transgressive systems tract. It onlaps the sharp erosional unconformity developed over the top of continental Tyumenskaya Formation. Overlying is the Shaly Part of the Lower Vasyugan Group that was deposited in deposited in an offshore environment, representing highstand deposits.

Podugol'naya Member. The lowermost U1-4 bed was formed as a result of regression that occurred during the Middle to Late Callovian (more precise age determination is impossible because of sparse ammonite data). This part of the section is recognized as a lowstand systems tract (Figure 28). The lack of a well-determined erosional surface at the base of U1-4 suggests only minor fall of relative sea-level and formation of a type 2 sequence boundary. The overlying uniform layer of sandy shales that separates U1-4 from U1-3 was deposited as a result of transgression and represents a transgressive systems tract (Figure 28). Subsequent sea-level fall, during which the U1-3 bed was deposited, occurred during the second half of the Early Oxfordian (age determined by ammonite biostratigraphy). We interpret U1-3 as a late highstand systems tract with a maximum flooding surface at its base.

Mezhugol'naya Member. In most localities U.1-3 is overlain by a surface of subaerial erosion that marks the base of the Mezhugol'naya Member. It is a classic representation of a type-1 sequence boundary. Mezhugol'naya is interpreted as the terrestrial part of lowstand systems tract. It consists of various facies of coastal plains such as fluvial channels, lacustrine, interfluvial zones, and exhibits significant lithological heterogenity.

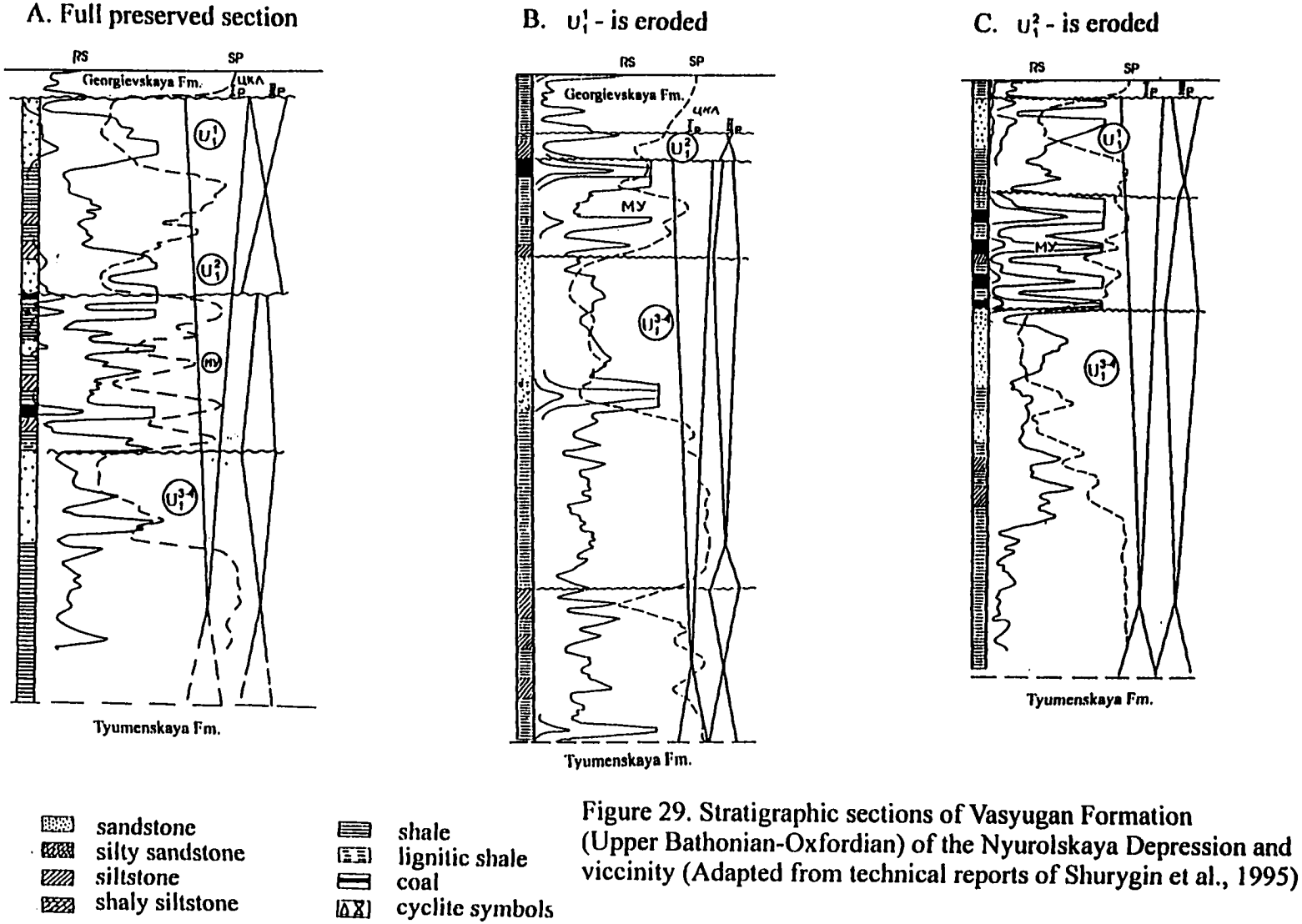

Figure 29. Stratigraphic sections of Vasyugan Formation (Upper Bathonian-Oxfordian) of the Nyurolskaya Depression and viccinity (Adapted from technical reports of Shurygin et al., 1995)

The maximum regional sea-level fall that occurred during the deposition of Mezhugol'naya Member resulted in subaerial exposure of the entire area of study (Nyurolskaya Depression and vicinity) as well as significant fluvial erosion. The interpreted channels (Figure 28) are parts of incised valley fill complexes (Bowen et al., 1993; Posamentier et al., 1988). Deltaic and marine equivalents of this rocks were deposited beyond the area of study representing a situation of forced regression (Posamentier et al., 1992). Most local experts conventionally the channel units to U1-1 sand bed. Our sequence stratigraphic interpretation (Figure 28) indicates that fluvial complexes are older than any units of the Nadugol'naya Member and younger than Podugol'naya, being time equivalents of terrestrial rocks of the Mezhugol'naya Member.

Nadugol'naya Member. Sequence stratigraphic interpretation was particularly difficult for this part of the section because of extensive erosion that resulted in stratigraphic incompleteness of many sections. The lower part of U1.2 is a transgressive systems tract, while the upper portion may partially represent highstand deposits. Relative sea-level fall that followed deposition of U1.2 resulted in significant erosion that in some cases eroded away the entire U1.2 bed. Presence of a coal layer at the boundary of U1.2 and U1.1 reported from the Igolskoe-Talovoe uplift zone (western Nyurolskaya Depression) (Tatianin and Volkov, 1982) provides an additional evidence of sea-level fall and subaerial exposure (without erosion in this case). In some stratigraphically complete sections (such as those of the Northern Kaimysov Arch), U1.2 is separated from U1.1 by a layer of shales which may represent transgressive or highstand deposits.

The U1.1 bed was formed during the following sea-level fall, as suggested by its regressive nature (coarsening upward shallow marine successions). It represents deposits of a late highstand or earliest lowstand phase of relative sea-level change. Continuous sea-level fall caused extensive erosion of U1.1 (sometimes the entire Nadugol'naya Member) and in a few cases led to the formation of coal beds.

Georgievskaya Formation. In the most complete sections, the base of Georgievskaya formation corresponds to that of the upper zone of the Late Oxfordian - Amoeboceras ravni (according to ammonite biostratigraphy). It overlies the Vasyuganskaya Formation with evidence of significant erosion in many cases. The basal transgressive layer of U1.0 consists of poorly sorted silty sandstones with abundant glauconite, phosphate nodules, and belemnite fragments. The overlying strata of the Georgievskaya formation display predominately fine-grained composition (siltstones and shales) and are also characterized by abundant glauconite (Vyachkileva et al., 1990). Paleogeographic data show that amplitude of Georgievskaya transgression was higher than those in the Oxfordian (Shurygin, per. comm.).

The overlying bituminous shales of the Bazhenovskaya formation formed during the next stage of the basin development when significant regional subsidence coincident with eustatic rise caused drowning of the entire basin.

As a final result of sequence stratigraphic and facies analyses I constructed an approximate curve of relative sea-level change for the late Bathonian-Volgian interval of the southeastern West Siberia (Figure 30).

Comparison to the QEC

Comparison of the sea-level events interpreted from Nyurolskaya and vicinity with those of our Quantified Eustatic Curve reveal close correspondence (>90%) of timing of sea-level events (Figure 31). This indicates that sea level events occurred simultaneously in West Siberia and the Russian Platform, and eustasy was the main factor controlling sedimentation in the area of during the Bathonian-Lower Kimmeridgian interval (the rate of eustatic changes overwhelmed tectonic subsidence). The discrepancies between the QEC and the Nyurolskaya Depression in the Upper Kimmeridgian-Volgian reflect the onset of a well recognized regional basin subsidence phase (Nezhdanov, 1990) which resulted in deposition of the black shales of the Bazhenov Formation.

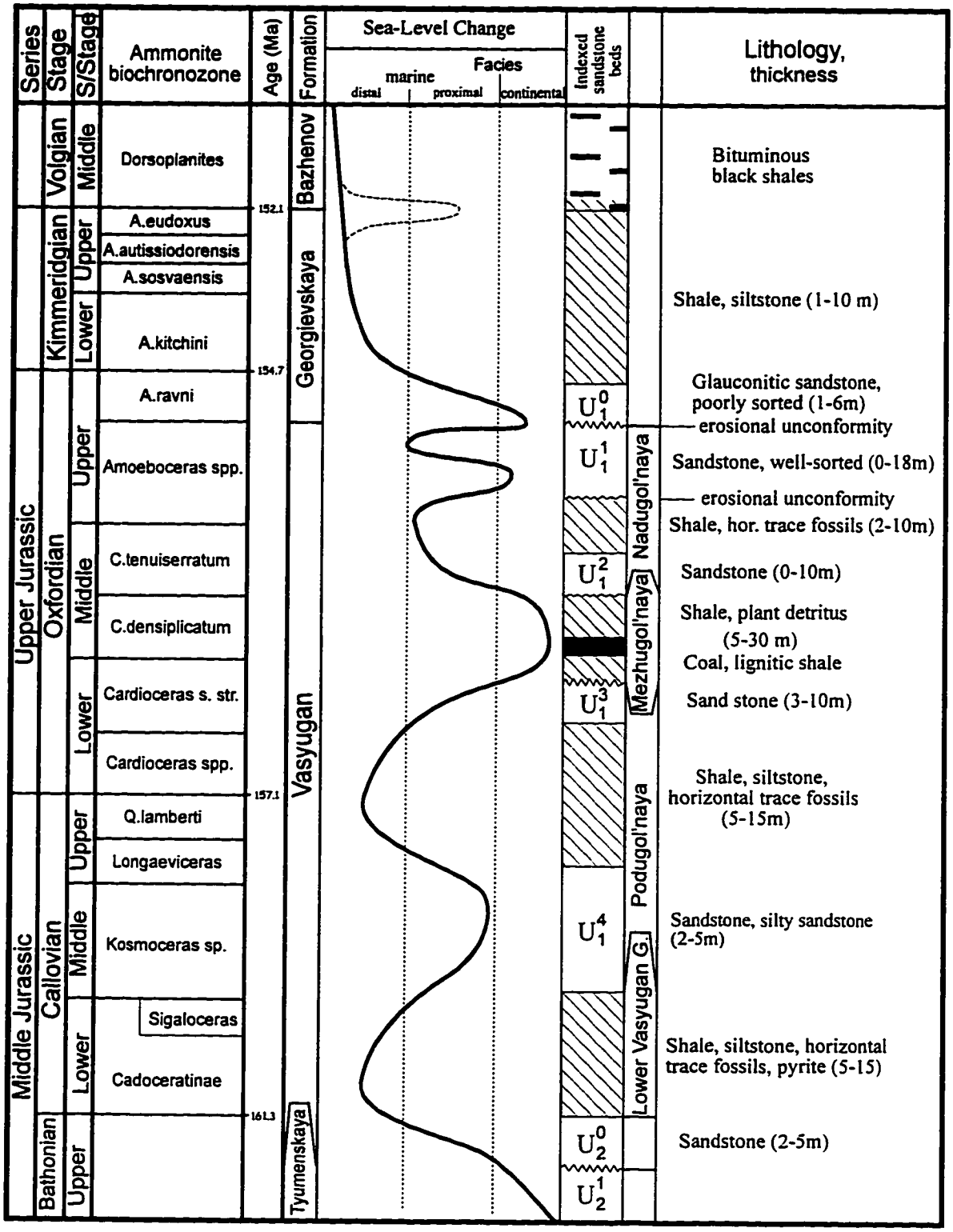

Figure 30. Sea-level interpretation of the Bathonian-Kimmeridgian of southeastern West Siberia.

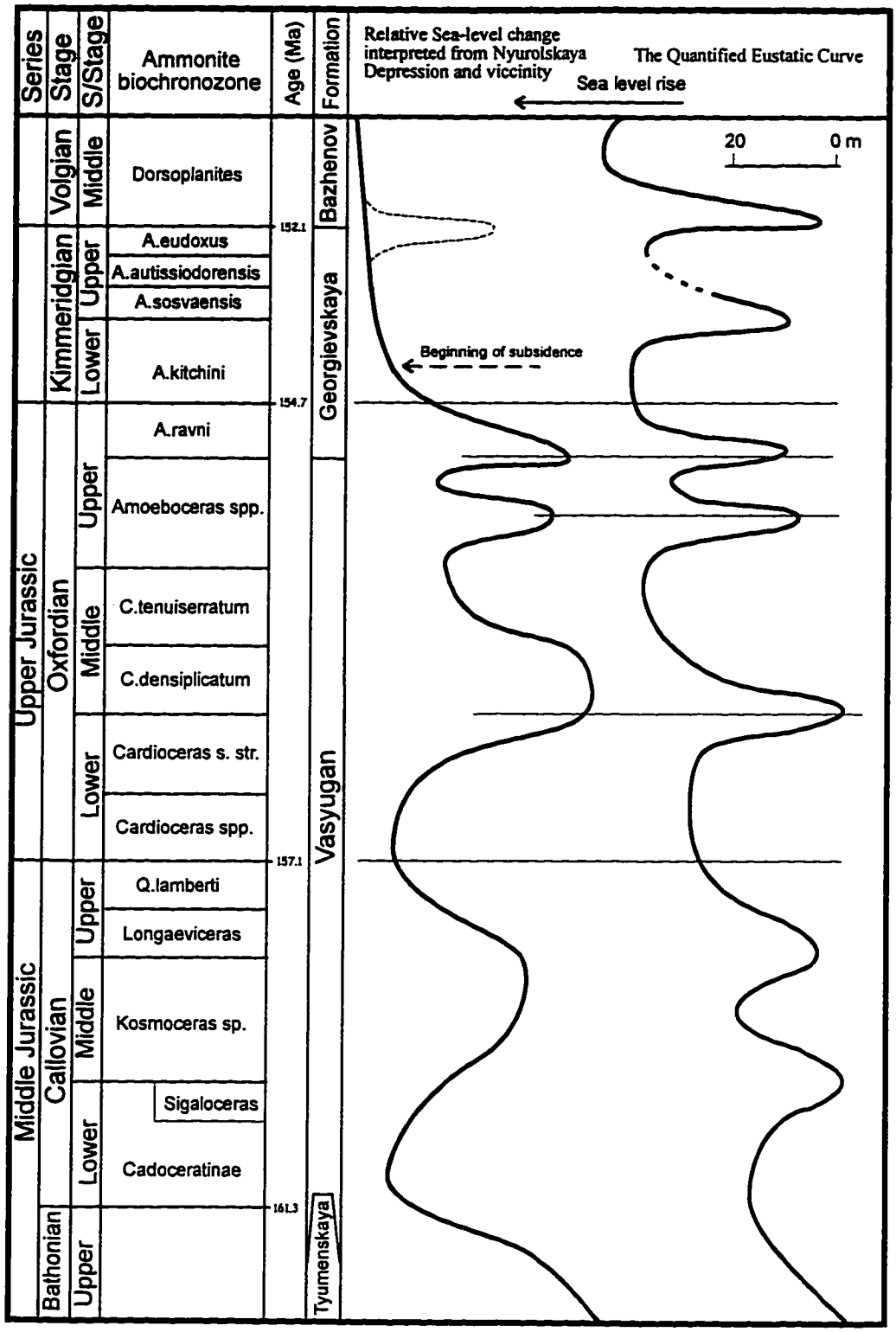

Figure 31. Comparison of sea-level change of the southeastern West Siberia with the Quantified Eustatic Curve

Conclusion

1. As a result of application of high-resolution sequence stratigraphic analysis, a sequence stratigraphic framework has been established for Bathonian-Kimmeridgian strata of Nyurolskay Depression and Viccinity. Based on analysis of wireline logs, lithologies, and sedimentary facies, four third-order depositional sequences have been identified within the Vasyugan Formation. The sequences exhibit different stratigraphic completeness and generally vary in thickness from 3 to 30 meters. In addition, history of regional relative sea-level change was reconstructed (Figure 30).

2. Incorporation of sequence stratigraphic framework into the correlation procedure helped to properly distinguish specific stratigraphic units (indexed sand beds) and thus improved correlation itself. For example, previously dated Mid-Oxfordian U1.2 beds from some wells of Pervomaiskaya and Lont-Yakhskaya fields were redetermined as Upper Oxfordian U1.1 beds. Sequence stratigraphic analysis helped to properly identify fluvial channel zones on the elevated parts of the positive structures and determine timing of their formation.

3. Comparison of the sea-level events interpreted from Nyurolskaya and vicinity with those of our Quantified Eustatic Curve (QEC) reveal close correspondence of timing of sea-level events (e.g. almost 100% for the Oxfordian). This indicates that sea level events occurred simultaneously in West Siberia and the Russian Platform, and that eustasy was the main factor controlling sedimentation in the area of during Bathonian-Lower Kimmeridgian interval (the rate of eustatic changes overwhelmed tectonic subsidence). In addition, it confirms biostratigraphic data for the region and provides mean for inter-regional correlation.

4. The good correspondence of the QEC to relative sea level curve based on the sequence stratigraphic study of the Nyurolskaya Depression and vicinity provides a good preliminary test of the validity of the QEC. The good biostratigraphic and sea level event correlation suggests that subsequent testing of the QEC in other regions and other intervals would yield similar results, within the variable limits of biostratigraphic correlation.

Neocomian

The Neocomian is the most important oil-producing interval of the West Siberian basin. At the present time it is a source for more than 90% of the total volume of oil production (Karagodin et al., 1996). The largest anticlinal petroleum reservoirs with simple structures (including giants such as the Samotlor, Salym, and other reservoirs) are concentrated in this interval. In addition there is a great number of smaller traps which collectively represent a significant total volume (Ulmishek, 1993). At the same time, the Neocomian is an extremely contentious interval among Russian geologists because of its complex geometry and diversity of depositional systems. As a result, exploration of this interval requires very detailed stratigraphic data and models because of its complicated structure and zoning.

Depositional history and stratigraphy

A major Volgian transgression resulted in significant water depth increase and expansion of the marine basin throughout the entire West Siberian Plain. Most of the basin was sediment starved, and the bituminous shales of Bazhenov formation were deposited. The Bazhenov Formation is the main oil bearer of West Siberia (accounts for

more than 85% of West Siberian oil) and is one of the largest oil-generating systems in the world (Peters et al., 1993).

In the Berriasian the rates of sedimentation dramatically increased and the accommodation created by the Volgian transgression was filled by prograding, longitudinally oriented clinoforms which met in the central part of the basin in the Early Barremian (Figure 24). In plan view the clinoforms are relatively large, lenticular bodies that trend basinward and overlap each other in the direction of the sediment source. These lenticular bodies are oriented parallel to the paleoshoreline and are laterally continuous for hundreds of kilometers. During the Barremian, marine sedimentation occurred in a long (about 2000 km) and narrow (50-150 km) submeridionally oriented zone in the central part of the basin. This zone has been termed the "remnant channel zone" by regional geologists (e.g. Kunin et al., 1993). The sediments were derived from the East-Siberian Highlands and the Urals with most of the sediment influx coming from the east. This resulted in asymmetrical basin fill, with thicker bodies with coarser sediments on the eastern flanks of the basin, where accommodation was filled by the westward-prograding clinoforms.

In the Middle Ob' region clinoforms generally consist of thick sands and silts (100-200m) separated by thin and mostly uniform shaly units (Nezhdanov et al., 1992), suggesting a series of short-term marine transgressions throughout the Neocomian. Generally, the clinoforms grade to thinner shales toward the west (central basin).

In contrast, clinoforms at the western flank of the basin mostly consist of fine-grained sediments. This was primarily caused by the difference in clastic source. During most of Mesozoic deposition, the Urals provided predominantly fine (shaly and silty) material to the West Siberian basin (Nezhdanov et al., 1992).

The richest petroleum fields were discovered in westward prograding clinoforms of the Shirotnoe Priobie area (Figure 24). Consequently, a wealth of stratigraphic

information is available for this area, and we chose it for our first sequence stratigraphic analysis.

"First-sight" analysis of seismic profiles

In order to identify and roughly estimate the main events of relative sea-level change that occurred in the Shirotnoe Priobie area during the deposition of the clinoform complex, we examined two latitudinal seismic profiles I-I and XIII-XIII (Figure 23). The most clearly defined seismic units are uniform shale horizons (e.g. Sarmanovskaya, Pimskaya, etc.) which are interpreted to have been deposited during transgressions and sea-level highstands. Being distinctive reflectors these numbered units are commonly used to subdivide the section into its component clinoform units (Figure 32). It is worth noting that the numbered shale units correlate well with eustatic highstands of the QEC (Figure 33). For example, two of the most important regional sea-level falls (which bracket the Lower Hauterivian) described in the literature (Karagodin et al., 1991; Shpilman et al., 1993) correspond to those of the QEC. Correspondence is particularly good for the Upper Valanginian-Hauterivian interval which is in general better biostratigraphically defined at the zonal level than is the Berriasian - Lower Valanginian.

Close agreement with the QEC indicates the importance of eustasy as a factor controlling Neocomian sedimentation in the Shirotnoe Priobie region. This makes the Neocomian section of Shirotnoe Priobie particularly favorable for sequence stratigraphic analysis and application of the QEC.

Sequence stratigraphic analysis

In this part of the study I undertook more comprehensive analysis of a latitudinal band of oil fields in the Shirotnoe Priobie region including the Asomkinskaya (6), Mamontovskaya (5), Salymskaya (4), Pravdinskaya (3), V-Shapshinskaya (2), and Priobskaya (1) oil fields (Figure 23). The clinoforms in these areas are younger toward

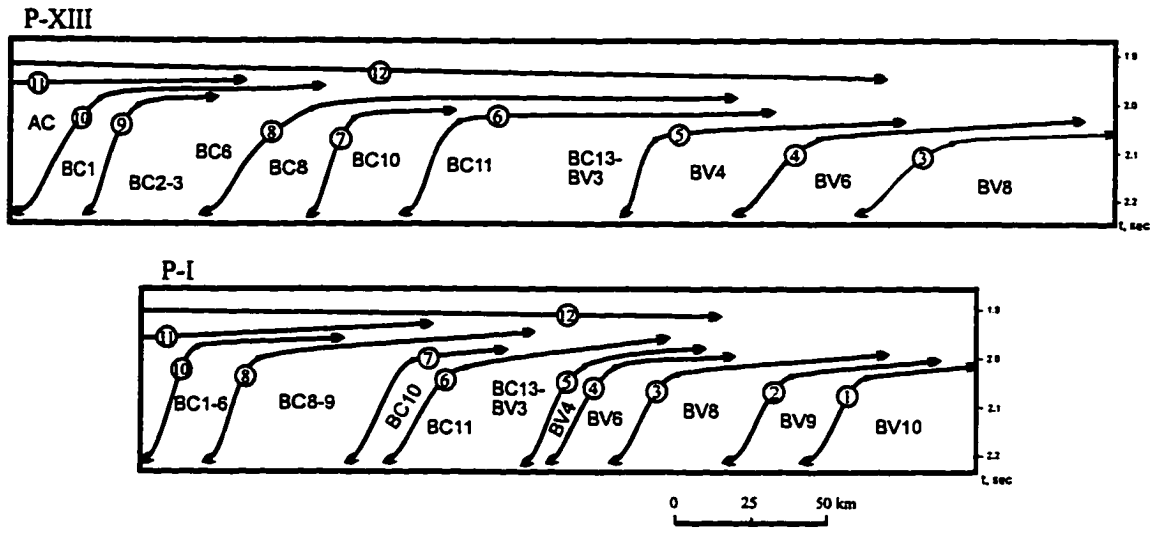

Based on 2 regional seismic profiles P-I and P-XIII, and data from Nezhdanov et al. (1990) and Mkrtchian (1990)
The strata are adjusted to the downlap surface - top of black shale Bazhenov Formation (Volgian - Valanginian)

Shale Horizons

Interpreted shelf break point

BC8-9 - Sand beds

1 - Tagrinskaya
2 - Uzunskaya
3 - Samotlorskaya
4 - Urievskaya
5 - Pokachevskaya
6 - Savuiskaya
7 - Cheuskinskaya
8 - Sarmanovskaya
9 - Pravdinskaya
10 - Pimskaya
11 - Bystrinskaya
12 - Koshaiskaya

Figure 32. Seismostratigraphic model of the "Clinoform Neocomian" Complex

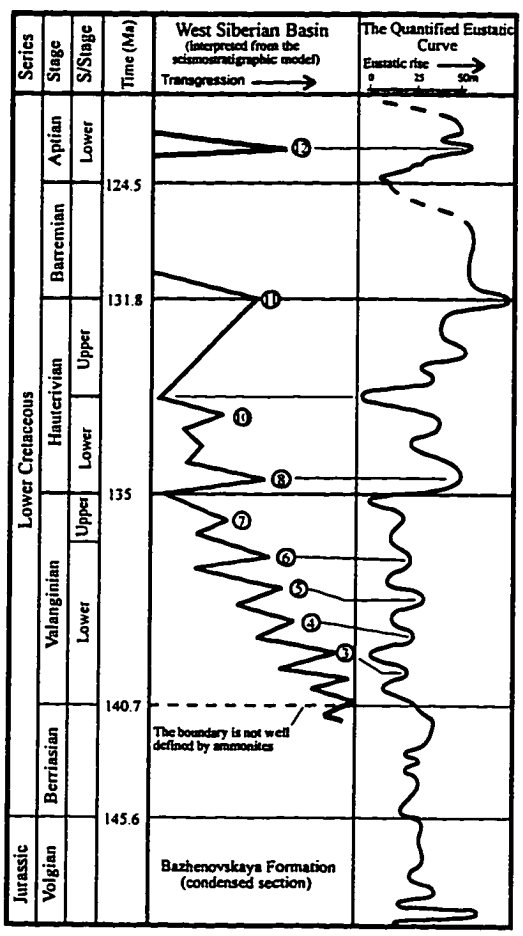

Figure 33. Interpretation of transgressive/ regressive history of the "Clinoform Neocomian" compared to the Quantified Eustatic Curve.

the west ranging from Lower Valanginian (Asomkinskaya) to Upper Hauterivian (Priobskaya).

The section generally consists of sandy clinoform units separated from each other by shale horizons (Figures 24). Owing to their lateral continuity and reliable biostratigraphic dating, the named shale horizons are commonly used to subdivide the section into its component clinoform units (Figure 34). These shale horizons are characterized by the typical attributes of condensed sections (pelagic content, abundant marine organic matter, thin and uniform nature, etc.), and thus, can be interpreted to be deposited during maximum sea-level highstand and maximum transgression of the shoreline (which were essentially simultaneous in this slowly subsiding part of the basin).

Nine depositional sequences have been identified (Figure 35). Age dating is based on ammonite biostratigraphy which has been generalized for the interval from published and unpublished sources (Figure 34). A relative sea-level curve was obtained by measuring onlap/offlap variations from seismic data and geologic profiles (Haq et al., 1988)

Comparison to the QEC

The major sea-level events inferred from the analysis generally correspond to those of the Quantified Eustatic Curve (Figure 36). This result demonstrates again the strong influence of eustasy on the deposition of the "Clinoform Neocomian" complex.

Direct comparison of the Quantified Eustatic Curve to the West Siberian sea-level curve enabled us to estimate regional tectonic subsidence during the Neocomian. This is interpreted to be varying from 12 - 20 m/Ma, which is considerably less than previous estimates (40-50 m/Ma).

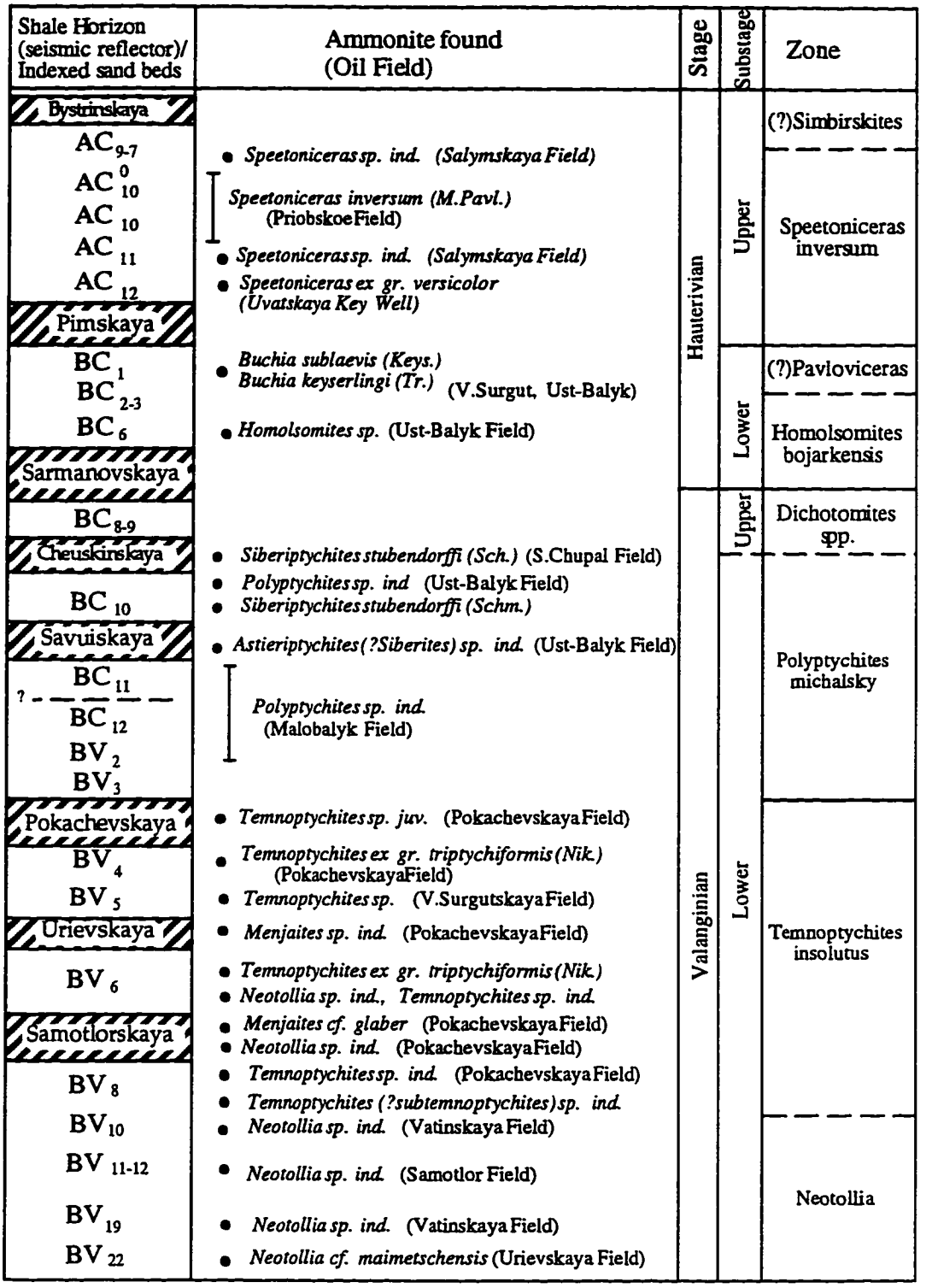

Figure 34. Summary on the ammonite biostratigraphy of the Neocomian strata of Shirotnoe Priobie Area.

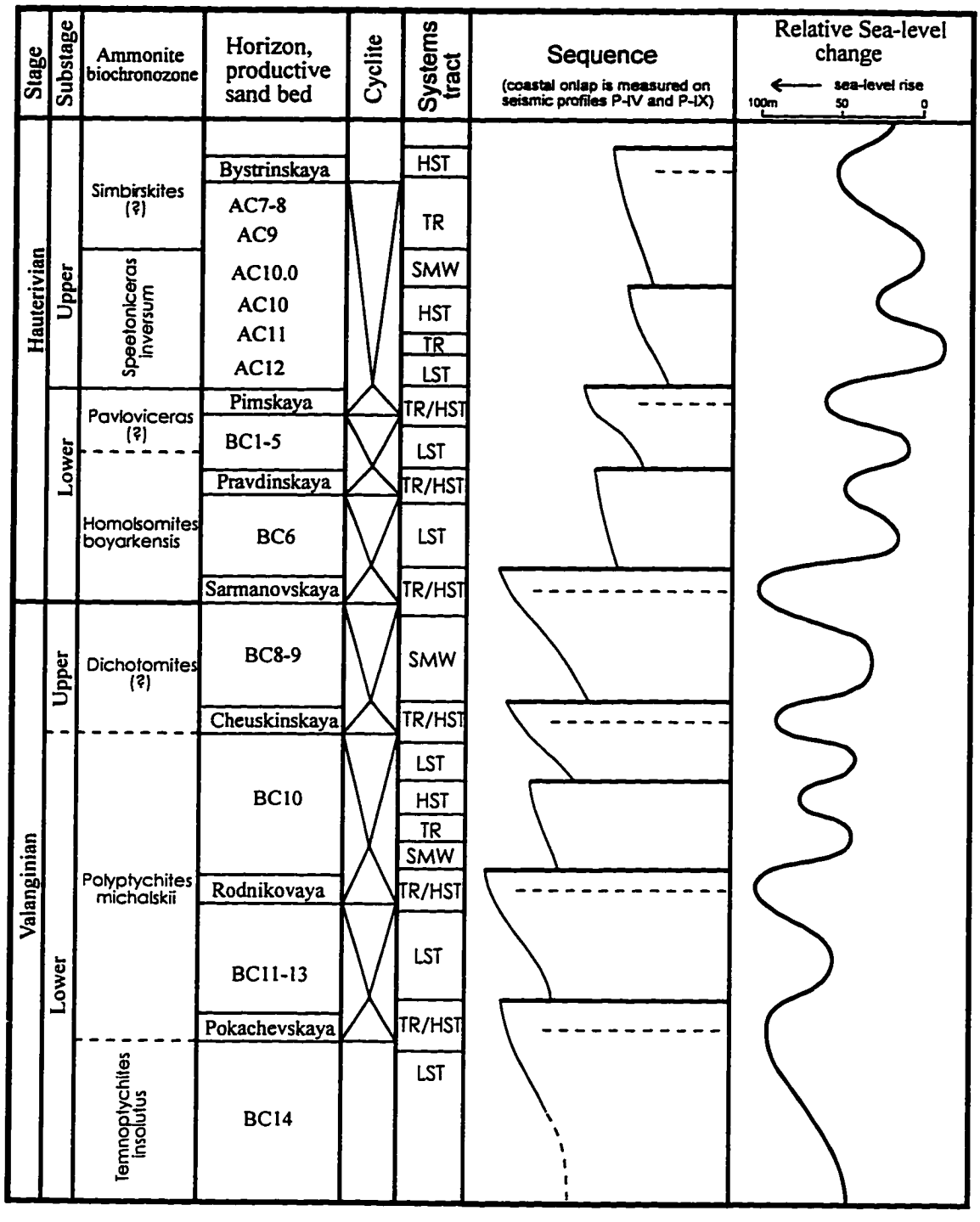

Figure 35. Sequence stratigraphic interpretation of Valanginian-Hauterivian strata of the Shirotnoe Priobie area.

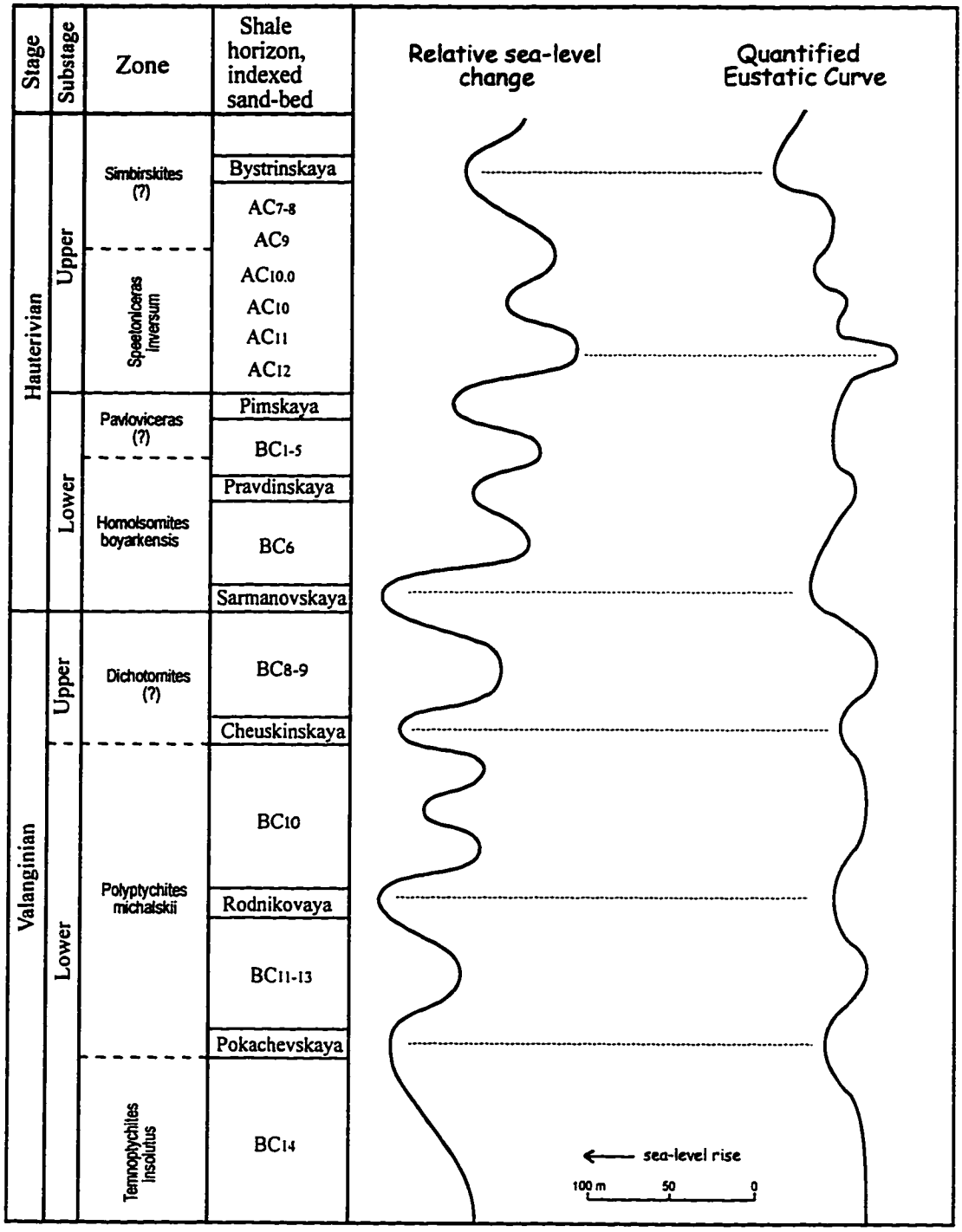

Figure 36. Comparison of Valanginian-Hauterivian sea-level change of the Shirotnoe Priobie area to the Quantified Eustatic Curve

Priobskoe Oil Field

We chose the Priobskoe Field as a site for detailed high resolution sequence stratigraphic examination due to the availability of copious stratigraphic data including seismic profiles, well logs, core descriptions, and biostratigraphic determinations.

General description and geological history.

The Priobskoe (literally: near the Ob River) petroleum field is one of the most prospective areas for petroleum exploration in West Siberia. This field is located in the central part of West Siberian plain, 60 km to the northeast of Khanty-Mansiysk (Figure 23), and contains wells drilled to depths of 2000-2500 m. Most reservoirs of this field are concentrated in the Hauterivian (Low Cretaceous) clinoform bed package which is bounded by shale horizons (Pimskaya and Bystrinskaya). The Hauterivian clinoform package is subdivided into 6 individual beds denoted AC7 through AC12 (Figure 37), which correspond to 6 cycles of sea-level change (regression-transgression-regression) (Karagodin et al., 1996). Most geologists interpret this unit as a deltaic system that formed under the strong influence of relative sea level changes (Karagodin et al., 1996; Shpilman et al., 1993). The entire system is characterized by the explicit cyclicity, making it favorable for sequence stratigraphic investigations.

The Priobskoe complex is at the western part of eastern side of the Neocomian clinoform supercomplex (Berriasian-Barremian), as appears on the regional seismic profiles (Figures 32, 33, 38).

The deltaic environments within the Priobskoe complex are reconstructed in beds AC_{12}, AC_{11} ,and AC_{10} (Karagodin et al., 1991). These are thick bodies consisting of sandstones, siltstones and shales. Analysis of contour maps suggests that the number of distributaries was changing through time(Karagodin et al., 1996). Nevertheless, it is possible to recognize three main channels and the mouth bars corresponding to their

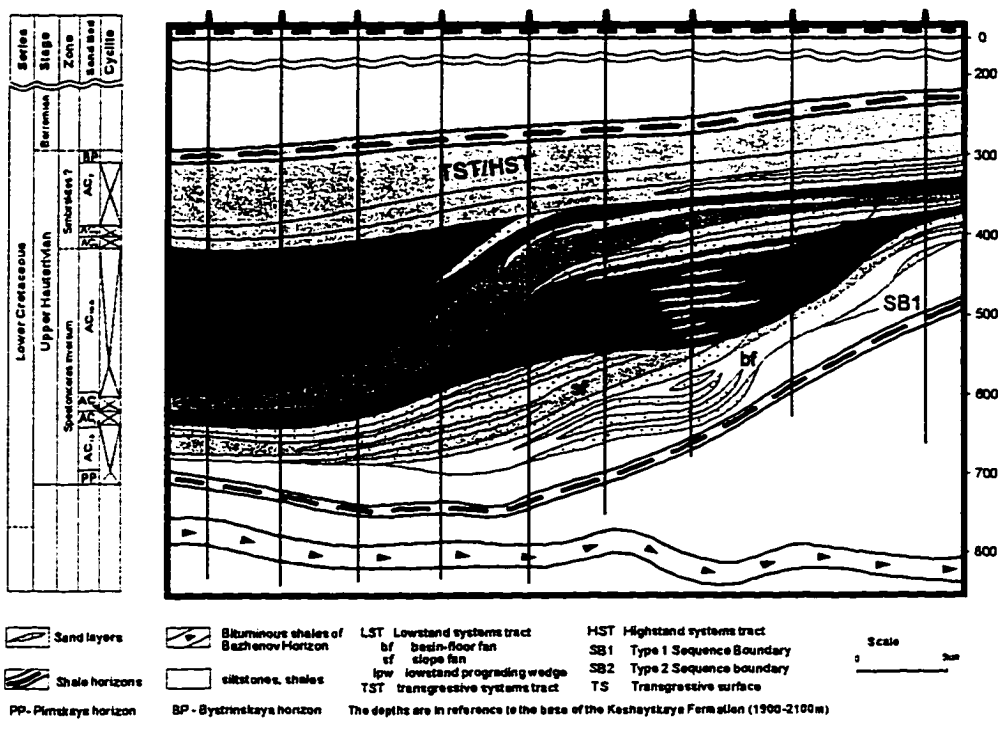

Figure 37. Stratigraphic Cross-Section and Sequence Stratigraphic Interpretation of the Priobskoe Oil Field Clinoform Complex (Upper Hauterivian)

distributaries - the main (central part), northern, and southern associated with the elongate complexes (Figure 39). The sand trends in bed AC12 are predominantly perpendicular to the shoreline. The shapes of lobes and fingers (predominantly lobate geometry) show evidence that the deltaic system was river dominated and influenced by wave processes (according to the classification of Bhattacharya and Walker, 1992).

Biostratigraphy.

One of the most important problems encountered in stratigraphic investigations of the Priobskoe complex is the lack of reliable biostratigraphic data. Rarity and poor preservation of fauna (ammonites, forams) do not allow a precise determination of the geological age of most beds (AC12-AC7). Most researchers accept the approximate age of the complex as Hauterivian-Barremian, basing on foraminifera and palynologic data (Nezhdanov et al., 1992; Vyachkileva et al., 1990).

However, the Upper Hauterivian ammonite *Speetoniceras ex gr. inversum Pavlov* is found in beds AC10-AC10.0 (Pinous, 1993). In addition *Speetoniceras sp. ind.* is reported from AC11 of the Salymskaya oil field (Vyachkileva et al., 1990). This makes it possible to assign AC11-AC10o to ammonite Zone *Speetoniceras versicolor*, and to determine the age of the whole complex (AC12-AC7) more precisely as Late Hauterivian (Pinous, 1993).

Sequence stratigraphic analysis.

The sequence stratigraphic interpretation is mostly based on data from the Mesozoic Stratigraphy Laboratory and the Laboratory for Mesozoic Oil and Gas (Institute of Geology, RAS, Novosibirsk) in addition to the published literature (Kunin et al., 1993; Mkrtchyan et al., 1990). The original data include geological cross sections constructed by S. Ershov (based on interpretations of numerous wells and seismic profiles), regional

seismic profile IX (Figure 38), well logs and lithologic descriptions of some important wells, and biostratigraphical/ paleoecological data.

Sequence stratigraphic analysis was conducted by using the approach suggested by the BP Exploration and Exxon groups (Emery and Myers, 1996; Posamentier et al., 1988), and includes:

- Analysis of seismic data (seismic facies analysis- configurations of reflection patterns, types of reflection terminations, external geometric shapes); correlation of seismic facies.
- Analysis of well data (lithostratigraphy and biostratigraphy from cores and well logs).
- Analysis of surfaces and condensed sections (frequency and nature, areal extent, association with facies distributions).
- Identification of systems tracts

The lowest stratum of the Priobskoe productive complex is the Pimskaya shale horizon (dashed horizon second from the bottom in Figure 37, which formed during the time of maximum regional transgression, and represents a typical condensed section (Loutit et al., 1988). After subsequent slow relative sea level fall, sediment supply from the east was restored. This resulted in progradation of clinoforms over the shelf break which eventually buried the downlap surface. The thickness of the upper Pimskaya horizon is increased at the shelf break as a result (Mkrtchyan et al., 1990) (Figure 37). The next phase of relative sea level change led to a prominent regression "AC_{12} bed" during most of the shelf was exposed. A noticeable onlap pattern can be distinguished on the seismic profiles (Figure 38). The boundary between the Pimskaya Formation and AC_{12} is thus a classic representative of type 1 sequence boundary (Van Wagoner et al., 1988). The deposition of the AC_{12} bed is associated with a lowstand systems tract and consists of three regressive phases. During the first phase, sea level fell to the level of

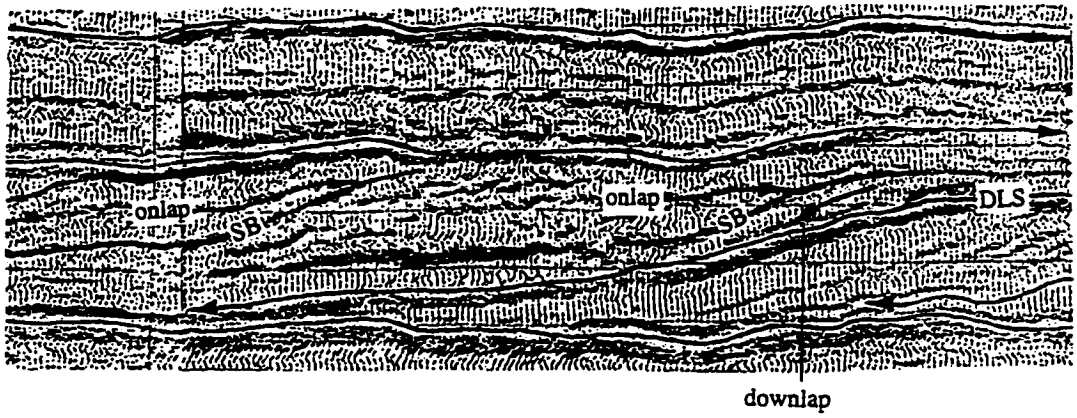

Figure 38. Fragment of seismic profile through the Priobskoe oil field. SB - sequence boundary; DLS - downlap surface

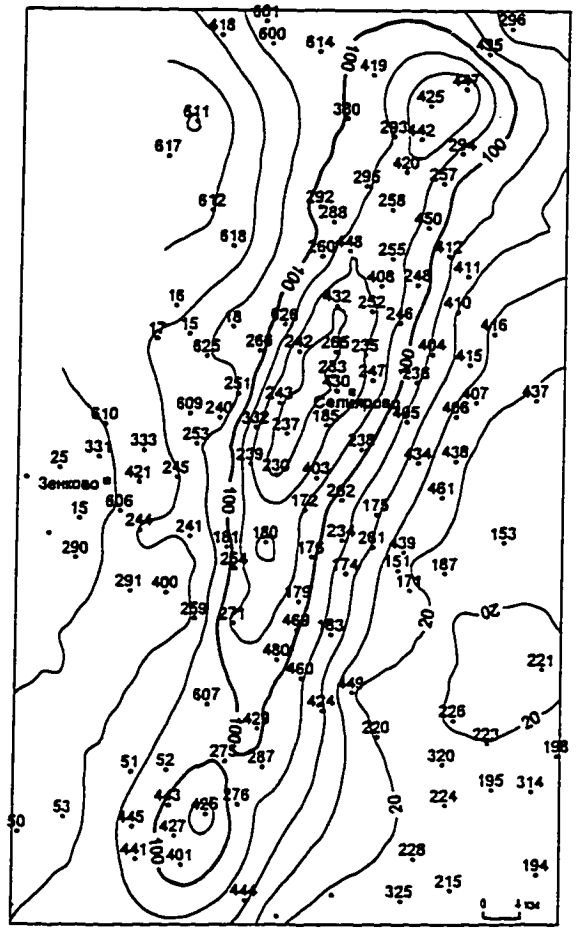

Figure 39. Sand thickness of the bed AC12-11 (expressed as a percent of total section). From Karagodin et al. 1996.

the shelf edge, and the broad area of the shelf platform became a fluvial delta plain. Major depocenters shifted to the slope, resulting in mass movements of sand and the deposition of lenticular bodies within fans at the base of slope. Sand was also deposited at the shelf break in mouth bars during that time. The second phase began as sea level dropped below the shelf edge, resulting in significant erosion of the exposed area, and an increase in sediment influx. Large lenticular sand bodies were deposited at the base of the slope. The result of these processes was to flatten the slope and deposit aggradational terraces. Further regression and fall of sea level to the level of the aggradational terraces characterized the third phase. Fluvial streams passed through aggradational terraces and partially eroded them. The main depocenters shifted basinward. Erosion of terraces and redistribution of material flattened the slope and deposited more lobate bodies of sediments.

The formation of unit AC11 began with the onset of another phase of sea-level rise. This part of the section corresponds to a lowstand wedge systems tract. High rates of sediment supply resulted in deposition of a thick (150 m) package of sands and shales. The aggradation exhibited by the sands indicates that the rate of subsidence was equal to or exceeded sediment influx for at least part of this time.

The formation of the AC10 bed began during rapid transgression which partially eroded the upper portion of AC11. Depocenters shifted back onto the shelf, where thin beds and lenses of coarse transgressive sediments were deposited as a transgressive systems tract. The upper part of AC10 is interpreted as a highstand systems tract.

The interval form AC10.0 to AC7 does not contain significant sand bodies and is interpreted to represent shelf margin wedge, transgressive, and possibly highstand systems tracts.

Summarizing, sequence stratigraphic analysis of Priobskoe indicates that:

- Units AC12 to AC10 represent a Type 1 sequence, and the lower boundary of AC12 is a type 1 sequence boundary. AC12 was formed mainly by turbidite processes during significant regression;
- Systems tracts and bounding surfaces can be identified within the sequence;
- Pimskaya and Bystrinskaya shale horizons contain condensed sections

Discussion.

The clinoform complex formed under conditions of strong sediment supply, continuous tectonic subsidence (caused mainly by sediment loading), and eustatic sea level change. In combination, these factors produced frequent relative sea level fluctuations, and caused the cyclicity of the strata (Sosedkov et al., 1987). Progradational clinoformal packages, alternate with aggradational packages (regional shale units) that formed during periods of transgressions and sea-level highstands and are the cap rocks for petroleum.

Whereas some regional experts argue that the clinoform complex was developed under the influence of local factors rather than eustasy, others generally people generally agree that the eustasy was the main factor driving the sedimentation, even though the rates of sediment supply were high.

It is clear, that at least the Priobskoe clinoform complex was formed under conditions of strong influence by local factors. The general regressive trend depicts enormous sediment influx during deposition, which significantly distorted evidence of the eustatic sea level changes. In many cases cyclicity was caused by local variations such as delta channel switching (avulsion). Nevertheless, some events, like the evident regression of the AC12 bed (during which time relative sea level dropped at least 150 m below the shelf break (interpretation of S. Ershov) as well as transgressions of the Pimskaya and Bystrinskaya horizons can not be explained as being caused mainly by local factors.

Comparison of the Priobskoe sequences to those of the Haq et al. chart (1988) do not reveal any correspondence. However, a similarity can be found with the QEC (based on stratigraphy of the central Russian Platform). It is particularly noteworthy that a major sea level fall in the central Russian Platform occurred at the Lower/Upper Hauterivian boundary (prior to Speetoniceras versicolor time). Therefore, there is a good possibility that this sea-level fall and AC12 regression of the Priobskoe field represent the same eustatic event. In addition, the Upper Hauterivian sea level maximum on the Russian Platform is associated with Hauterivian/Barremian boundary, which in turn, may correspond to highstand of the Bystrinskaya Horizon of the Priobskoe. The biostratigraphic data of the Priobskoe field (see Biostratigraphy chapter) support this interpretation. Thus, the age of the Priobskoe complex (AC12 - AC7) can be assigned as upper Hauterivian (AC12-AC10o - *Speetoniceras versicolor* Zone), and the boundary between Pimskaya/AC12 can be assigned as the Lower/Upper Hauterivian boundary.

Conclusion

Summarizing, sequence stratigraphic analysis of Priobskoe indicates that:

- Units AC12 to AC10 represent a Type 1 sequence, and the lower boundary of AC12 is a type 1 sequence boundary. AC12 was formed mainly by turbidite processes during the forced regression;
- Systems tracts and bounding surfaces can be identified within the sequence;
- The Pimskaya and Bystrinskaya shale horizons formed as highstand and transgressive systems tracts and contain condensed sections

The Priobskoe complex was formed under conditions of strong sediment supply in a deltaic depositional system. In many cases cyclicity was caused by local variations such as channel switching (avulsion). Nevertheless, some events, like the evident regression of the AC12 bed as well as transgressions of Pimskaya and Bystrinskaya horizons cannot be

explained as being caused mainly by local factors and are attributed to eustatic sea level changes.

While little correspondence of sea-level events was found with the Haq et al. curve (1988), the main sea-level change events inferred from Priobskoe correspond well to those of the Russian Platform - the locality where deposition was driven solely by eustasy. Thus the application of sequence stratigraphy may enhance biostratigraphic dating by correlation on the basis of synchroneity of eustatic events. In this analysis the correlation with the Russian Platform confirmed the previous biostratigraphic age interpretations (Pinous, 1993). The age of the Priobskoe complex (AC_{12} - AC_7) can be assigned as Upper Hauterivian (AC_{12}-$AC_{10.0}$ - *Speetoniceras versicolor* Zone), and the boundary between Pimskaya/AC_{12} can be assigned as the Lower/Upper Hauterivian boundary.

This study is only one of the first attempts to interpret the West Siberian Neocomian strata by the methods of sequence stratigraphy. More detailed investigations of the whole Neocomian supercomplex should lead to more significant and global results and should demonstrate the applicability of sequence stratigraphy to clastic epicontinental basins.

CHAPTER IV

GENERAL CONCLUSIONS

The Quantified Eustatic Curve (Figure 14) was constructed on the basis of stratigraphic data from the central part of the Russian Platform. Analysis of stratal geometry of this region suggests tectonic stability throughout most of the period of Mesozoic marine deposition. The paleogeography of the region led to extremely low rates of sediment influx. As a result, accommodation potential was limited and is interpreted to have been determined primarily by eustatic variations. Thus, the Quantified Eustatic Curve generated from central part of the Russian Platform can be considered as a representation of global eustasy. Incorporation of Northern Siberian stratigraphic data enabled us to fill the gaps left by hiatuses on the Russian Platform, and thus compile a more complete eustatic curve than would be possible on the basis of Russian Platform stratigraphy alone.

The Quantified Eustatic Curve represents a tool that makes it possible to filter the eustatic signal from basin stratigraphic data. It thus may potentially be applied to any basin world wide to:

- Estimate the influence of local factors (subsidence and sedimentation rates) by removing the eustatic signal from stratigraphic data;
- Determine or refine geological correlation (where there is poor biostratigraphic control) on the basis of synchroneity of *major* eustatic events;
- Provide the eustatic parameter for computer modelling of basin sedimentation.

In order to confirm that the Quantified Eustatic Curve represents a reliable representation of eustasy for Bajocian-Santonian time I compared it against other sea-level curves derived from basins with contrasting tectonic environments. The eustatic nature can be inferred if age equivalency (within limits of biostratigraphic resolution) of sea-level events is demonstrated between the QEC and sea-level records from other regions.

Comparison of the Quantified Eustatic Curve to various other sections and relative sea-level curves (Western European and the U.S. Western Interior) showed that many sea-level events can be recognized globally. This enables me to confirm the eustatic origin of the following events depicted on the QEC:

- Eustatic rise in the Late Bathonian
- Late Callovian eustatic rise and subsequent highstand during the Earliest Oxfordian
- Eustatic fall during the late Early Oxfordian to the minimum at the Early/Middle Oxfordian boundary
- Significant eustatic rise in the Middle Oxfordian with maximum highstand in transversarium (=ilovaisky) Zone
- Eustatic fall in the late Oxfordian (uppermost serratum Zone)
- Significant sea-level rise in the Late Oxfordian (base of pseudocordata/ravni Zone) continued to Early Kimmeridgian

Subsequent more extensive testing is needed for the following intervals that demonstrate good agreement between the curve but include some minor discrepancies:

- Early to Middle Callovian
- Kimmeridgian
- Hauterivian
- Aptian
- Late Albian - Turonian.

The first application of sequence stratigraphic techniques to selected regions of the West Siberian Basin enabled me to establish sequence stratigraphic framework and reconstruct sea-level history for Bathonian-Kimmeridgian of the southeastern West Siberia and Neocomian of the Shirotnoe Priobie.

Four third-order depositional sequences have been identified within the Vasyugan Formation of the southeastern West Siberia based on analysis of wireline logs, lithologies, and sedimentary facies. Incorporation of a sequence stratigraphic framework into the correlation procedure helped properly distinguish specific stratigraphic units (indexed sand beds) and thus improved correlation itself. Comparison of the interpreted sea-level events with those of the QEC reveal close correspondence of timing (e.g. almost 100% for the Oxfordian). This indicates that sea level events occurred simultaneously in West Siberia and the Russian Platform, and that eustasy was the main factor controlling sedimentation in the area of during Bathonian-Lower Kimmeridgian interval.

Nine depositional sequences were identified in the Neocomian sections of the extensively drilled areas of Priobskoe and seven other oil fields in the central part of West Siberia. Age dating is based on ammonite biostratigraphy which has been generalized for the interval from published and unpublished sources. A relative sea-level curve was obtained by measuring onlap/offlap variations from seismic data and geologic profiles. The major sea-level events inferred from the West Siberian data generally correspond to those of the QEC. This result demonstrates the strong influence of eustasy on the deposition of the "Clinoform Neocomian" complex.

To summarize, close correlation of the QEC to relative sea-level curves based on two regions and stratigraphic intervals of the West Siberian Basin demonstrates the dominance of eustasy in controlling sedimentation in these regions. In addition, it provides another good test of the validity of the QEC as a global stratigraphic tool. Subsequent application of the QEC to West Siberia will make it possible to filter the eustatic signal from basin stratigraphic data and thereby estimate basin subsidence and

sedimentation history more accurately than previously possible. Accurate reconstructions of site-based relative sea-level histories will provide the basis for these analyses. The accuracy for these reconstructions can be greatly improved by integration of all the available multidisciplinary stratigraphic data including seismic, wire-line logs, and sedimentology/ biostratigraphy.

REFERENCES

Angevine, C. L., 1989, Relationship of eustatic oscillations to regressions and transgressions on passive continental margins, *in* R. A. Price, ed., Origin and Evolution of Sedimentary Basins and Their Energy and Mineral Resources: Geophysical Monograph, Littleton, Col., American Geophysicsal Union-International Union of Geodesy and Geophysics, p. 29-36.

Angevine, C. L., P. L. Heller, and C. Paola, 1990, Quantitative sedimentary basin modeling: American Association of Petroleum Geologists Continuing Education Course Notes, v. 32: Tulsa, AAPG, 133 p.

Arkell, W. J., 1933, The Jurassic System in Great Britain: Oxford, Clerendon Press, 681 p.

Arthur, M. A., S. O. Schlanger, and H. C. Jenkyns, 1987, The Cenomanian-Turonian anoxic event, II. Paleoceanographic controls on organic production and preservation, *in* J. Brooks, and A. J. Fleet, eds., Marine petroleum source rocks: Spec. Publ. Geol. Soc. London, p. 401-420.

Baraboshkin, E. Y., 1992, Lower Albian of the central regions of the Russian Platform, *in* S. M. Shick, ed., Phanerozoic stratigraphy of the Central East European Platform, Moscow, Centrgeologia, p. 20-36.

Baraboshkin, E. Y., and I. A. Mikhailova, 1987, Ammonites and stratigraphy of Middle Albian of north Moscow Region. Paper 1. Stratigraphy: BMOIP, v. 62, p. 91-100.

Barron, E. J., 1985, Explanations of the Tertiary global cooling trend: Palaeogeogr. Palaeoclim. Palaeoecol, v. 50, p. 45-61.

Barron, E. J., S. L. Thompson, and S. H. Schneider, 1981, An ice-free Cretaceous? Results from climate model simulations: Science, v. 212, p. 501-508.

Belozerov, V. B., 1989, Kinematic model of deposition of Jurassic-Cretaceous sediments of West Siberian Plate, Geologic structure and oil-gas potential of south-east of West Siberia, Novosibirsk, SNIIGGiMS, p. 99-106.

Belozerov, V. B., N. A. Brylina, and E. E. Danenberg, 1989a, Lithostratigraphy of Vasyugan Formation in south-east of the West Siberian Plate, Geologic structure and oil-gas potential of south-east of West Siberia, Novosibirsk, SNIIGGiMS, p. 75-83.

Belozerov, V. B., N. A. Brylina, and E. e. Danenberg, 1989b, Perspectives of exploration in non-structural traps of Upper Jurassic sediments of Middle Vasyugan Mega-swell, Geologic structure and oil-gas potential of south-east of West Siberia, Novosibirsk, SNIIGiMS, p. 99-106.

Benedict, G., and K. Walker, 1978, Paleobathymetric analysis in Paleozoic sequences and its geodynamic significance: Am. J. Sci., v. 278, p. 579-607.

Bill, M., P. O. Baumgartner, J. C. Hunziker, and Z. D. Sharp, 1995, Carbon isotope stratigraphy of the Liesberg Beds member (Oxfordian, Swiss Jura): Eclog. Geol. Helv., v. 88, p. 135-155.

Blank, M. Y., D. P. Naidin, and A. G. Olferiev, 1992, Relief of Cenomanian roof in Dniepr-Donetz Trough, Voronezh Anticlyse and adjacent structures of East-European Platform: Bull. Moscow Soc. Natural., v. 67, p. 43-47.

Bowen, D., P. Weimer, and A. Scott, 1993, The relative success of siliciclastic sequence stratigraphic concepts in exploration: Examples from incised valley fill and turbidite systems reservoirs, *in* P. Weimer, and H. Posamentier, eds., Silicclastic Sequence Stratigraphy: Recent Developments and Applications, Tulsa, AAPG, p. 15-43.

Braduchan, Y. V., F. G. Gurari, V. A. Zakharov, and a. others, 1986, Bazhenov Horizon of West Siberia (stratigraphy, paleogeography, ecosystem, oil potential): Trudy IGiG, v. 649: Novosibirsk, Nauka, 216 p.

Brett, C., A. Boucot, and B. Jones, 1993, Absolute depths of Silurian benthic assemblages: Lethaia, v. 26, p. 25-40.

Bromley, R., 1967, Marine phosphorites as depth indicators: Mar. Geol., v. 5, p. 503-509.

Brylina, N. A., and E. E. Danenberg, 1989, Paleogeomorphologic factors for oil-gas exploration in non-structural traps in deposits of Vasyugan Formation in south-east of West Siberian Plate, Geologic structure and oil-gas potential of south-east of West Siberia, Novosibirsk, SNIIGiMS, p. 115-123.

Bushinski, G., 1964, On shallow water origin of phosphatic deposits, *in* L. V. Straaten, ed., Deltaic and shallow marine deposits, Amsterdam, Elsevier, p. 62-70.

Christie-Blick, N., 1990, Tectonic and eustatic controls on sedimentary successions on passive continental margins: AAPG Bull., v. 74, p. 628.

Clifton, H. E., 1988, Sedimentological approaches to paleobathymetry, with applications to the Merced Formation of Central California: Palaios, v. 3, p. 507-522.

Cloetingh, S., 1988, Intraplate stresses: A tectonic cause for third-order cycles in apparent sea level?, *in* B. H. Lidz, ed., Sea-Level Changes: An Integrated Approach, Tulsa, Society of Economic Paleontologists and Mineralogists, p. 19-29.

Eicher, D. L., 1969, Paleobathymetry of Cretaceous Greenhorn Sea in eastern Colorado: AAPG Bull., v. 53, p. 1075-1090.

Ekdale, A., 1988, Pitfalls of paleobathymetric interpretations based on trace fossil assemblages: Palaios, v. 3, p. 464-472.

Emery, D., and K. J. Myers, 1996, Sequence stratigraphy, Cambridge, Blackwell Science, p. 297.

Ericksen, M., and R. Slingerland, 1990, Numerical simulations of tidal and wind-driven circulation in the Cretaceous Interior Seaway of North America: Geol. Soc. Amer. Bull., v. 102, p. 1499-1516.

Evseev, G., 1981, Communities of bivalves in postglacial sediments of the Japanese Sea shelf: Moscow, Nauka, 160 p.

Fedynsky, V. V., B. A. Sokolov, N. A. Strakhova, and V. G. Fel'dt, 1976, The Central Russian aulacogen-an ancient equivalent of modern rift systems: Intern. Geol. R. , v. 18, p. 509-514.

Gerasimov, P., 1962, Jurassic and Cretaceous deposits of the Russian platform, Regional sketches of the Geology of the USSR, *in* I. Lyubimov, ed., Moscow, Moscow University Press, p. 196 .

Gerasimov, P., 1969, Upper substage of the Volgian stage in the central part of the Russian platform; Paleontologic, stratigraphic, and lithologic investigations, Interdepartmental Stratigraphy Comission, Moscow, Academy Nauk, p. 132.

Gerasimov, P., 1971, Jurassic System, Central Part of European USSR: Geological description: Geology of the USSR, Moscow, Nedra, p. 373-416.

Golbert, A. V., I. G. Klimova, and V. N. Sachs, 1972, Reference section of the Neocomian of West Siberia in the Subarctic Urals: Novosibirsk, Nauka, 184 p.

Gygi, R. A., 1986, Eustatic sea level changes of the Oxfordian (Late Jurassic) and their effect documented in sediments and fossil assemblages of an epicontinental sea: Eclogae geol. Helv., v. 79, p. 455-491.

Hallam, A., 1963, Eustatic control of major cyclic changes in Jurassic sedimentation: Geological Magazine, v. 100, p. 444-450.

Hallam, A., 1967, The depth significance of shales with bituminous laminae: Mar. Geol., v. 5, p. 473-480.

Hallam, A., 1978, Eustatic Cycles in the Jurassic: palaeogeography, Palaeoclimatology, Palaeoecology, v. 23, p. 1-32.

Hallam, A., 1985, A review of Mesozoic climates: Journal of the Geological Society of London, v. 142, p. 433-445.

Hallam, A., 1988, A re-evaluation of Jurassic eustasy in the light of new data and the revised Exxon curve, *in* C. W. e. al., ed., Sea-Level Change: An Integrated Approach, Soc. Econ. Paleont. Mineral., p. 261-273.

Hallam, A., 1992, Phanerozoic Sea Level Changes: N.Y., Columbia, 266 p.

Haq, B. U., J. Hardenbol, and P. R. Vail, 1988, Mesozoic and Cenozoic chronostratigraphy and cycles of sea-level change, *in* B. H. Lidz, ed., Sea-Level Changes: An Integrated Approach: SEPM Special Publication No. 42, Tulsa, The Society of Economic Paleontologists and Mineralogists, p. 71-108.

Harland, W., R. L. Armstrong, A. V. Cox, L. E. Craig, A. G. Smith, and D. G. Smith, 1990, A geologic time scale 1989, Cambridge, Cambridge University Press, p. 263.

Heydari, E., and W. J. Wade, 1993, Sedimentology and geochemistry of the lower mudstone member of the Smackover Formation, U.S. Gulf Coast: implications for Late Jurassic seawater composition, paleoceanography, and anoxic events: Pangea, Carboniferous to Jurassic, CSPG Annual Convention, p. 138.

Hoffman, A., M. Gruszczynski, K. Malkowski, S. Halas, B. A. Matyja, and A. Wierbowski, 1991, Carbon and oxygen isotope curves for the Oxfordian of central Poland: Acta Geol. Polon., v. 43, p. 157-164.

Jacobs, D. K., and D. L. Sahagian, 1993, Climate-induced fluctuations in sea level during non-glacial times: Nature, v. 361, p. 710-712.

Jenkyns, H. C., 1996, Relative sea-level change and carbon isotopes: data from the Upper Jurassic (Oxfordian) of central and Southern Europe: Terra Nova, v. 8, p. 75-85.

Jervey, M. T., 1988, Quantitative geological modeling of siliciclastic rock sequences and their seismic expression, *in* B. H. Lidz, ed., Sea-Level Changes: An Integrated Approach, Tulsa, Socity of Economic Paleontologists and Mineralogists, p. 47-70.

Karagodin, Y., and A. Nezhdanov, 1988, Lithmologic features of space distribution of reservoirs and hydrocarbon accumulations of Western and Eastern Siberia: Geology and Geophysics, p. 3-7.

Karagodin, Y. N., and J. M. Armentrout, 1996, Analysis of basic concepts and terms of lithmology and sequence stratigraphy: Geology and Geophysics, v. 37, p. 3-11.

Karagodin, Y. N., S. V. Ershov, V. S. Safonov, and a. m. others, 1996, The Priob' oil zone in West Siberia: system-lithmological aspect: Novosibirsk, SB RAS SPC UIGGM, 252 p.

Karagodin, Y. N., M. A. Levchuk, and S. V. Ershov, 1991, Structure of Jurassic-Neocomian sedimentary complex of the Surgut Trough and adjacent areas, Institute of Geology, Russian Academy of Sciences, Siberian Branch, Novosibirsk.

Karner, G. D., 1986, Effects on lithospheric in-plane stress on sedimentary basin stratigraphy: Tectonics, v. 5, p. 573-588.

Kendall, C. G. S. C., and I. Lerche, 1988, The rise and fall of eustasy, *in* B. H. Lidz, ed., Sea-Level Changes: An Integrated Approach, Tulsa, Society of Economic Paleontologists and Mineralogists, p. 3-17.

Kliger, J., 1994, Sedimentation, zoning of reservoir rocks in W. Siberian oil fields: Oil & Gas J., v. 92, p. 69-71.

Krymholts, G., 1972, The Jurassic system, *in* D. V. Nalivkin, ed., Stratigraphy of the USSR, Moscow, Izdatelstvo Nedra, p. 26-135.

Krymholts, G., M. Mesezhnikov, and G. Westeermann, 1988, The Jurassic Ammonite Zones of the Soviet Union, GSA Special Paper, GSA, p. 118.

Krymholts, G. Y., 1984, The Jurassic-Cretaceous boundary and the Ryazanian horizon, *in* V. V. Menner, ed., The Jurassic and Cretaceous boundary stages, Moscow, Nauka, p. 5-8.

Kump, L. R., and A. C. Hine, 1986, Ooids as sea-level indicators, *in* O. Van de Plassche, ed., Sea-Level Research: A Manual for the Collection and Evaluation of Data, Norwich, Geo Books, p. 175-193.

Kunin, N. Y., S. P. Filippova, S. G. Kuzmenkov, S. P. Tyunegin, and A. N. Zadoenko, 1993, The structural model and seismostratigraphic scale of Neocomian sediments in the Middle Ob' region, *in* B. S. Sokolov, ed., Seismostratigraphic investigations in Eurasia, Moscow, Nauka, p. 67-82.

Lawrence, D., 1993, Evaluation of Eustasy, Subsidence, and Sediment Input as Controls on Depositional Sequence Geometries and the Synchroneity of Sequence Boundaries, *in* P. Weimer, and H. Posamentier, eds., Siliciclastic Sequence Stratigraphy: AAPG Memoir, Tulsa, AAPG.

Loutit, T. S., J. Hardenbol, and P. R. Vail, 1988, Condensed sections: The key to age determination and correlation of contenental margin squences, *in* B. H. Lidz, ed., Sea-Level Change: An Integrated Approach: SEPM Special Publication, Tulsa, The Society of Economic Paleontologists and Mineralogists, p. 183-213.

Maksimova, S., 1949, Characteristics of distribution and preservation of mollusc shells: Tr. Inst. Okeanol. AN SSSR, v. 4, p. 165-171.

Marcher, M. V., and R. G. Stearns, 1962, Tuscaloosa formation in Tennessee: U.S. Geology Survey Bulletin, v. 73, p. 1365-1386.

Meledina, S. V., 1994, Boreal Middle Jurassic of Russia: Novosibirsk, Nauka, 182 p.

Mesezhnikov, M., 1984, Zonal subdivision of the Ryazanian horizon, *in* V. Menner, ed., Boundary stages of the Jurassic and Cretaceous systems: Transactions, Moscow, Nauka, p. 54-66.

Mesezhnikov, M., 1989, Practical aspects of detailed biostratigraphic studies in hydrocarbon-rich basins, Methodical aspects of stratigraphic studies in hydrocarbon-rich basins: VNIGRI publications, Leningrad.

Miall, A. D., 1992, Exxon global cycle chart: an event for every occasion?: Geology, v. 20, p. 787-790.

Milanovsky, E., 1987, Geology of the USSR, v. 1: Moscow, Ak. Nauk. USSR, 416 p.

Mitta, V. V., 1993, Ammonites and zonal stratigraphy of Middle Volgian substage of the central Russia: Kiev, 132 p.

Mkrtchyan, O., I. Grebneva, V. Igoshkin, M. Karneev, A. Nezhdanov, and S. Filina, 1990, Seismogeological study of clinoform sediments of the Middle Ob Region: Moscow, Nauka, 108 p.

Moore, G., D. Hayashida, C. Ross, and S. Jacobson, 1992, Paleoclimate of the Kimmeridgian/Tithonian (Late Jurassic) world: I. Results using a general circulation model: Paleogeogr. Paleoclimat. Paleoecol., v. 93, p. 113-150.

Naidin, D., 1959, On the paleogeography of the Russian platform during the Upper Cretaceous epoch: Stockholm Contr. Geol., v. 3, p. 127-138.

Naidin, D., V. Benyamovsky, and L. Kopayevitch, 1984, Scheme of biostratigraphic division of the Upper Cretaceous of the European part of the paleogeographic realm: Moscow Univ. Bull., v. 4, p. 3-15.

Naidin, D. P., 1981, The Russian Platform and the Crimea, *in* R. A. Reyment, and P. Bengtson, eds., Aspects of Mid-Cretaceous Regional Geology, Academic Press, p. 29-69.

Naidin, D. P., V. Pokhialainen, V. Katz, and V. Krassilov, 1986, Cretaceous period: Paleogeography and paleooceanology: Nauka: Moscow, 262 p.

Nalivkin, D. V., 1973, Geology of the USSR: Toronto, University of Toronto Press, 855 p.

Naumov, A. L., T. M. Onishuk, and M. M. Binshtok, 1977, Features of deposition of the Neocomian section in Shirotnoe Priobie, Geology and exploration of oil and gas accumulations in West Siberia, Tyumen, TII, p. 39-49.

Nezhdanov, A. A., 1990, Theoretical problems of cyclic sedimentation, *in* Y. N. Karagodin, ed., Lithologic features of distribution of reservoirs and hydrocarbon accumulations, Novosibirsk, Nauka.

Nezhdanov, A. A., V. V. Ogibenin, M. I. Kurenko, S. V. Sapozhnikova, and E. B. Topychkanova, 1992, Regional lithmostratigraphic correlation of the Mesozoic and Cenozoic of West Siberia and main systematic distributions of non-anticlinal traps for hydrocarbons: Petroleum Geology, v. 26, p. 71-92.

Norris, M., and A. Hallam, 1995, Facies variations across the Middle-Upper Jurassic boundary in western Europe and the relationship to sea-level changes: Palaeogeography, Palaeoclimatology, Palaeoecology, v. 116, p. 189-245.

Olferiev, A., 1986, Stratigraphy of Jurassic deposits of the Moscow Synclise, *in* M. Mesezhnikov, ed., Jurassic deposits of the Russian Platform, Leningrad, Vses. Neft. Nauchn. Issled. Geologorazved, p. 48-61.

Olferiev, A., 1988, Composition of the lower Cretaceous of the central and southern part of the Moscow Synclise in accordance with the distribution of essential minerals, Inst. MGRI.

Peters, K., A. E. Kontorovich, J. M. Moldovan, V. E. Andrusevich, B. J. Huizinga, G. J. Demaison, and O. F. Stasova, 1993, Geochemistry of selected oils and rocks from the central portion of the West Siberian Basin, Russia: AAPG Bull., v. 77, p. 863-887.

Pinous, O., 1993, New data on stratigraphy of Upper Jurassic and Neocomian deposits of Shirotnoe Priobie (West Siberia): XXXI international student conference, p. 70-82.

Pitman, W. C., 1978, Relationship between eustasy and stratigraphic sequences of passive margins: Geo. Soc. Am. Bull., v. 89, p. 1389-1403.

Porrenga, D., 1967, Glauconite and chamosite as depth indicators in the marine environment: Mar. Geol., v. 5, p. 495-501.

Posamentier, H. W., G. P. Allen, D. P. James, and M. Tesson, 1992, Forced regressions in a sequence stratigraphic framework: concepts, examples, and exploration significance: AAPG Bull., v. 76, p. 1687-1709.

Posamentier, H. W., M. T. Jervey, and P. R. Vail, 1988, Eustatic controls on clastic deposition I-conceptual framework, *in* B. H. Lidz, ed., Sea-Level Changes: An Integrated Approach: Spec. Publ. Soc. econ. Paleont. Mineral., Tulsa, Society of Economic Paleontologists and Mineralogists, p. 109-124.

Rovenskaya, A., and N. Nemchenko, 1992, Prediction of hydrocarbons in the West Siberian Basin: Bull. Cent. Rech. Expl. Prod. Elf Aquitaine, v. 16, p. 285-318.

Ruffell, A., 1991, Sea-level events during the Early Cretaceous in western Europe: Cret. Res., v. 12, p. 527-551.

Sachs, V. N., 1969, Reference section of the Upper Jurassic of the Kheta River basin, Moscow, Nauka, p. 208.

Sachs, V. N., 1975, The Jurassic-Cretaceous boundary and the Berriasian stage in the boreal realm, Jerusalim, Keter Pub. House, p. 345.

Sachs, V. N., 1976, Stratigraphy of the Jurassic System of the North of the USSR, Moscow, Nauka, p. 436.

Sachs, V. N., V. A. Basov, V. A. Zakharov, M. S. Mesezhnikov, Z. Z. Ronkina, N. I. Shulgina, and E. G. Judovnyi, 1965, Stratigraphy of the Upper Jurassic and Lower Cretaceous sediments of Khatanga Depression, *in* V. N. Sachs, ed., Stratigraphy and Paleontology of Mesozoic sediments of Northern Siberia, Moscow, Nauka, p. 27-60.

Sahagian, D., 1988, Ocean temperature-induced chage in lithospheric thermal structure: a mechanism for long-term eustatic sea level change: J. Geology, v. 96, p. 254-261.

Sahagian, D., and S. Holland, 1991, Eustatic sea-level curve based on a stable frame of reference: Preliminary results: Geology, v. 19, p. 1209-1212.

Sahagian, D., and M. Jones, 1993, Quantified Middle Jurassic to Paleogene eustatic variations based on Russian Platform Stratigraphy: Stage-level resolution: Geol. Soc. Amer. Bull., v. 105, p. 1109-1118.

Sahagian, D., O. Pinous, A. Olferiev, V. Zakharov, and A. Beisel, 1994, Eustatic curve for the Middle Jurassic through Cretaceous based on Russian Platform stratigraphy: Zonal resolution: GSA Nat'l Mtg. 1994 Abstracts, v. 26, p. 246.

Sahagian, D. L., 1987, Epeirogeny and eustatic sea level changes since the mid-Cretaceous: Application to central and western United States: JGR, v. 92, p. 4895-4904.

Sazonov, N. P., and I. G. Sazonova, 1967, Paleogeography of the Russian Platform in the Jurassic and Early Cretaceous, *in* B. Khain, ed., Trans. VNIGRI, Leningrad, Nedra, p. 227.

Sazonov, N. T., 1957, Jurassic sediments of the central regions of Russian platform: Leningrad, Gostoptehizdat, 156 p.

Sazonova, I. G., 1958, Lower Cretaceous deposits in central regions of the Russian Platform, *in* O. V. Flerovoi, ed., Mesozoic and Tertiary deposits of the central regions of the Russian Platform, Moscow, VNIGRI, p. 31-184.

Seilacher, A., 1967, Bathymetry of trace fossils: Mar. Geol., v. 5, p. 413-428.

Shpilman, V., G. Myasnikova, and L. Trusov, 1993, Depositional breaks during formation of Neocomian clinoforms in West Siberia: Geologiya nefti i gaza, p. 2-5.

Slavkin, V. S., N. S. Shik, A. A. Guseynov, and T. E. Yermolova, 1996, Prediction of sandstone bodies in Upper Jurassic sediments of Kaimysov Arch: Petroleum geology, v. 30, p. 235-242.

Sleep, N. H., 1976, Platform subsidence mechanisms and "eustatic" sea level changes: Tectonophys., v. 36, p. 45-56.

Sloan, R., 1964, The Cretaceous system in Minnesota: Rept. Inv. Minn. Geo. Surv., v. 5, p. 64.

Sloss, L. L., 1991, The tectonic factor in sea-level change: A countervailing view: J. Geophys. Res, v. 96, p. 6609-6618.

Sosedkov, V. S., Y. N. Surkov, and S. A. Levchenko, 1987, Cyclicity of the Neocomian sediments from northern part of West Siberia (seismic exploration data), *in* A. A. Trofimuk, ed., Application Problems of Sedimentary cyclicity and Oil Presence, Novosibirsk, Nauka, p. 20-23.

Steckler, M. S., and A. B. Watts, 1978, Subsidence of the Atlantic-type continental margin of New York: Earth Planet. Sci. Lett, v. 41, p. 1-13.

Sun, S. Q., 1989, A new interpretation of the Corallian (Upper Jurassic) cycles of the Dorset coast, southern England: Geological Journal, v. 24, p. 139-158.

Sykes, R. M., and F. A. Surlyk, 1976, A revised ammonite zonation of the boreal Oxfordian and its application in northeast Greenland: Lethaia, v. 9, p. 421-436.

Talbot, M. R., 1973, Major sedimentary cycles in the Corallian Beds of southern England: Palaeogeography, Palaeoclimatology, Palaeoecology, v. 14, p. 293-317.

Tatianin, G. M., and B. M. Volkov, 1982, Stratigraphy and features of distribution of productive beds of Vasyugan Formation in south-east of West Siberian Plain, Stratigraphy of Triassic and Jurassic sediments of oil and gas bearing basins of USSR, Leningrad, VNIGRI, p. 75-87.

Ulmishek, G., 1993, Geology and Exploration Potential of major Petroleum Basins in the Former Soviet Union: AAPG Bull., v. 77, p. 2022.

Ulmishek, G., and C. Masters, 1993, Oil, gas resources estimated in the Former Soviet Union: Oil and Gas Journal, v. 91, p. 59-62.

Underhill, J., 1991, Controls on late Jurassic seismic sequences, Inner Moray Firth, UK North Sea: A critical test of a key segment of Exxon's original global cycle chart: Basin Research, v. 3, p. 79-98.

Underhill, J., and M. Partington, 1993, Use of sequence stratigraphy in defining and determining a regional tectonic control on the "Mid Cimmerian unconformity": implications for North Sea Basin development and the global sea-level chart, *in* P.

Weimer, and H. Posamentier, eds., Siliciclastic sequence stratigraphy: recent development and applications, Tulsa, AAPG Memoir, p. 449-484.

Van Wagoner, J. C., H. W. Posamentier, R. M. Mitchum, P. R. Vail, J. F. Sarg, T. S. Loutit, and J. Hardenbol, 1988, An overview of the fundamentals of sequence stratigraphy and key definitions, *in* B. H. Lidz, ed., Sea-Level Changes: An Integrated Approach, Tulsa, Society of Economic Paleontologists and Mineralogists, p. 39-45.

Vinogradov, A. P., 1968, Atlas of the lithological-paleogeographical maps of the USSR: Ministry of geology of the USSR.

Vyachkileva, N., I. Klimova, A. Turbina, Y. Braduchan, V. Zakharov, S. Meledina, and A. Aleinikov, 1990, Atlas of Molluscs and foraminiferas of Upper Jurassic and Neocomian Marine Sediments of the West Siberian Oil Province, v. 1: Moscow, Nedra, 285 p.

Walker, R. G., 1984, Shelf and shallow marine sands, *in* R. G. Walker, ed., Facies models, St. John's, Newfoundland, Geological Association of Canada.

Walker, R. G., and A. G. Plint, 1992, Wave- and storm-dominated shallow marine systems, *in* R. G. Walker, ed., Facies Models: Reponse to sea level change, St. John's, Newfoundland, Geol. Assoc. Canada, p. 219-238.

Watts, A. B., 1988, Gravity anomalies, crustal structure and flexure of the lithosphere at the Baltimore Canyon Trough: Earth Planet. Sci. Lett., v. 89, p. 221–238.

Watts, A. B., 1989, Lithospheric flexure due to prograding sediment loads: implications for the origin of offlap/onlap patterns in sedimentary basin: Basin. Res., v. 2, p. 133-144.

Weimer, P., and H. Posamentier, 1993, Recent Develpments and Applications in Siliciclastic Sequence Stratigraphy, *in* P. Weimer, and H. Posamentier, eds., Siliciclastic Sequence Stratigraphy: AAPG Memoir, AAPG, p. 3-13.

Weimer, R. J., 1984, Relation of unconformities, tectonics, and sea-level changes, Cretaceous of Western Interior, USA: AAPG, v. Memoir 36, p. 7-35.

Weissert, H., and A. Lini, 1991, Ice age interludes during the time of Cretaceous greenhouse climate, *in* D. W. Muller, J. A. McKenzie, and H. Weissert, eds., Controversies in modern geology, London, Academic Press, p. 173-191.

Wignall, P. B., 1991, Test of the concepts of sequence stratigraphy in the Kimmeridgian (Late Jurassic) of England and northern France: Marine and Petroleum Geology, v. 8, p. 430-441.

Wright, J. K., 1986, A new look at the stratigraphy, sedimentolgy and ammonite fauna of the Corallian Group (Oxfordian) of South Dorset: Proceedings of Geological Association, v. 97, p. 1-21.

Yanin, B., 1983, Basics of taphonomy: Moscow, Nedra, 184 p.

Zakharov, V., 1966, Late Jurassic and Early Cretaceous bivalves of northern Siberia and their paleoecology. Order Anisomyaria: Trans. Inst. Geol. Geophys. Sib. Branch Acad. Sci. USSR, v. 113: Moscow, Nauka, 189 p.

Zakharov, V., 1984, Taphonomy and paleoecolgy of the marine invertebrates: Novosibirsk, Novosibirsk State University, 78 p.

Zakharov, V., and O. Khomentovsky, 1989, New data on stratigraphy of marine Upper Cretaceous of the Ust-Yenisey trough, *in* V. Solovyev, ed., Stage and zonal scales of the Boreal Mesozoic of the USSR, Moscow, Nauka, p. 176-184.

Zakharov, V., M. Mesezhnikov, and a. m. others, 1983, Jurassic paleogeography of northern USSR: Trudy IGiG, v. 573: Novosibirsk, Nauka, 191 p.

Zakharov, V. A., A. L. Beisel, and V. P. Pokhialainen, 1989a, Discovery of the marine Cenomanian of the North of Siberia: Sov. Geol. Geophys., v. 30, p. 7-10.

Zakharov, V. A., A. L. Beisel, K. V. Zverev, N. K. Lebedeva, and O. V. Khomentovsky, 1989b, Stratigraphy of the Upper Cretaceous Deposits of Northern Siberia (Yangoda River Section): Novosibirsk, Ins. Geol. Geophys., 70 p.

Zakharov, V. A., and J. I. Bogomolov, 1984, The correlation of the boreal and subtethyan Valanginian on Buchias and ammonites, Boundary stages of the Jurassic and Cretaceous System, Moscow, Nauka, p. 18-27.

Zakharov, V. A., and E. G. Judovnyi, 1974, Sedimentary processes and paleoenvironments of fauna in the Khatanga Early Cretaceous Sea, *in* A. S. Dagis, and V. A. Zakharov, eds., Mesozoic Paleobiogeography of the Northern Eurasia, Novosibirsk, Nauka, p. 127-174.

Zakharov, V. A., Y. N. Zanin, K. V. Zverev, and H. K. Lebedeva, 1986, Stratigraphy of the Upper Cretaceous deposits of the Northern Siberia (Ust-Jenisey depression): Novosibirsk, Ins. Geol. Geophys., 82 p.

Zenkevitch, L. A., 1977, Biological Producivity of the Ocean: Oceanologia. Biologia oceana, v. 2: Moscow, Nauka, 309 p.

Zhukov, V., and A. Konstantinovich, 1951, Development of paleorelief on the top of Carboniferous sediments in the Southwestern region of the Moscow Paleozoic Depression: Acad. A.D.Arkhangelskyi memoires, Moscow, p. 433-474.

Ziegler, P. A., 1982, Geological Atlas of Western and Central Europe, Shell Internationale Petroleum maatschappij B.V., 1-110 p.

APPENDIX

STRATIGRAPHIC DESCRIPTIONS

Russian Platform stratigraphy is subdivided into lithostratigraphic formations. The correlation of formations to biostratigraphic zonation is shown on figures 5 and 6.

Teplyi Stan (M1)

This well is located in southern Moscow city near the Teplyi Stan metro station, altitude 253 m, depth 144.6 m.

Unit	Lithology	Thickness (m)
Quaternary		
34	Clay and mud with pebbles, moraine deposits	11.8
Cretaceous		
Tentikovskaya Formation (Upper Santonian)		
33	Silty clay with silica; greenish gray; lenses and layers of quartz-glauconitic silt and very fine sand; fragments of light gray siliceous ooze	2.4
Dmitrovskaya Formation (Upper Santonian)		
32	Clayey sand; greenish gray, brown limonite mottles; micaceous; thin layers of quartz-glauconitic sandstone; erosional unconformity at the lower contact	1.0
Zagorskaya Formation (Upper Coniacian-Lower Santonian)		
31	Unsorted quartz sand; rusty yellow; predominantly fine-medium grained with quartz gravel; layers of greenish gray silty clays; quartz-glauconitic sandstone concretions with siliceous cement	5.8
30	Unsorted predominantly fine sand; light brown; quartz and chert gravel with basal erosional unconformity	2.5
Jakhromskaya Formation (Lower Cenomanian-Upper Albian)		
29	Fine quartz sand; greenish gray; massive, ferrous in lower part	3.8
28	Fine sand; greenish to light gray; clayey erosional unconformity at the lower contact	1.4
Paramonovskaya Formation (Upper Albian)		
27	Clayey silt; greenish gray to dark gray; brown limonite mottles, micaceous; thin layers of black clay; *Nereites* and *Zoophycos* trace fossils	16.6
26	Silty clay to fine clayey silt; dark gray to black; horizontally laminated rare small horizontal trace fossils	5.0
25	Very fine quartz-glauconitic clayey sand; black, massive	0.8
24	Intercalation of dark gray clayey silts, black silty clays, and fine clayey sands; clayey phosphorite concretions; lenses of very fine sand in the lower part	6.1
23	Fine-medium glauconitic-quartz sand, dark gray to black; quartz gravel and phosphorite pebbles in the lower part; erosional unconformity at the lower contact	0.7
Gavrilkovskaya Formation (Middle Albian)		
22	Medium-fine quartz sand; dark gray; small sandy phosphorite concretions in the lower part; erosional unconformity at the base	5.1

Volgushinskaya Formation (Upper Aptian)

21 Fine sand and silt; light to bluish gray; clayey, micaceous; thin lenses and layers of clay in the lower part, flaser bedding sedimentary structure 5.7

20 Poorly sorted, predominantly medium sand; brownish gray; quartz gravel thin layer of phosphorite in the lower part 1.5

Vorokhobinskaya Formation (Lower Aptian)

19 Fine clayey quartz sand; dark gray; micaceous, horizontal trace fossils layer of sandstone with siderite cement; wavy erosional surface at the base 7.1

Ikshinskaya Formation (Lower Aptian)

18 Fine sand; dark to brownish gray; clayey, micaceous; horizontally laminated, thin layers of black clay; plant detritus; erosional surface at the base 3.8

Butovskaya Formation (Barremian)

17 Intercalation of black silty clays and brown fine sands; mean thickness of layers is ~5cm; trough cross-bedding in sands, flaser bedding in some places; concretion of siderite sand in the lower part; lower contact is very distinct but with no evidence of erosion 4.7

Kotelnikovskaya Formation (Upper Hauterivian)

16 clay; dark gray to black; massive 1.4

Gremyachevskaya Formation (Upper Hauterivian)

15 Unsorted quartz sand and sandstone; grayish brown; predominantly fine-grained, small quartz gravels; siderite cement 5.7

Savelievskaya Formation (Upper Hauterivian)

14 Fine quartz sand; dark gray; clayey, micaceous; layers of clay; hummocky cross-stratified; erosional unconformity at the lower contact 4.6

Jurassic

Kuntsevskaya Formation (Upper Volgian, zone C. nodiger)

13 Fine quartz sand; gray; micaceous, clayey; lenticular bedding in lower part 13.6

12 Fine sand; greenish gray; micaceous, clayey; plant detritus; wavy to lenticular bedding 4.6

Lopatinskaya Formation (Middle-Upper Volgian)

11 Fine clayey sand; greenish black; shell detritus, fragments of belemnites, fragment of mid Volgian ammonite; erosional surface at the base 3.7

Philevskaya Formation (Middle Volgian)

10 Coarse silt; brownish to dark gray; clayey, micaceous, limy in some places fragments of thin bivalve shells; Virgatites sp. 4.5

Egorievskaya Formation (Middle Volgian, zone V.virgatus)

9 Fine sand; black; clayey, glauconite; abundant shell detritus; abundant phosphorite concretions in the lowermost part; Erosional unconformity at the base, ammonite imprints: Virgatites sp. 0.9

Ermolinskaya Formation (Lower Kimmeridgian-Upper Oxfordian)

8 Silty rich clay; dark gray to black; abundant shell detritus, pyrite; bivalve shells and ammonite imprints; Amoeboceras sp., Cylindrotheutis costromensis 11.2

Kolomenskaya Formation (Upper Oxfordian)

7 Silty clay; gray; small shell detritus; small deformed ammonites 1.0

Podmoskovnaya Formation (Middle-Upper Oxfordian)

6 Lean clay; brownish gray; fine horizontal lamination; fine shell detritus; small ammonites in the lower part 0.6

5	Clay; dark gray; fine laminated; small lenses of light gray silt; large ammonites erosional unconformity at the lower contact	2.0
Podosinkovskaya Formation (Upper Callovian-Lower Oxfordian)		
4	Clay; greenish gray; compact, shell detritus, small lenses of light gray silt; small ammonites	2.6
3	Clay; light greenish gray; fine lamination; pyrite; rare horizontal trace fossils; erosional unconformity at the base	1.5
Kriushskaya Formation (Middle Callovian)		
2	Oolitic clay-marl; rusty brown with light gray mottles; erosional unconformity	0.1
Carboniferous		
1	Limestone	0.8

Varavino (M456b)

Well is located in Moscow Province, Sergiev-Posad County, 0.2 km south-east of village Varavino
Altitude 201m, depth 222.3 m.

Unit	Lithology	Thickness (m)
Quaternary		
27	Silty clay and silt with pebble and boulders, moraine deposits; erosional unconformity at the base	32.5
Cretaceous		
Jakhromskaya Formation (Upper Albian-Lower Cenomanian)		
26	Clayey silt; greenish gray; thin clay layers; bioturbation erosional unconformity at the lower contact	8.2
Paramonovskaya Formation (Upper Albian)		
25	Clay; black; compact, sometimes silty; thin layers of medium sand; rare phosphorite concretions; erosional unconformity at the lower contact	26.2
Gavrilkovskaya Formation (Middle Albian)		
24	Fine to medium sand; grayish green; glauconitic-quartz, clayey; clayey and sandy-clayey phosphorite concretions of irregular shapes; erosional unconformity at the lower contact	7.6
Volgushinskaya Formation (Upper Aptian)		
23	Clayey silt; gray and dark gray; horizontally laminated, micaceous; in the lower part more clayey and abundant plant detritus	3.2
Vorokhobinskaya Formation (Lower Aptian)		
22	Fine to silty sand; dark gray; thin coaly layers, very micaceous wavy erosion at the base	8.8
Ikshinskaya Formation (Lower Aptian)		
21	Fine to medium quartz sand; dark brown; micaceous,	0.3
20	Fine to silty sand; light brownish gray to white; clayey, micaceous; abundant coaly plant detritus in the lower part	6.5
19	Silty quartz sand; snow white; coaly pellets, erosional surface at the base	4.4
Kotelnikovskaya Formation (Upper Hauterivian)		
18	Fine to medium quartz sandstone; grayish brown; clayey ferruginous cement	2.9

17	Clayey-coaly silt; black; small phosphorite nodules and concretions	0.5
16	Clay; grayish brown; fine laminated, micaceous	2.8
Gremyachevskaya Formation (Upper Hauterivian)		
15	Fine to medium quartz sand; greenish brown; glauconite; clayey-ferruginous cement; two layers of coaly clay in the upper part	8.2
14	Fine sand; dark gray to black; silty, micaceous; erosional unconformity at the base	1.2
Rostovskaya Formation (Lower Hauterivian)		
13	Fine quartz sand; white; micaceous, glauconitic	9.8
12	Fine silty sand; greenish dark gray; clayey, micaceous, rare coaly fragments	1.5
11	Fine sand; brownish gray; small lenses of white sand; numerous phosphorite sandy and clayey nodules; fragments of coalified wood	1.5
10	Fine to medium quartz sand; black; clayey, glauconitic; thin layers of coaly clay; erosional unconformity at the base	7.7
Jurassic		
Kostromskaya Formation (Mid Volgian)		
9	Quartz glauconitic sandstone; phosphate cement; abundant bivalve shells and ammonites; erosional unconformity at the base	0.8
Gorkinskaya Formation (Upper Kimmeridgian)		
8	Silty clay; dark gray; micaceous	0.7
7	Clay; black; well-rounded clayey phosphorite nodules, carbonate detritus wavy erosional surface at the lower contact	2.5
Ermolinskaya Formation (Upper Oxfordian-Lower Kimmeridgian)		
6	Compact clay; dark gray; horizontally laminated; abundant carbonate detritus; abundant *Zoophycos* and *Nereites* trace fossils in the lower part with marcasite; large bivalve shells, small ammonites and belemnites; erosional unconformity at the base	7.6
Podmoskovnaya Formation (Mid-Upper Oxfordian)		
5	Compact clay; dark gray to brownish; abundant carbonate detritus and and foraminifera; limonitized in the lower part; erosional surface at the base	5.2
Podosinkovskaya Formation (Upper Callovian-Lower Oxfordian)		
4	Compact clay; light gray; fine laminated; abundant *Zoophycos* and *Rhizocorallium* trace fossils with silt and marcasite; thin carbonate detritus; erosional surface at the base	0.8
Velikodvorskaya Formation		
3	Clay; light to bluish gray; fine laminated; abundant carbonate detritus, with fine sand in the lower part	4.0
Kriushskaya Formation		
2	Clay; brownish gray; horizontally laminated; abundant iron oolites, layer of light gray oolitic marl; erosional unconformity at the base	0.8
Carboniferous		
1	Dolomite; dark brown	16.1

Savelievo (M163)

Well is located in Vladimir Province, Kirzhach County, 1.2 km south of village Savelievo. Altitude 204 m, Depth 155.8 m

Unit	Lithology	Thickness (m)
Quaternary		
33	Sandy clay; brownish gray; erosional unconformity at the base	2.5
Cretaceous		
Tentikovskaya Formation (Upper Santonian)		
32	Siliceous ooze; light gray; massive, clayey in some places	8.0
31	Compact siliceous ooze; light to brownish gray; with lenses and layers of fine glauconitic quartz sand in the lower part	7.5
30	Fine siltstone with siliceous cement; small lenses of quartz glauconitic sand; small horizontal trace fossils	0.4
Dmitrovskaya Formation (Upper Santonian)		
29	Fine to very fine quartz sandstone; light to dark gray; glauconitic wavy erosional surface at the base	2.6
Zagorskaya Formation (Upper Coniacian-Lower Santonian)		
28	Siliceous ooze and clayey siliceous ooze; gray; with *Inoceramus sp.*	6.5
27	Unsorted sandstone; dark gray; predominantly fine; gravel and pebbles in the basal part; erosional unconformity at the base	0.5
Chernevskaya Formation (Mid-Upper Turonian)		
26	Sandy marl; brownish gray; with gravel	2.7
25	Fine to medium sand; light to purplish gray; clayey, calcareous; small phosphorite concretions in basal part	1.5
24	Poorly sorted, predominantly fine to medium sand; light gray; marly; erosional unconformity at the base	1.2
Lyaminskaya Formation (Lower Cenomanian)		
23	Fine to very fine sandstone; gray; coarse grains, calcareous in the upper part; erosional unconformity at the lower contact	2.8
Paramonovskaya Formation (Upper Albian)		
22	Clayey glauconitic siltstone; dark gray to black; pyrite; small phosphorite concretions in the upper part; abundant small horizontal trace fossils in lower part	17.8
21	Silty clay, dark gray to black; horizontal lamination; abundant small horizontal trace fossils; pyrite	11.2
20	Compact rich clay; dark gray to black; very small lenses of silt and very fine sand	5.6
19	Clayey silt; gray; massive	1.7
18	Unsorted quartz glauconitic sand; greenish gray; very fine to coarse with dominating fine grains; abundant well-rounded small (0.5-1 cm) pebbles of clayey phosphorite; erosional unconformity at base	0.3

Gavrilkovskaya Formation (Mid Albian)		
17	Unsorted quartz glauconitic sand; grayish green; fine to coarse with dominance of medium grains; small (3-5 cm) coarse sandy phosphorite nodules; erosional unconformity at base	9.2
Kolokshinskaya Formation (Lower Albian)		
16	Fine to very fine quartz sandstone; dark gray; clayey, glauconitic	14.0
15	Clayey glauconitic silt; light to purplish gray; thin layers and lenses of very fine sand in the lower part; erosional unconformity at base	1.4
Vorokhobinskaya Formation (Lower Aptian)		
14	Very fine sand; brownish gray; silty; wavy erosional surface at lower contact	6.9
Kotelnikovskaya Formation (Upper Hauterivian)		
13	Clayey silt; dark gray; massive or horizontally laminated	5.4
Gremyachevskaya Formation (Upper Hauterivian)		
12	Unsorted quartz sand; dark to greenish gray; fine to coarse with dominance of medium grains; clayey; clayey silt in the upper part	4.1
11	Fine to very fine quartz sand; light gray;	6.4
Savelievskaya Formation (Upper Hauterivian)		
10	Clayey silt; brownish gray; in the upper part - micaceous, pyrite, coalified plant detritus	8.5
Sobinskaya Formation (Upper Hauterivian)		
9	Clayey silt; dark gray; lenses of unsorted sand; sandy in the lower part sedimentary structures resembling hummocky cross stratification	1.0
8	Unsorted sand; dark to brownish gray; fine to coarse with dominance of fine grains; micaceous; layers and lenses of silty and calcareous clay	2.1
7	Fine to very fine sand; dark to brownish gray; micaceous fragments of fine calcareous sandstone with ammonites *Simbirskites cf. coronatiformis*	2.0
6	Fine sand; dark gray to black; calcareous, clayey, with pyrite erosional unconformity at base	1.4
Rostovskaya Formation (Lower Hauterivian)		
5	Fine to very fine quartz sand; light gray; ?glauconite, clayey in lower part	4.4
4	Very fine sand; smoky gray; micaceous, clayey; calcareous in lower part	6.5
3	Sandy conglomerate; brownish to dark gray; angular to well rounded pebbles of gray to black clayey phosphorite (several generations), small (0.5-1 cm) pebbles dominate, largest can be 4-5 cm; matrix consist of fine calcareous sand; erosional unconformity at base	2.4
Jurassic		
Ermolinskaya Formation (Upper Oxfordian-Lower Kimmeridgian)		
2	Silty clay; brownish gray to black; dark gray phosphorite pebbles in lower part	1.5
1	Silty clay; dark gray; horizontal lamination; abundant fauna of ammonites and bivalves: *Rasenia stephanoides, Amoeboceras sp., Melagrinella subtilis, Loripes kostromensis, Buchia ex. gr. bronni, Astarte cordata, Parallelodon sp., Dicroloma sp.*	5.2

Lasitsy (M121)

Well is located in eastern Ryazan Province, 850 m south of village Lasitsy
Altitude 145.5 m, depth 105 m.

Unit	Lithology	Thickness (m)
Quaternary		
25	Clay, sand, erosional unconformity at the base	25.7
Cretaceous		
Maidanskaya Formation (Lower Aptian, D.weissi zone)		
24	Clayey quartz silt; light gray; micaceous; horizontal lamination	2.7
23	Silty and clay; brownish green gray; fragments of coalified wood; sandy siderite concretions in the upper portion; with fine to medium sand	1.8
22	Clayey silt; light to smoky gray; micaceous; thin layers of dark brown clay horizontal lamination; plant detritus	5.7
21	Clayey silt and fine quartz sand; light gray; micaceous	2.8
22	Silt and fine sand; light gray; clayey, micaceous; massive; small plant detritus	4.6
21	Lean clay; gray; numerous small lenses of fine quartz sand; erosional surface at the lower contact	0.7
Lasitskaya Formation (Lower Aptian, M.ridzewskyi zone)		
20	Fine top medium quartz sand; yellowish gray; grains are well rounded	3.0
19	Fine quartz sand; brownish gray to dark gray; silty and clayey	2.6
18	Fine quartz sand; dark gray to black; clayey, micaceous; abundant pyrite nodules (0.5-4 cm); erosional unconformity at base	2.4
Okshovskaya Formation (Upper Hauterivian)		
17	Silty clay; dark gray to black; micaceous; abundant quartz grains and chamosite oolites in middle part	4.2
16	Silty clay; light gray to rusty brown; abundant iron (chamosite) oolites; erosional unconformity at base	2.2
Izhevskaya Formation (Lower Hauterivian)		
15	Phosphorite; brown gray; well rounded quartz sand and gravel; abundant iron oolites and oncoids; phosphate cement; abundant bivalves: *Buchia sublaevis*; erosional unconformity at base	1.2
Jurassic		
Elatminskaya Formation (Lower Callovian)		
14	Fine silt; light gray to gray; clayey, micaceous; horizontal lamination; large bivalve shells and belemnite fragments	7.6
13	Clayey silt; light to smoky gray; fine horizontal lamination; small horizontal trace fossils; small poorly preserved ammonites	3.6
12	Clayey silt; dark gray; micaceous; wavy lamination, abundant horizontal trace fossils; coalified wood fragments; well preserved lower Callovian ammonites	3.2

11	Silty clay; gray; micaceous; fragments of coalified wood; bioturbated; small horizontal trace fossils	2.8
10	Silty clay; brownish gray; micaceous; plant detritus; coalified and pyritized fragments of wood and belemnite fragments in the basal part; well preserved ammonites in middle part; erosional unconformity at base	7.6
Mokshinskaya Formation (Mid-Late Bathonian)		
9	Clay; light gray; silty in the lower part; horizontal lamination	5.2
8	Coarse silt; light gray; micaceous, quartz-glauconitic; massive	1.2
7	Clay; gray; fine horizontal lamination; thin layers of silt	3.3
6	Silty clay; brownish to light gray; sandy in upper and lower parts; horizontal lamination	1.9
5	Clay; light gray; horizontal lamination	1.5
4	Silty clay; gray; abundant plant remnants and detritus; horizontal lamination	1.5
Vyazhnevskaya Formation (Upper Bajocian-Lower Bathonian)		
3	Clay; brownish to dark gray; coalified plant remnants; shell detritus	2.5
2	Oolitic marl; brownish to dark gray; shell detritus; abundant iron oolites erosional unconformity at the base	1.0
Carboniferous		
1	Limestone	1.5

Boyarka River section (Valanginian-Hauterivian part)
Section is located in southern Taimyr Peninsula at 97.5 E, 70.7 N and is exposed in several outcrops along Boyarka River.

Unit	Lithology	Thickness (m)
Lower Hauterivian		
zone Homolsomites bojarkensis		
28	Sandy silt; bluish-gray; fine sand in the upper part; *Arctichnus* trace fossils	3.5
27	Silt clayey; dark gray	2.5
26	Silty clay; bluish gray, massive; lenses of greenish gray sand in upper part	18.0
25	Clayey silt; gray; sandy in some parts; rare carbonate concretions; 7.0 lower contact - wavy erosional surface	
24	Silt, fine sand; dark to yellow gray; abundant *Arctichnus* trace fossils	6.8
23	Silt; gray; lenses of jarosite	4.2
22	Sandy silt/clay; gray; lenses of silty sand with brown limonite mottles; wavy erosion at the lower contact	4.1

21	sandy silt - sand; greenish gray; small jarosite lenses	9.9
20	Silty clay; dark gray; rare carbonate concretions Fauna: *Homolsomites sp. ind.*	2.4
19	Sandy silt; light gray; *Arctichnus* trace fossils	7.1
18	Fine sand; gray; abundant *Arctichnus* trace fossils	2.9
17	Silt; gray; micaceous, sandy in the lower part Ammonites: *Homolsomites bojarkensis*	2.0
16	Silt sandy and clayey; dark gray; erosional unconformity at the lower contact; Fauna: *Neocraspedites kotschetkovi, Polyptychites cf. bidichotomoides, Homolsomites sp.,*	6.7

Upper Valanginian
zone Dichotomites bidichotomus

15	Fine sand and sandy silt; light gray; coarse-grained light-greenish sand with mineralized wood and rare carbonate concretions in the lower part; *Arctichnus* trace fossils in lower and upper (sandier) parts Fauna: *Polyptychites (Dichotomites) aff. bidichotomus*	5.8
14	Clayey silt; dark gray; shell accumulation of "shell pavement" type at the base; *Arctichnus* trace fossils Fauna: *Polyptychites polyptichus, Polyptychites bidichotomus, Polyptychites bidichotomoides*	2.9
13	Sandy silt; greenish gray; carbonate concretions; abundant *Arctichnus* trace fossils; wavy erosion at the lower contact Fauna: *Polyptychites polyptychus, P. triplodiptychus, P. bidichotomus, P. bidichotomoides*	8.2

Lower Valanginian
zone Polyptychites polyptychus

12	Sandy silt; greenish gray Fauna: *Temnoptychites mediatus, Polyptychites polyptychus, P. triplodiptichus, P. beani, P.bidichotomus*	2.0
11	Sand; greenish gray; ferruginous, silty in the lower part, rare carbonate concretions; abundant *Arctichnus* trace fossils Fauna: *Siberites rectangulatus, Temnoptychites mediatus, P. beani, Polyptychites polyptychus,*	4.3
10	Clay and clayey silt; dark gray; rounded shape carbonate concretions, sandy in the lower part	5.1
9	Sand and silty sand; greenish gray to bluish gray; rare scattered carbonate concretions, ferrous in some parts; abundant *Arctichnus* in the lower part; mineralized wood patterns in the middle part and horizon of carbonate concretions in the lower part; shell accumulation of "shingled" type in the middle part;	14.7

wavy erosion at the lower contact
Fauna: *Siberites rectangulatus, S.ramulicostata*

zone Temnoptychites syzranicus

8	Fine sand and sandy silt; yellowish to greenish gray; rare nodules of lime sandstone; abundant *Arctichnus* trace fossils; abundant mineralized wood in the upper part; trough cross-bedding in the lower part; Fauna: *Neocraspedites menjaiteformis, Siberites rectangulatus, S.ramulicostata, Temnoptychites sp. ind.*	14.4
7	Sandy silt; gray; rare carbonate nodules; *Arctichnus* trace fossils and small trough cross-bedding in the upper part	7.8
6	Clay; dark to greenish gray	5.0
5	Fine sand and silty sand; greenish gray; ferruginous, high content of leptochlorite; tabular/trough crossbeds and concretions of limy sandstone in the lower part; wavy erosion at the lower contact; *Arctichnus* trace fossils and shell accumulations of "shingled" type in the lower part; Fauna: *Neotollia maimetschensis*	10.3
4	Sand; greenish gray; leptochlorites; abundant trough and tabular cross-beds; sandy carbonate concretions; Rhizocorallium and *Zoophycos* trace fossils; "regularly distributed" accumulations of shells; Fauna: *Neotollia klimovskiensis*	17.0
3	Sand; greenish gray; plant detritus; trough cross-beds flasers of clay in the lower part; abundant *Arctichnus*, and *Rhizocorallium* only in the lower part; shell accumulations of "shell pavement" type; Fauna: *Tollia sp. ind., Temnoptychites sp. ind.*	8.6
2	Fine sand; greenish gray; limonite mottles around some mineralized wood patterns; trough cross-beds and clay flasers; abundant *Arctichnus* and *Rhizocorallium* trace fossils;	14.5

Berriasian
zone Bojarkia mesezhnikovi

1	Silty clay; dark gray; massive	20.0

Yangoda River section

Section is located in southern Taimyr peninsula at 88 E, 70.7 N and is exposed in several outcrops along the Yangoda River.

Unit	Lithology	Thickness (m)
Lower Coniacian		
layers with Inoceramus schulginae - I. jangodaensis		
20	Fine sand; greenish gray; massive, sandy concretions in the lower part climbing ripples, vertical trace fossils (*Arctichnus*)	5.0

19	Fine sand; greenish gray; massive, well sorted; numerous phosphorite and siderite nodules in the basal part; lower contact is an erosional unconformity Fossils: shark teeth, fragments of vertebras of Pliosauroids	2.5
18	Fine quartz sand; light gray; climbing ripples	7.5
17	Intercalation of fine- medium sand with clay layers; abundant siderite concretions of different shapes; abundant trace fossils including *Arctichnus*, *Rhizocorallium* Fossils: *Inoceramus jangodaensis, I. schulginae*	3.0
16	Fine sand; greenish gray; small trough cross-bedding in the upper part; rare phosphorite and siderite concretions; *Ophiomorpha* burrows; wavy erosional surface at the lower contact; Fossils: *Inoceramus jangodaensis, I. schulginae*	3.0
15	Fine sand, same lithology as unit 11 Fossils: *Inoceramus schulginae, I. jangodaensis, I. lamarcki, I.websteri, I. aff. monopterus, I. sp.*	3.0

zone Volviceramus subinvolutus

14	Fine sand; light gray; large trough cross-bedding, abundant siderite concretions; abundant fragments of wood; Fossils: *Cremnoceramus incostans, Volviceramus subinvolutus, Inoceramus lamarcki, I. jangodaensis, I.websteri, I. aff. monopterus, I. sp., Arctica sp., Euspira sp.*	6.0
13	Unsorted sand; dark green; small lenses of clay and silt; sandy phosphorite concretions in the lower part; abundant *Arctichnus* and *Rhizocorallium* trace fossils; wavy erosion at the lower contact Fossils: *Inoceramus schulginae, I. jangodaensis, I. lamarcki, I. cf. websteri, I. sp., I. aff. monopterus, Protocardia sp., Nuculoma (?) sp., Euspira sp., Serrifusus sp., shark teeth, Elasmosauridae* vertebrae	3.0
12	Fine sand and silty sand; dark gray; thin layers of silt; plant detritus and small fragments of wood; rare vertical trace fossils in the upper part Fossils: *Cremnoceramus incostans, Volviceramus subinvolutus, I. sp., Inoceramus schulginae*	10.5
11	Silty sand; light gray; thin layers of clay and silt; plant detritus, abundant mineralized wood in the upper part Fossils: *Inoceramus schulginae, I. jangodaensis, I. cf. pseudocancellatus, Cremnoceramus incostans*	5.7
10	Fine sand; light to dark green; numerous layers of silty clay, lenses of unsorted siderite sand, sandy phosphorite concretions, small trough crossbedding, abundant *Arctichnus* trace fossils; erosional wavy surface at the lower contact Fossils: *Inoceramus inaequivalvis, I. lamarcki, Cremnoceramus incostans, Volviceramus subinvolutus, I. cf. pseudocancellatus*	2.6

Upper Turonian
zone Inoceramus inaequivalvis

9	Clay and silty clay; bluish gray to dark brown; lenses and thin layers of fine cross-bedded and bioturbated sand; abundant jarosite in the lower part; rare *Rhizocorallium* trace fossils	5.0
8	Clayey silt and silty clay, micaceous; dark gray to black; small sandy siderite concretions in the lower part; small pyrite nodules	7.4
7	Fine sand; dark gray to brown; concretions of sandy siderite, rare fragments of wood; abundant *Rhizocorallium* and rare *Arctichnus* trace fossils; wavy erosion at the lower contact Fossils: *Inoceramus pseudocancellatus, I. inaequivalvis, I. shulginae*	3.0
6	Fine sand; light gray; thin layers of clay and plant detritus in the lower part, well sorted with trough cross-beds in the upper part; rare fragments of mineralized wood	21.0
5	Black clay; small pyrite nodules, layer of carbonate concretions in the lower part	3.0
4	Clayey silt; dark gray; phosphorite and sandy siderite concretions in the lower part, and accumulations of shell fragments, erosional unconformity at the lower contact Fossils: fragments of Inoceramus pseudocancellatus	2.0
3	Clayey silt; greenish gray; abundant sandy phosphorite concretions in the lower part, abundant *Arctichnus* trace fossils and coprolites Fossils: *Scaphites spp., Baculites sp., Inoceramus pseudocancellatus, inaequivalvis, I. shulginae, I. lamarcki, Lopatinia jenisseae, Nuculana sp., Nucula sp., Astarte sp., Arctica sp., Malletia nitens, Saturnia sp., Tankredia sp, Goniomya sp., Modiolus sp., Euspira sp., Drepanocheilus sotnikovi, Graphidula sp., Serrifusus sp.*	1.7
2	Fine or medium sand; grayish green; bioturbated; phosphorite concretions; abundant siderite and glauconite; Abundant *Rhizocorallium* and *Arctichnus* trace fossils; wavy erosion at the lower contact Fossils: *Inoceramus pseudocancellatus, I. inaequivalvis, Lopatinia jenisseae, Falcimytilus lanceolatus, Arctica sp., Pleuromya sp., Modiolus sp., Lucina sp., Protocardia sp., Euspira sp., Cylichna sp.*	5.7
1	Fine sand; light gray to greenish gray; ferrous in the middle part; thin clay layers, phosphorite concretions; *Arctichnus* trace fossils,pellets and coprolites; climbing ripples Fossils: *Inoceramus sp. ind., Lopatinia jenisseae, Falcimytilus lanceolatus,* gastropods, teeth of marine lizards	10.2

Agapa River

The section is located in southern Taimyr peninsula at 86 N, 70 E and is exposed in several outcrops along Agapa River.

Unit	Lithology	Thickness (m)
Lower Turonian, Inoceramus labiatus zone		
11	Fine sand; light gray; massive; large concretions of sandstone in the upper part; *Inoceramus labiatus*	8.5
10	Clayey silt; greenish dark gray; extensively bioturbated; small (3-4 cm) phosphorite concretions; soiderite concretions in the upper part (8-10 cm); abundant shell detritus and accumulations; Fossils: *Proplacenticeras sp., Borissiakoceras sp., Inoceramus labiatus , Nuculana sp., Malletia sp., Lopatinia jenissiae, Eusprira sp., Falcimytilus lanceolatus , Pyropsis sp.*	11.0
9	Leptochlorite silt; greenish gray; extensively bioturbated; accumulation of accumulation of shell detritus in the lower part; numerous siderite concretions in the middle part; Fossils: *Proplacenticeras sp., Aporrhais sp., Fasciolaria sp., Cylichna sp., Pyropsis sp.*	1.5
8	Silty clay; bluish dark gray; massive or fine horizontal lamination; bioturbated in the uppermost part; rare*Inoceramus labiatus*	12.0
Upper Cenomanian, Inoceramus pictus zone		
7	Leptochloritic silt; green gray; abundant phosphate nodules and fossil accumulations (bivalves, ammonites, gastropods, etc.), including Inoceramus pictus Sow.	3.5
6	Silt and silty clay; gray; bioturbated; limonite mottles; accumulations of small shells (bivalves and gastropods)	6.8
5	Fine sand; greennish gray and green; two layers of calcareous sand in the upper part and siderite concretiuons with abundant fauna including *Inoceramus pictus*	5.5
Not observed (~30 m)		
4	Clayey silt; gray; horizon of siderite concretions with inoceramids in the lower part; scattered shells and accumulations of *Lopatinea*, ctenodontids; gastropods and belemnite rostra	12.5
3	Intercalation of sand, silt, and clay; light to dark gray; horizontal lamination chained horizons of siderite concretions; clayey breccias; plant detritus	9.2
2	Quartz fine and medium sand; light gray; lens-like accumulations of lignitic wood; and associated amber resins (retinites); large trough and tabular cross--bedding;	25.0